



Field Observations During the Third Microwave Water and Energy Balance Experiment (MicroWEX-3): June 16 - December 21, 2004¹

Tzu-yun Lin, Jasmeet Judge, Kai-Jen Calvin Tien, Joaquin Casanova, Mi-young Jang, Orlando Lanni, Larry Miller, and Fei Yan²

-
1. This document is Circular 1483, one of a series of the Agricultural and Biological Engineering Department, Florida Cooperative Extension Service, Institute of Food and Agricultural Sciences, University of Florida. First published November 2005. Please visit the EDIS Web site at <http://edis.ifas.ufl.edu>.
 2. Jasmeet Judge is an Assistant Professor and Director of Center for Remote Sensing (email: jasmeet@ufl.edu); Joaquin Casanova is an Undergraduate Research Assistant; and Kai-Jen Tien, Mi-young Jang, and Fei Yan are Graduate Research Assistants. All authors are affiliated with the Agricultural and Biological Engineering Department, Institute of Food and Agricultural Sciences, University of Florida, Gainesville, 32611

The Institute of Food and Agricultural Sciences (IFAS) is an Equal Opportunity Institution authorized to provide research, educational information and other services only to individuals and institutions that function with non-discrimination with respect to race, creed, color, religion, age, disability, sex, sexual orientation, marital status, national origin, political opinions or affiliations. U.S. Department of Agriculture, Cooperative Extension Service, University of Florida, IFAS, Florida A. & M. University Cooperative Extension Program, and Boards of County Commissioners Cooperating. Larry Arrington, Dean.

TABLE OF CONTENTS

1. INTRODUCTION	1
2. OBJECTIVES	1
3. FIELD SETUP	1
4. SENSORS	4
4.1 University of Florida C-band Microwave Radiometer (UFCMR) System	4
4.1.1 Theory of operation	5
4.2 Eddy Covariance System	7
4.3 Net Radiometer	8
4.4 Thermal Infrared Sensor	9
4.5 Soil Moisture and Temperature Probes	9
4.6 Soil Heat Flux Plates.....	10
4.7 Rain gauges	10
4.8 Canopy temperatures	10
5. SOIL SAMPLING	10
5.1 Surface Roughness	10
5.2 Gravimetric Soil Moisture	11
5.3 Soil Temperature and Moisture.....	12
6. VEGETATION SAMPLING	12
6.1 Height and Width.....	12
6.2 Leaf Area Index (LAI)	12
6.3 Green and Dry Biomass	12
6.4 Root Sampling	12
6.5 Lint Yield.....	12
7. WELL SAMPLING	13
7.1 Groundwater sampling	13
7.2 Water level measurement	13
8. FIELD LOG	14
ACKNOWLEDGEMENT	23
REFERENCES	23
A. FIELD OBSERVATIONS	24

1. INTRODUCTION

For accurate prediction of weather and near-term climate, root-zone soil moisture is one of the most crucial components driving the surface hydrological processes. Soil moisture in the top meter is also very important because it governs moisture and energy fluxes at the land-atmosphere interface and it plays a significant role in partitioning of the precipitation into runoff and infiltration.

Energy and moisture fluxes at the land surface can be estimated by Soil-Vegetation-Atmosphere-Transfer (SVAT) models. These models are typically used in conjunction with climate prediction models and hydrological models. Even though the biophysics of moisture and energy transport is well-captured in most current SVAT models, the computational errors accumulate over time and the model estimates of soil moisture diverge from reality. One promising way to improve significantly model estimates of soil moisture is by assimilating remotely sensed data that is sensitive to soil moisture, for example microwave brightness temperatures, and updating the model state variables.

The microwave brightness at low frequencies (< 10 GHz) is very sensitive to soil moisture in the top few centimeters in most vegetated surfaces. Many studies have been conducted in agricultural areas such as bare soil, grass, soybean, wheat, pasture, and corn to understand the relationship between soil moisture and microwave remote sensing. Most of these experiments conducted in agricultural regions have been short-term experiments that captured only a part of growing seasons. It is important to know how microwave brightness signature varies with soil moisture, evapotranspiration (ET), and biomass in a dynamic agricultural canopy with a significant biomass ($4-6$ kg/m²) throughout the growing season.

2. OBJECTIVES

The goal of MicroWEX-3 was to understand the land-atmosphere interactions during the growing season of cotton, and their effect on observed microwave brightness signatures at 6.7 GHz, matching that of the two satellite-based microwave radiometers (AMSR-E and AMSR). Specific objectives of MicroWEX-3 are:

1. To collect passive microwave and other ancillary data to develop and calibrate a dynamic microwave brightness model for cotton.
2. To collect energy and moisture flux data at land surface and in soil to develop and calibrate a dynamic SVAT model for cotton.
3. To evaluate feasibility of soil moisture retrievals using passive microwave data at 6.7 GHz for the growing cotton canopy.
4. To evaluate feasibility of using Mid Infrared Reflectance for estimating vegetation water content and biomass during the cotton growing season

3. FIELD SETUP

MicroWEX-3 was conducted by the Center for Remote Sensing, Agricultural and Biological Engineering Department, at the Plant Science Research and Education Unit (PSREU), IFAS, Citra, FL. Figures 1 and 2 show the location of the PSREU and the study site for the MicroWEX-3, respectively. The study site was located at the west side of the PSERU. The dimensions of the study site were a 183 m X 183 m. A linear move system was used for irrigation. The experiment began on June 16 with microwave radiometer observing bare soil. The cotton was planted on June 21 (DoY 173) at an orientation of 60° from East as shown in Figure 3 and sensors were installed on DoY 182 (Eddy covariance system), DoY 183 (Northwest station), and DoY 189 (East station). Root fungus destroyed the seedling and the cotton was re-planted on July 9 (Day of Year in 2004, DoY 191). The crop spacing was about 8 cm and the row spacing was 76.2 cm (30 inches). Instrument installation took place on July 14 (DoY 196). The instruments consisted of a ground-based microwave radiometer system and micrometeorological stations. The ground-based

microwave radiometer system was installed at the location shown in Figure 3, facing south to avoid the radiometer shadow interfering with the field of view as seen in Figure 3.

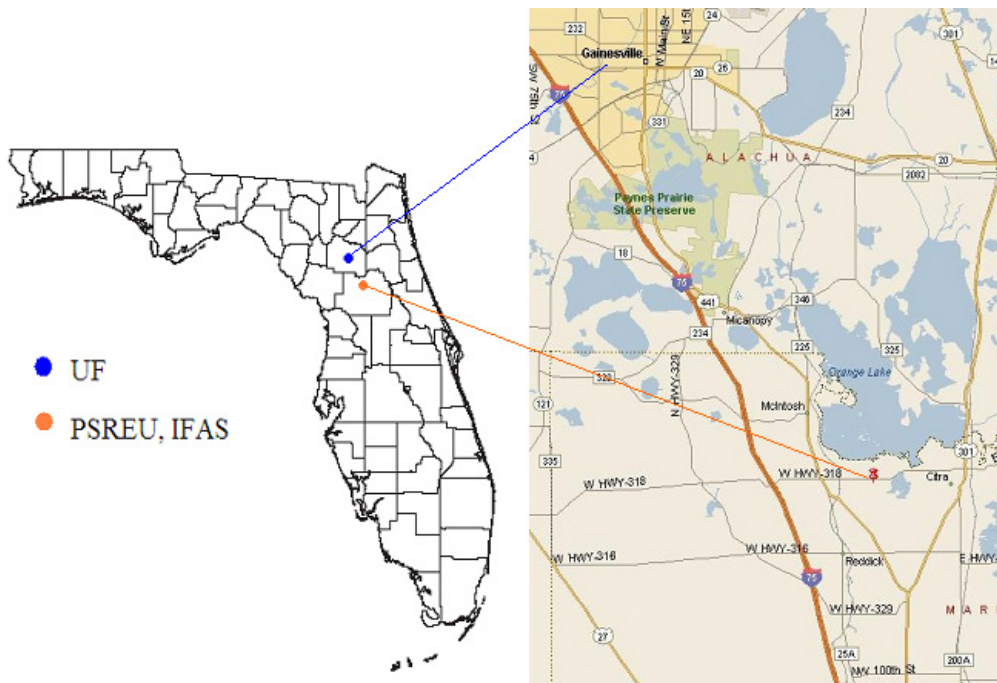


Figure 1. Location of PSREU/IFAS.

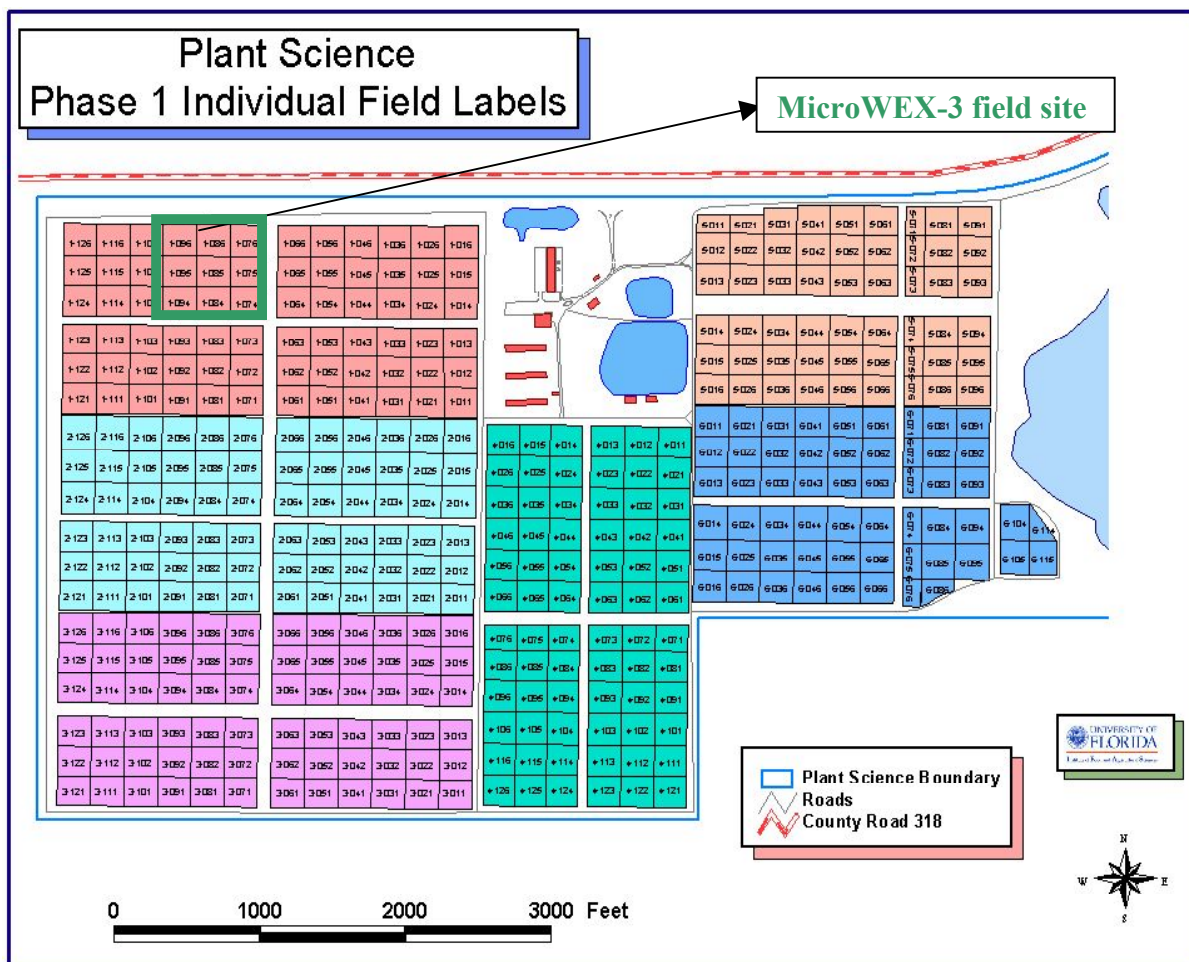
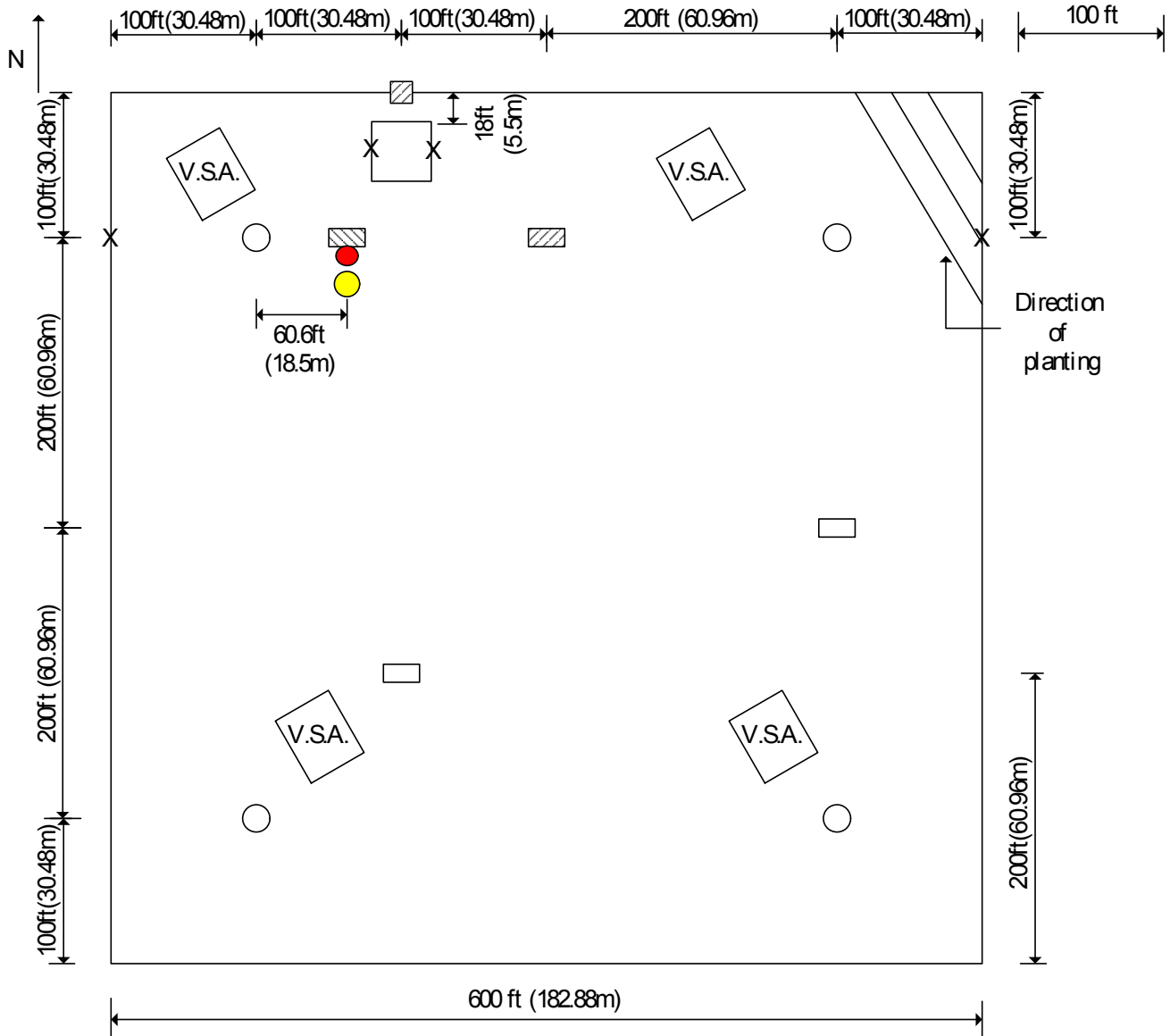


Figure 2. Location of the field site for MicroWEX-3 at the UF/IFAS PSREU.

The micrometeorological station was installed at the center of the field and included soil heat flux plates and the eddy covariance system. Two raingauges were installed at the east and west edge of the radiometer footprint. Two additional raingauges also were installed at the east and west edge of the field to capture the irrigation. Three stations with soil moisture, soil heat flux, and soil temperature sensors installed were set up at the location shown in Figure 3. The Northwest station was installed with a Thermal infrared camera and a net radiometer. This report provides detailed information regarding sensors deployed and data collected during the MicroWEX-3.



- : Wells □ : Footprint (12.5m* 12.5m or 41ft* 41ft) X : Raingauges ▨ : Radiometer
 - ▨ : CR23x, with soil moisture, soil temperature, and soil heat flux* ● (red) : TIR ● (yellow) : CNR
 - ▨ (diagonal lines) : CR23x, with ECS
 - (white) : CR10, with soil moisture, soil temperature, and soil heat flux*
 - ◇ (V.S.A.) : Vegetation Sampling Area
- *: The sensors are installed at depth: 2, 4, 8, 16, 32, 64, and 120 cm

Figure 3. Layout of the sensors during MicroWEX-3.

4. SENSORS

MicroWEX-3 had three major types of instrument subsystems: the ground-based University of Florida C-band Radiometer (UFCMR), the micrometeorological subsystem, and the soil subsystem

4.1 University of Florida C-band Microwave Radiometer (UFCMR) System

Microwave brightness temperatures at 6.7GHz ($\lambda = 4.48$ cm) were measured every 30 minutes using the University of Florida's C-band Microwave Radiometer system (UFCMR) (Figure 4 (a)). The radiometer system consisted of a dual polarization total power radiometer operating at the center frequency of 6.7 GHz housed atop a 10 m tower installed on a 16' trailer bed. UFCMR was designed and built by the Microwave Geophysics Group at the University of Michigan. It operates at the center frequency at 6.7 GHz that is identical to one of the center frequencies on the space borne Advanced Microwave Scanning Radiometer (AMSR) aboard the NASA Aqua Satellite Program. UFCMR observed a footprint of size 11 m x 11 m from a height of 7.6 m. A rotary system was used to rotate the look angle of the UFCMR both for field observations and sky measurements. The brightness temperatures were observed at an incidence angle of 55 degrees, matching that of the space borne AMSR-E sensor. The radiometer was calibrated every two weeks with a microwave absorber as warm load and measurements of sky at several angles as cold load. Figures 4 (b) and 4 (c) show the close-up of the rotary system and the antenna of the UFCMR, respectively. Table 1 lists the specifications of UFCMR. Figure A-1 shows the V- & H-pol brightness temperatures observed during MicroWEX-3.

Table 1. UFCMR specifications

Parameter	Qualifier	Value
Frequency	Center	6.7 GHz
Bandwidth	3 dB	20 MHz
Beamwidth	3 dB V-pol elevation	23 ^{oa}
	3 dB V-pol azimuth	21 ^{ob}
	3 dB H-pol elevation	21 ^{oc}
	3 dB H-pol azimuth	23 ^{od}
Isolation		> 27 dB
Polarizations	Sequential	V/H
Receiver temp		437 K ^e
Noise Figure	From Trec	3.99 dB
RF gain		85 dB
Gain tempco	dTsys/dTset	-2 K/C ^f
NEDT	1 sec	0.71 K ^g
	8 sec	0.25 K ^h
Tempature	Control – rms	5 mK ⁱ
SetPoint	Max	40° C ^j
	Min	0° C
Ambient	Max	48° C ^k
	Min	< 0° C ^l
RF cutout	McShane or RF1 thermistor	42° C ^m
Thermal shutdown	Case thermistor	62° C ⁿ

(a). sidelobes < -33 dB, (b). sidelobes < -28 dB, (c). sidelobes < -27 dB, (d). sidelobes < -35 dB, (e). +/- 20 K uncertainty, (f). looking at reference load, (g). tracking of absorber to reference load in lab, Tset = 305 K with PID = 0.75, 0.94, 0, (h). tracking of absorber to reference load in lab, Tset = 305 K with PID = 0.75, 0.94, 0, (i). Tset = 305 K in lab environment, on RF2, over 0.5 hour, after a day running, (j). active components rated to 65 C, filters to 40 C, (k). estimated absolute max Tamb-Tset = 15 C at TEC 100% cooling, (l). estimated, (m). RF power cut only, user recovery only, (n). RF and TEC power, user recovery only.

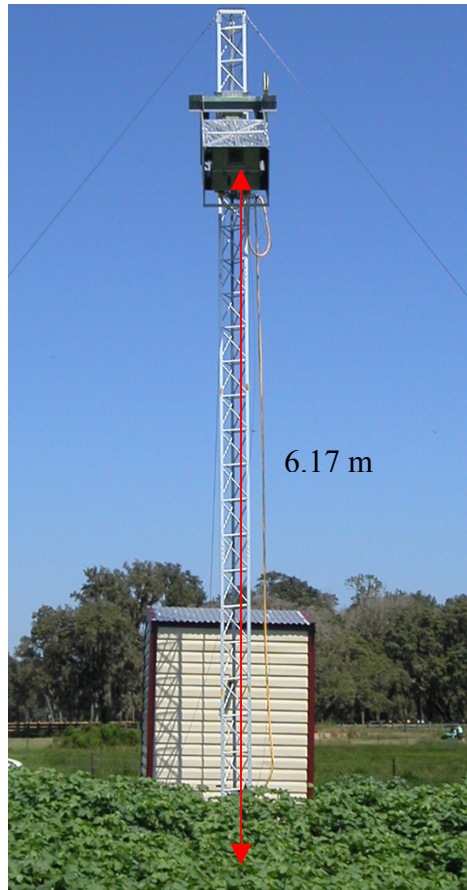


Figure 4 (a). The UFCMR system

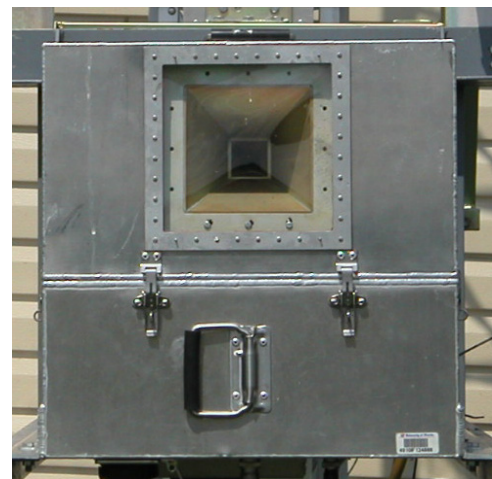


Figure 4 (b) and (c). The side view of the UFCMR showing the rotary system and the front view of the UFCMR showing the receiver antenna.

4.1.1. Theory of operation

UFCMR uses a thermoelectric cooler (TEC) for thermal control of the Radio Frequency (RF) stages for the UFCMR. This is accomplished by the Oven Industries “McShane” thermal controller. McShane is used to cool or heat by Proportional-Integral-Derivative (PID) algorithm with a high degree of precision at 0.01°C. The aluminum plate to which all the RF components are attached is chosen to have sufficient thermal mass to eliminate short-term thermal drifts. All components attached to this thermal plate, including the TEC, use thermal paste to minimize thermal gradients across junctions.

The majority of the gain in the system is provided by a gain and filtering block designed by the University of Michigan for the STAR-Light instrument (De Roo, 2003). The main advantage of this gain block is the close proximity of all the amplifiers, simplifying the task of thermal control. This gain block was designed for a radiometer working at the radio astronomy window of 1400 to 1427 MHz, and so the receiver is a heterodyne type with downconversion from the C-band RF to L-band. To minimize the receiver noise figure, a C-band low-noise amplifier (LNA) is used just prior to downconversion. To protect the amplifier from saturation due to out of band interference, a relatively wide bandwidth, but low insertion loss, bandpass filter is used just prior to the amplifier. Between the filter and the antenna are three components: a switch for choosing polarization, a switch for monitoring a reference load, and an isolator to minimize changes in the apparent system gain due to differences in the reflections looking upstream from the LNA.

The electrical penetrations use commercially available weatherproof bulkhead connections (Deutsch connectors or equivalent). The heat sinks have been carefully located employing RTV (silicone sealant) to seal the bolt holes. The radome uses 15mil polycarbonate for radiometric signal penetration. It is sealed to the case using a rubber gasket held down to the case by a square retainer.

The first SMA connection electromechanical latching, which is driven by the Z-World control board switches between V- and H-polarization sequentially. The SMA second latching which switches between the analog signal from the first switch and the reference load signal from a reference load resistor sends the analog signal to a isolator, where the signals within 6.4 to 7.2 GHz in radiofrequency are isolated. Then the central frequency is picked up by a 6.7 GHz bandpass filter, which also protects the amplifier to saturation. A Low Noise Amplifier (LNA) is used to eliminate the noise figure and adjust gain. A mixer takes the input from the LNA and a local oscillator to output a 1.4 GHz signal to STAR-Lite. After the Power Amplifier and Filtering Block (Star-Lite back-end), the signal is passed through a Square Law Detector and a Post-Detection Amplifier. UFCMR is equipped with a microcontroller that has responsibility for taking measurements, monitoring the thermal environment, and storing data until a download is requested. A laptop computer is used for running the user interface named FluxMon to communicate with the radiometer through Radiometer Control Language (RadiCL). The radiometer is configured to maintain a particular thermal set point, and make periodic measurements of the brightness at both polarizations sequentially and the reference load. The data collected by the radiometer is not calibrated within the instrument, since calibration errors could corrupt an otherwise useful dataset. Figure 5 shows the block diagram of UFCMR.

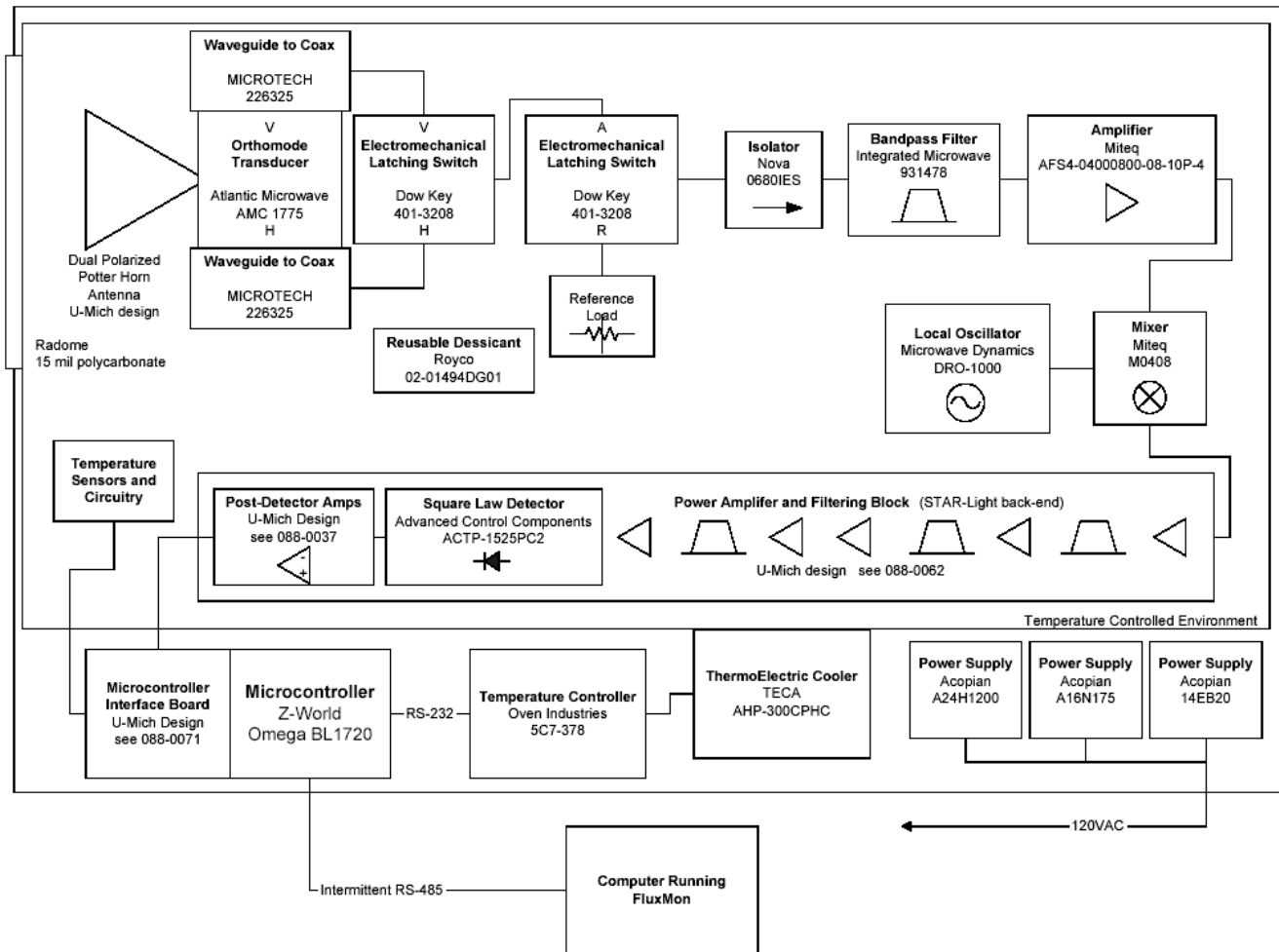


Figure 5. Block diagram of the University of Florida C-band Radiometer (De Roo, 2002).

4.2 Eddy Covariance System

A Campbell Scientific eddy covariance system was located at the center of the field toward the north edge as shown in Figure 3. The system included a CSAT3 anemometer and KH20 hygrometer. Figure 6 shows a close up of the sensor. CSAT3 is a three dimensional sonic anemometer, which measures wind speed and the speed of sound on three non-orthogonal axes. Orthogonal wind speed and sonic temperature are computed from these measurements. KH20 measures the water vapor in the atmosphere. Its output voltage is proportional to the water vapor density flux. Latent and sensible heat fluxes were measured every 30 minutes. The height of the eddy covariance system was set to 2.1m in the beginning of experiment and was changed to 1.2 m on DoY 202, and the orientation of the system was 220° toward southwest. The height of the eddy covariance system was moved to 2.25 m from the ground on DoY 246. Table 2 shows the list of specifications of the CSAT3. Data collected by the eddy covariance system have been processed for coordinate rotation (Kaimal and Finnigan, 1994; Wilczak et al., 2001), WPL (Web et al., 1980), oxygen (van Dijk et al., 2003, 2004), and sonic temperature corrections (Schotanus et al., 1983). Figure A-2 shows the processed latent and sensible heat fluxes observed during MicroWEX-3.



Figure 6. Eddy covariance system

Table 2. Specifications of the CSAT3 (Campbell Scientific, 1998)

Description	Value
Measurement rate	1 to 60 Hz
Noise equivalent wind	1 mm/sec in horizontal wind speed and 0.5 mm/sec in vertical wind speed
Wind measurement offset	$< \pm 4$ cm/sec over -30 to 50°C
Output signals	Digital SDM or RS-232 and Analog
Digital output signal range	± 65.535 m/sec in wind speed and 300 to 366 m/sec in speed of sound
Digital output signal resolution	0.25 to 2 mm/sec in vertical wind speed and 1 mm/s in speed of sound
Analog output signal range	± 32.768 to ± 65.536 m/sec in wind speed and 300 to 366 m/sec in speed of sound
Analog output signal resolution	± 8.192 mm/sec in vertical wind speed and 16 mm/sec in speed of sound
Measurement path length	10.0 cm vertical and 5.8 cm horizontal
Transducer path angle from horizontal	60 degrees
Transducer	0.64 cm in diameter
Transducer mounting arms	0.84 cm in diameter
Support arms	1.59 cm in diameter
Dimensions: anemometer head	47.3 cm x 42.4 cm
Dimensions: electronics box	26 cm x 16 cm x 9 cm
Dimensions: carry case	71.1 cm x 58.4 cm x 33 cm
Weight: anemometer head	1.7 kg
Weight: electronics box	2.8 kg
Weight: shipping	16.8 kg
Operating temperature range	-30°C to 50°C
Power requirement: voltage supply	10 to 16 VDC
Power requirement: current	200 mA at 60 Hz measurement rate and 100 mA at 20 Hz measurement rate

4.3 Net Radiometer

A Kipp and Zonen CNR-1 four-component net radiometer (Figure 7) was located at the center of the field to measure up- and down-welling short- and long-wave infrared radiation. The sensor consists of two pyranometers (CM-3) and two pyrgeometers (CG-3). The sensor was installed at the height of 2.5 m above ground and facing south. Table 3 shows the list of specifications of the CNR-1 net radiometer. Figure A-3 shows the up- and down-welling solar (shortwave) wave radiation observed during MicroWEX-3. Figure A-4 shows the up- and down-welling far infrared (longwave) radiation observed during MicroWEX-3. Figure A-5 shows the net total radiation observed during MicroWEX-3.



Figure 7. CNR-1 net radiometer

Table 3. Specifications of the CNR-1 net radiometer (Campbell Scientific, 2004a)

Description	Value
Measurement spectrum: CM-3	305 to 2800 nm
Measurement spectrum: CG-3	5000 to 50000 nm
Response time	18 sec
Sensitivity	10 to 35 $\mu\text{V}/(\text{W}/\text{m}^2)$
Pt-100 sensor temperature measurement	DIN class A
Accuracy of the Pt-100 measurement	± 2 K
Heating	Resistor 24 ohms, 6 VA at 12 volt
Maximum error due to heating: CM-3	10 W/m^2
Operating temperature	-40° to 70°C
Daily total radiation accuracy	$\pm 10\%$
Cable length	10 m
Weight	4 kg

4.4 Thermal Infrared (TIR) Sensor

An Everest Interscience thermal infrared sensor (4000.3ZL) was collocated with the net radiometer to observe skin temperature at nadir. Table 4 shows the list of specifications of the thermal infrared sensor. The sensor was installed at the height of 2.5 m. With the sensor field of view of 15° , the size of the footprint for the thermal infrared sensor was 66 cm X 66 cm. Figure A-6 shows the surface thermal infrared temperature observed during MicroWEX-3.

Table 4. Specifications of the thermal infrared sensor (Everest Interscience, 2005)

Description	Value
Accuracy	$\pm 0.5^\circ\text{C}$
Resolution	0.1°C
Measurement range	-40° to 100°C
Measurement spectrum	8 to 14 μm
Field of view	15°
Response time	0.1 sec
Operating distance	2 cm to 300 m
Power requirement: voltage supply	5 to 26 VDC
Power requirement: current	10 mA
Output signal	RS-232C and analog mV ($10.0 \text{ mV}/^\circ\text{C}$)

4.5 Soil Moisture and Temperature Probes

Three standard Vitel Hydra soil moisture and temperature probes and twenty-six Campbell Scientific time-domain water content reflectometers (CS616, see Table 5 for specifications) were used to measure temperature and soil volumetric water content at the depths of 2, 4, 8, 16, 32, 64, and 120 cm in row every 15 minutes. The observations of soil moisture were duplicated at the depths of 2 cm and 4 cm near the root zone. The calibration coefficients for the CS616 probes are listed in Table 5. Figures A-7, A-8 and A-9 show the soil temperatures observed at the northwest station during MicroWEX-3. Figures A-10, A-11 and

A-12 show the soil temperatures observed at the east station. Figures A-13, A-14 and A-15 show the soil temperatures observed at the southwest station. Figures A-16, A-17 and A-18 show the volumetric soil moisture content observed at the northwest station and Figure A-19 shows the volumetric soil moisture content observed at the depth of 1.7m located near the northwest monitoring well. Figures A-20, A-21 and A-22 show the volumetric soil moisture content observed at the east station. Figures A-23, A-24 and A-25 show the volumetric soil moisture content observed at the southwest station.

Table 5. The calibration coefficients for the CS616 probes (Campbell Scientific, 2004b)

Coefficient	Value
C ₀	-0.187
C ₁	0.037
C ₂	0.335

4.6 Soil Heat Flux Plates

Two Campbell Scientific (2003) soil heat flux plates (HFT-3) were used to measure soil heat flux at the depths of 2 and 5 cm, in row and near the root area, respectively. Table 6 shows the list of specifications of the soil heat flux plate. Figure A-26 shows the soil heat fluxes observed at 2cm and 5cm at northwest station during MicroWEX-3. Figure A-27 shows the soil heat fluxes observed at 5cm at CSAT station. Figure A-28 shows the soil heat fluxes observed at 5cm at the east station. Figure A-29 shows the soil heat fluxes observed at 5cm at southwest station.

Table 6. Specifications of the soil heat flux plate (Campbell Scientific, 2003)

Description	Value
Operating temperature	-40° to 55°C
Plate thickness	3.91 mm
Plate diameter	38.2 mm
Sensor	Thermopile
Measurement range	± 100 W/m ²
Signal range	± 2.4 mV
Accuracy	± 5%
Thermal conductivity	1.22 W/m/K

4.7 Rain gauges

Four rain gauges were installed in the field to measure the precipitation/irrigation. There were two rain gauges individually installed on the east and west edge of the footprint of the radiometer and were connected to the Northwest station. The amounts of precipitation/irrigation were recorded every 15 minutes. Figure A-30 shows the rainfall recorded by these two rain gauges. The other two rain gauges were set up on the east and west edge of the field and connected with Onset Hobo rainfall event datalogger to record the rainfall/irrigation. The time of every rainfall/irrigation event, which represents 0.2 mm of rainfall/irrigation, was recorded. Figure A-31 shows rainfall recorded by these rain gauges.

4.8 Canopy temperatures

Six thermistors were installed in the canopy to measure the temperatures of canopy at 4 cm, 10 cm, 20 cm, 50 cm, 75 cm, and 90 cm. Perforated metal cans (painted white) were used as radiation shield to protect the sensor from direct sun and rain. Figure A-32 and A-33 show the canopy temperature at different heights.

5. SOIL SAMPLING

Extensive soil sampling was conducted to provide additional information of the spatial distribution of the surface soil moisture, temperature, and surface roughness.

5.1 Surface Roughness

Surface roughness was measured using metal grid plate on DoY 195 (July 13). The measurements were located at the east, south, and west side and near the footprint of the radiometer. Figures A-79 to A-84 show the surface roughness observations.

5.2 Gravimetric Soil Moisture

The gravimetric soil moisture (GSM) was sampled at 3-6, 13-16, and 33-36 cm by a coring tool. Gravimetric soil moisture samplings were conducted four times during MicroWEX-3 on days: Sep. 9 (DoY 253), Sep. 14 (DoY 258), Sep. 23 (DoY 267), and Dec. 04 (DoY 339) in 2004. During each day, GSM was sampled from 8 locations in Row A and Row B as shown in Figure 8. GSM was converted to volumetric soil moisture (VSM) by bulk density as follows:

$$VSM = GSM \times \left(\frac{\rho_B}{\rho_w} \right) \quad (1)$$

$$\rho_B = \frac{w_s}{V_s} \quad (2)$$

where ρ_w is the density of water which is $1000 \text{ kg}\cdot\text{m}^{-3}$, ρ_B is bulk density which is approximately $1530 \text{ kg}\cdot\text{m}^{-3}$ for the sandy soil, w_s is the weight of the soil, and V_s is the volume of the soil (internal diameter of the coring tool = 4.3cm). Figure A-34 shows the average VSM of Row A and B sampled during the four days.

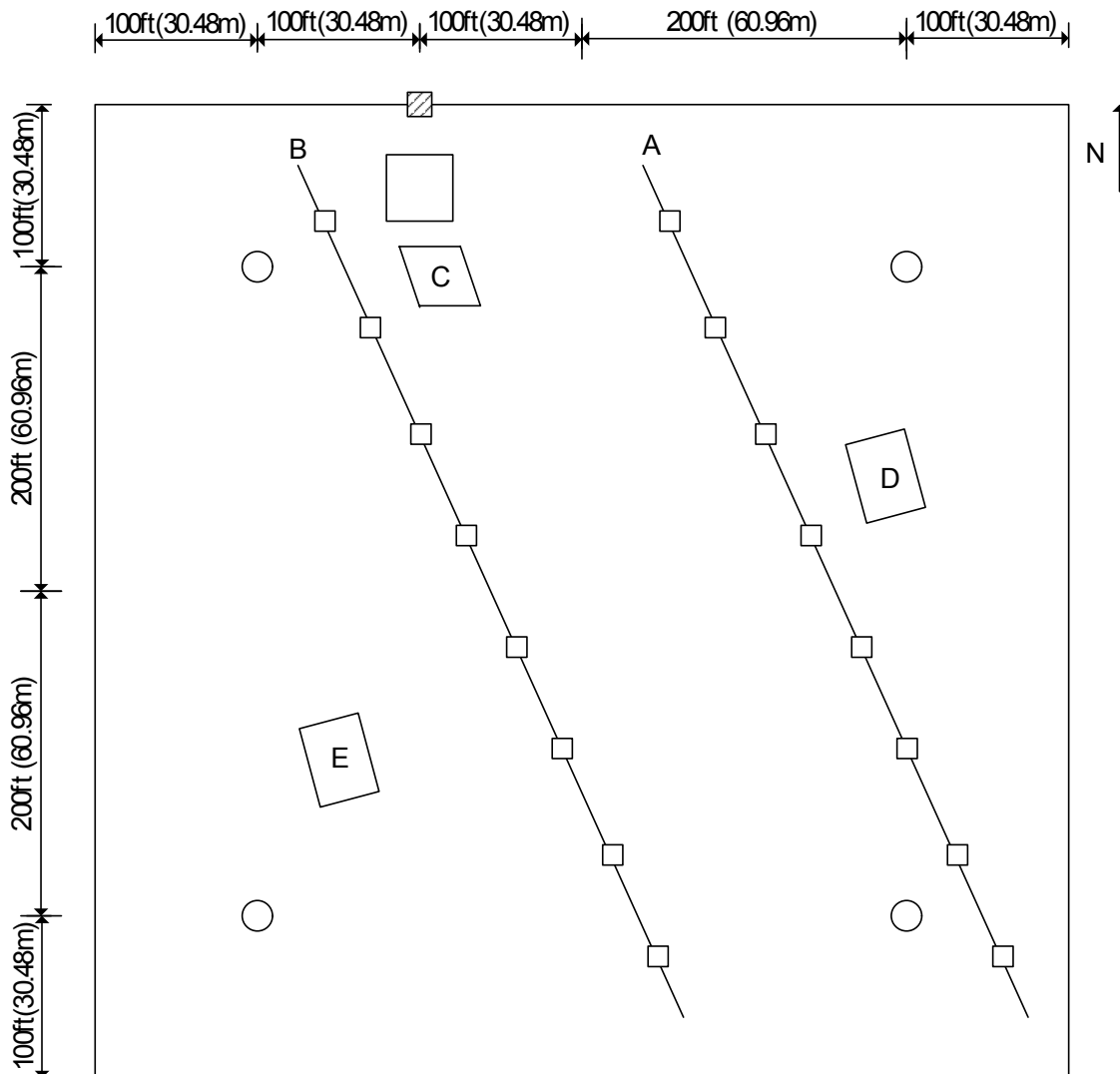


Figure 8. Layout of the soil sampling locations

5.3 Soil Temperature

A Max/Min waterproof digital thermometer from Forestry Supplier was used to measure the soil temperature at the depths of 2, 4, and 8 cm at locations A to E shown in Figure 8. An ML2 theta probe volumetric soil moisture sensor from Delta-T Devices was used to measure the soil moisture at the locations of in-row; 1/4 row; 1/2 row at the locations A to B shown in Figure 8. Figure A-35 to A-52 show soil temperature and figure A-53 to A-70 show soil moisture observed during the soil sampling.

6. VEGETATION SAMPLING

Vegetation properties such as stand density, row spacing, height, biomass, and LAI were measured bi-weekly during the field experiment. The crop density derived from the stand density and row spacing was measured during the first two sampling. The cotton seeds were planted in the fixed spacing and the germination rate is over 90% throughout the field. The bi-weekly measurements included height, width, biomass, LAI, and crop development. In the whole season, the vegetation samplings were conducted on four spatially distributed sampling locations (Figure 3) to characterize the spatial variability of vegetation properties in the study site.

6.1 Height and width

Crop height was measured by placing a measuring tape at the soil surface to average height of the crop. The width was measured in the direction of maximum width. The heights inside the vegetation sampling areas were taken for each vegetation sampling. Figure A-71 to A-72 show the crop heights and widths during MicroWEX-3.

6.2 LAI

LAI of the footprint was approximated by measuring 4 locations around the footprint bi-weekly. LAI was measured with a Li-Cor LAI-2000 in the inter-row region with 4 cross-row measurements. The LAI-2000 was set to average 4 locations into a single value so one observation was taken above the canopy and 4 beneath the canopy; in the row, 1/4 of the way across the row, 1/2 of the way across the row, and 3/4 of the way across the row. This gave a spatial average for row crops of partial cover. Figure A-73 shows the LAI observed during MicroWEX-3.

6.3 Green and Dry Biomass

Each vegetation sampling was conducted along one row. The sampling length was measured the same as during stand density measurement. The plants within this length were cut at the base and put in plastic bags to prevent losing moisture. In the laboratory, the canopy samples were separated into leaves, stems, and bolls to measure their wet weights. The vegetation samples were put into paper bags and dried in the oven at 75°C for 48 hours. Then the vegetation samples were removed from the oven and the dry weights were measured. At the time of harvest, lint yield was measured in certain area to estimate the yield of the whole field. Figure A-74 shows the wet biomass and dry biomass of different plant components observed during MicroWEX-3.

6.4 Root Sampling

Root sampling was conducted in three of the four vegetation sampling areas (Northeast, Southeast, and Southwest). The root samples were taken at five depths: 0-15 cm, 15-30 cm, 30-60 cm, 60-90 cm, and 90-120 cm. The samples were then washed and scanned to obtain the structure of the roots. Figure A-75 shows the total root lengths at different depths. Figure A-76 shows the dry root mass at different depths.

6.5 Lint Yield

The lint yield of cotton was estimated twice during MicroWEX-3. The first measurement was on DoY 356 (see Table 7) immediately after removal of sensors. The second time was on DoY 17 (see Table 8) in 2005, when harvest would have typically taken place based upon the numbers of open bolls. Harvest was

conducted in the four vegetation-sampling areas. A 20ft (6.10 m) section of a row was selected in each area. The bolls were manually collected from these marked areas and separated into open and closed bolls. Wet biomass of the bolls was measured. The samples were oven-dried at 70 degrees Celsius for 24 hours to obtain the dry biomass. The lint yield was estimated by the following equation:

$$\text{yield} = \frac{\text{dry biomass}}{\text{sampling area}} \times 0.4 \quad (3)$$

Table 7. First measurement of lint yield data on DoY 356 in 2004

			Open Bolls			Closed Bolls			Total
	distance (m)	sampling area(m ²)	bag(g)	dry(g)	yield(kg/ha.)	bag(g)	dry(g)	yield(kg/ha.)	yield(kg/ha.)
NW	7.10	5.41	55.39	368.11	231.21	55.68	643.03	434.25	665.46
NE	7.23	5.51	55.66	483.98	310.98	55.66	561.68	367.40	678.38
SW	7.06	5.38	55.27	262.24	153.89	55.31	631.65	428.53	582.42
SE	7.20	5.49	55.12	352.42	216.75	55.23	574.34	378.47	595.22
Average	7.15	5.45	55.36	366.69	228.21	55.47	602.68	402.16	630.37

Table 8. Second measurement of lint yield data on DoY 017 in 2005

			Open Bolls			Closed Bolls			Total
	distance (m)	sampling area(m ²)	bag(g)	dry(g)	yield(kg/ha.)	bag(g)	dry(g)	yield(kg/ha.)	yield(kg/ha.)
NW	7.24	5.52	54.09	524.57	341.12	54.35	197.33	103.67	444.79
NE	7.02	5.35	54.07	582.22	394.93	54.01	278.89	168.16	563.09
SW	7.09	5.40	54.20	436.85	283.31	54.08	322.26	198.56	481.87
SE	7.16	5.46	53.94	477.9	310.83	54.17	398.09	252.14	562.97
Average	7.13	5.43	54.08	505.39	332.55	54.15	299.14	180.63	513.18

7. WELL SAMPLING

7.1 Groundwater sampling

The groundwater sampling was conducted by Dr. Michael Dukes and his research team (ABE). The sampling was conducted monthly for the four wells in the field. The groundwater sampling included groundwater level measurement by water level sounder, samples for N₂ analysis. Figure A-77 shows the results of N₂ analysis.

7.2 Water level measurement

The water level was measured by the Levellogger from Solinst Canada Ltd.. The Levelloggers were installed in each well and recorded the water level every 30 minutes. Figure A-78 shows the observation of water level. The groundwater level went over the maximum volume recordable by the levellogger from DoY 276 to DoY 310, and the data during the period was filtered out.

8. FIELD LOG

Note: Time is in Eastern Standard Time.

The cotton was planted on June 21 (DoY173). Root fungus destroyed the seedlings. Cotton was re-planted on July 09 (DoY 191). The field log below was generated from July 09 (DoY191). There were three hurricanes during MicroWEX-3. The UFCMR was disconnected in order to prevent possible damages. UFCMR was overheated once during MicroWEX-3. The events and data gaps for UFCMR are listed in Table 9:

Table 9. The events and dates of data gaps for UFCMR during MicroWEX-3

Event	Hurricane Charley	Hurricane Frances	Hurricane Jeanne	Overheating
Dates	Aug. 14, DoY 227	Sep. 06, DoY 250	Sep. 26, DoY 270	Nov. 02, DoY 307
Dates of data gap	DoY 225-229	DoY 247-253	DoY 269-273	DoY 307-309

The stations of dataloggers were also disconnected to power supply during the hurricanes. The data gaps of stations of dataloggers are listed in Table 10 below:

Table 10. The events and dates of data gaps of dataloggers at Northwest, East, and Southwest stations during MicroWEX-3

Event	Hurricane Frances	Hurricane Jeanne
Dates	Sep. 06, DoY 250	Sep. 26, DoY 270
Dates of data gap	DoY 247-253	DoY 269-273

July 09 (DoY 191)

07:10	Land preparation, finished at 11:30
08:30	Planting, 09:30 to 11:50, 12:40 to 15:00

July 12 (DoY 194)

07:30	Marked the footprint of radiometer
08:00	Set up tripods for all dataloggers
09:30	Connected sensors to Northwest station (by Miller)
10:30	Connected sensors to East station (by Miller)

July 13 (DoY 195)

09:30	Set up TIR, CNR, and CSAT (by Lanni and Miller), the cal.# of CSAT is -0.206, the height of CSAT was 2.1 m.
10:30	Surface roughness measurement near footprint
	Cotton germination observed

July 14 (DoY 196)

08:30	Buried the sensors at East station
10:30	Measurement of the height of CNR(2.66m), TIR(2.5m)

July 19 (DoY 201)

07:30	Set up raingauges at the east and west edge of field
10:30	The #2 thermistor (at 8cm) at Northwest station was not working due to broken cable, fixed on DoY 202

July 20 (DoY 202)

07:40	Changed the height of CSAT to 1.2 m
09:30	Set up tripod at Southwest station
10:00	Hand-planted in the footprint (done by 10:40)
10:30	Replaced #2 thermistor (at 8cm) at Northwest station (by Miller)

July 21 (DoY 203)

07:40	Changed desiccant in radiometer; Sky calibration: absorber temperature = 32.85° C(306K)
-------	---

July 22 (DoY 204)

08:40	Found TDR cable of 1.2m depth at the East station and connected it to the datalogger
11:00	Program bug found on East station, fixed by 13:30 (by Miller)

July 23 (DoY 205)

07:15	Found TDR cable of 1.7m depth at the Northwest station and connected to the datalogger; the initial reading for volumetric soil moisture was 40%
-------	--

July 26 (DoY 208)

07:20	Hand-plant in the sensor area of Northwest station, the area around tripods of Northwest and CSAT station
10:30	Checked TDR at 1.7m at Northwest station: reading = 32%

July 27 (DoY 209)

09:15	Marked the soil sampling rows and points
10:15	Marked the soil sampling point near the area of sensors at East and Northwest station
11:30	Hand-planted in area of sensor and the tripod of East station
13:00	Marked vegetation sampling area (13 rows × 66 feet)

July 29 (DoY 211)

12:20	Soil sampling
13:40	Vegetation sampling
15:00	Changed the battery of CSAT

August 02 (DoY 215)

07:30	Observed the area of hand-planted, cotton had germinated
-------	--

August 05 (DoY 218)

12:40	Soil sampling
13:30	Well sampling
14:00	The angle of radiometer was changed to 55.2° (until 14:30), Lin accidentally touched the controller

August 09 (DoY 222)

08:05	Changed desiccant in radiometer; Sky calibration: absorber temperature = 30.30° (303.45K)
-------	---

August 11 (DoY 224)

07:30	Connected sensors to Southwest station, done by 14:45 (by Miller)
07:30	Buried sensors at Southwest station (by Lin)
15:00	Connected soil heat flux sensor to CSAT station (by Miller)

August 12 (DoY 225)

08:00	Soil sampling
11:30	Shut down radiometer (preparation of Hurricane Charley)

August 13 (DoY 226)

07:30	Connected soil heat flux sensor to Southwest station, done by 7:50
08:00	Uploaded new program to Southwest station

August 16 (DoY 229)

08:00	Turned on the radiometer power on
08:30	Replaced battery of CSAT
09:00	Modified the program of Southwest station; find #1 thermistor (at 2cm) not working, fixed on DoY 232
09:30	Started the radiometer to take reading

August 19 (DoY 232)

13:00	Replaced KH ₂ O with the one from Dr. Jacobs (by Miller), the cal.# is -0.185
13:30	Soil sampling
14:30	Vegetation sampling
15:00	Modified the program at Northwest station (by Tien)

August 20 (DoY 233)

08:30	Connected thermistors #3~#8 (for canopy temperature, at 4cm, 10cm, 20cm, 50cm, 75cm, and 90cm) at Northwest station, done by 10:00
10:00	Found #4 thermo-couple (at 120 cm) at Northwest station not working, fixed at DoY 234
10:30	LAI measurement
12:00	Program bug found at Northwest station (by Miller)

August 21 (DoY 234)

06:20	Uploaded the new program at Northwest station to fix the problem of #4 thermo-couple
	Cotton square observed

August 24 (DoY 237)

08:00	Soil sampling
-------	---------------

August 26 (DoY 239)

07:45	Change desiccant in radiometer; Sky calibration: absorber temperature = 29.57° (302.72K)
10:00	Replace battery of CSAT
10:30	Set up thermistors #3 to #8 for canopy temperatures at Northwest station

August 31 (DoY 244)

10:30	Soil sampling
13:00	Well sampling

September 02 (DoY 246)

07:30	Vegetation sampling and LAI measurement
10:30	Changed the height of CSAT to 2.25 meters

September 03 (DoY 247)

08:00	Disconnected CSAT and KH2O, store in Room #5 in preparation of Hurricane Frances
08:30	Disconnected radiometer, brought back to CRS
09:00	Disconnected power supply of Northwest station from trailer; disconnect the batteries from all stations

September 08 (DoY 252)

13:00	Connected the batteries to all the station and uploaded the program to all stations
-------	---

September 09 (DoY 253)

08:00	Set up radiometer
09:30	Connected CSAT and KH2O
10:30	Gravimetric soil sampling (by Casanova)
11:00	Sky calibration: absorber temperature = 29.79° (302.94K)
	50% Flowering

September 11 (DoY 255)

06:30	Checked the angle that CSAT is facing (232° from north), and change it to 220° from north
07:45	Found the battery of CSAT was low voltage; the system stopped logging data from Sep. 10(DoY 254) 22:45; replaced battery; data collection resumed at 08:00

September 14 (DoY 258)

07:30	Soil sampling and gravimetric soil moisture sampling
08:30	Downloaded data from Hobologger

	Observed 70% to 80% of cotton with flower
--	---

September 15 (DoY 259)

07:30	Replaced the KH2O with the one of CRS (disconnected the one from Dr. Jacobs and stored in Room#5), the cal.# is -0.206
-------	--

September 16 (DoY 260)

07:30	Vegetation sampling and LAI measurement
09:00	Found the battery of CSAT was low voltage; the system stopped logging data from Sep. 16(DoY 260) 06:00; replace battery, data collection resumed at 10:30

September 18 (DoY 262)

08:00	Found the battery of Northwest station was low voltage; the system stopped logging data from Sep. 17(DoY 261) 00:45; connected the power cable; data collection resumed at 09:00
-------	---

September 20 (DoY 264)

13:30	Replaced battery of CSAT
-------	--------------------------

September 23 (DoY 267)

07:30	Soil sampling and gravimetric soil moisture sampling
09:00	Conducted Cropscan in northeast vegetation sampling area
10:00	Checked the battery of CSAT (12.8 volt)

September 25 (DoY 269)

06:30	Found the battery of CSAT was low voltage; the system stopped logging data from Sep. 24 (DoY 268) 16:30; replace battery
08:00	Shut down radiometer in preparation of Hurricane Jeanne
10:30	Disconnected all batteries from all stations; disconnect all power supply cable
12:00	Disconnected radiometer and brought back to CRS
12:30	Disconnected KH2O and CSAT and stored in Room #5 at Pine Acres

September 28 (DoY 272)

07:00	Connected all batteries to the stations and reload the programs
08:00	Soil sampling
09:00	Connected CSAT and KH2O
	Observed 10% to 15% of cotton with bolls
	The radiometer could not be started because the booting sequence of radiometer and laptop was mistaken

September 29 (DoY 273)

13:00	Changed desiccant in radiometer and reboot radiometer
13:30	Sky calibration: absorber temperature = 33.4° (306.55K)

14:15	Staredt the radiometer to log data
15:00	Replace dbattery of CSAT

September 30 (DoY 274)

07:30	Vegetation sampling and LAI measurement
-------	---

October 01 (DoY 275)

14:50	Well sampling
-------	---------------

October 02 (DoY 276)

08:30	Replaced battery of CSAT
	The groundwater level went over the range of the levellogger. Data filtered

October 07 (DoY 281)

08:00	Soil sampling
	Observed 35% to 45% of cotton with bolls

October 09 (DoY 283)

08:30	Found the power supply pole broken due to vehicle operation; took pictures; verified the power supply is working
-------	---

October 12 (DoY 286)

09:30	Vegetation sampling and LAI measurement
-------	---

October 14 (DoY 288)

07:15	Soil sampling
08:30	Conducted Cropscan in northeast and northwest vegetation sampling area
	Observed 50% of cotton with bolls

October 19 (DoY 293)

09:30	Sky calibration: absorber temperature = 30.66° (303.81K)
-------	--

October 21 (DoY 295)

07:30	Soil sampling
08:00	Modified the program of Southwest station and added a reference temperature sensor (by Miller)

October 23 (DoY 297)

06:30	Replaced battery of CSAT
08:00	Downloaded data from Hobologger

October 26 (DoY 300)

09:30	Vegetation sampling and LAI measurement
	Observed open bolls from the cotton that first planted on June 21 (DoY 173)

October 28 (DoY 302)

07:30	Soil sampling
-------	---------------

October 29 (DoY 303)

12:30	Well sampling
-------	---------------

November 04 (DoY 309)

08:30	Radiometer overheated; stopped logging from November 02 (DoY 307) 16:49 due to debris in the cooling fan; Cleaned the cooling fan and restarted the radiometer
10:00	Soil sampling
11:00	Conducted Cropscan in northeast vegetation sampling area
12:00	Changed the cable length of well levelloggers

November 06 (DoY 311)

08:45	Sky calibration: absorber temperature = 21.91° (295.06K)
09:30	Root sampling
11:00	Checked the reading of well levelloggers

November 09 (DoY 314)

09:30	Vegetation sampling and LAI measurement
11:30	LAI measurement at four edges of footprint
	Observed 5% to 10% of cotton with open bolls

November 11 (DoY 316)

09:00	Soil sampling
-------	---------------

November 13 (DoY 318)

09:00	Found the cooling fan of radiometer not working; clean the fan
-------	--

November 16 (DoY 321)

09:00	LAI measurement at four edges of footprint
09:30	Conducted Sunscan (by Lanni and Lin); enter footprint from 09:30 to 10:00
11:00	Conducted Cropscan in northeast vegetation sampling area

November 18 (DoY 323)

08:40	Soil sampling
10:00	Replaced battery of CSAT

November 20 (DoY 325)

	Observed 15% to 20% of cotton with open bolls
--	---

November 23 (DoY 328)

08:40	Vegetation sampling and LAI and Sunscan measurement
-------	---

10:30	LAI measurement at four edges of footprint
-------	--

November 25 (DoY 330)

09:00	Sky calibration: absorber temperature = 21.53° (294.68K)
09:30	V _{offset} measurement: -0.791 Volt

November 28 (DoY 333)

09:00	Soil sampling
	Observed 30% to 35% of cotton with open bolls

November 30 (DoY 335)

10:20	LAI measurement at four edges of footprint
	Observed 35% to 40% of cotton with open bolls

December 01 (DoY 336)

13:30	Well sampling
	Observed 40% to 45% of cotton with open bolls

December 04 (DoY 339)

09:40	Gravimetric soil moisture sampling
10:30	Checked the cable length of well leveloggers
	Observed 50% of cotton with open bolls

December 07 (DoY 342)

10:30	Defoliator applied (by PSREU staff)
-------	-------------------------------------

December 10 (DoY 345)

10:30	Soil sampling
11:00	Cleared the cooling fan of radiometer
11:30	Soil moisture measurement around TDR sensors by theta probe

December 11 (DoY 346)

09:30	Vegetation sampling
10:30	Soil moisture measurement around TDR sensors by theta probe
11:00	Conducted Cropscan in northeast and northwest vegetation sampling area

December 13 (DoY 348)

10:17	Shut down the Southwest station
10:30	Removed sensor of Southwest station and store in Room #5

December 15 (DoY 350)

12:02	Shut down the East Station
12:20	Removed sensor of East station and store in Room #5

<i>13:00</i>	Removed TDR at 1.7m at Northwest station; conducted gravimetric soil moisture sampling at: 0.0m, 0.6m, 1.2m, 1.7m
<i>14:00</i>	LAI measurement at vegetation sampling areas and footprint

December 16 (DoY 351)

<i>10:00</i>	Shut down the Northwest Station
<i>10:20</i>	Removed sensor of Northwest station and stored in Room #5
<i>12:00</i>	Cleared dead leaves in footprint

December 18 (DoY 353)

<i>15:30</i>	Cut off leaves on cotton in footprint
--------------	---------------------------------------

December 20 (DoY 355)

<i>12:10</i>	Harvested in the footprint; weighed the bolls that were not open; measured the lint yield
--------------	---

December 21 (DoY 356)

<i>10:00</i>	Shut down CSAT
<i>10:30</i>	Sky calibration: absorber temperature = 16.90° (290.05K)
<i>11:20</i>	Disconnected radiometer and brought back to CRS
<i>12:20</i>	Harvested the specified areas in the four vegetation sampling areas; weighed the bolls that were not open; measured the lint yield (630.37 kg/ha.)
<i>14:00</i>	Downloaded data from well leveloggers; restarted the leveloggers at December 22 (DoY 357) 00:00

January 17 (DoY 017 in 2005)

<i>08:00</i>	Repeated yield measurement (513.18 kg/ha.)
--------------	---

ACKNOWLEDGEMENT

The authors would like to acknowledge Mr. James Boyer and his team at the PSREU, Citra, Florida for excellent field management. We also thank Dr. Wendy Graham, Dr. James Jones, and Dr. Jennifer Jacobs for their scientific advice in experimental design. MicroWEX-3 was supported by grant from the Earth Science Directorate of the NSF (Grant number: EAR-0337277).

REFERENCES

- Campbell Scientific, *CSAT3 Three Dimensional Sonic Anemometer Instruction Manual*, Campbell Scientific Inc., Logan, UT, 1998.
- Campbell Scientific, *HFT3 soil heat flux plate instruction manual*, Campbell Scientific Inc., Logan, UT, 2003.
- Campbell Scientific, *CNR1 Net Radiometer Instruction Manual*, Campbell Scientific Inc., Logan, UT, 2004a.
- Campbell Scientific, *CS615 and CS625 water content reflectometers instruction manual*, Campbell Scientific Inc., Logan, UT, 2004b.
- Everest Interscience, *Model 4000.3ZL Infrared Temperature Sensor*, Everest Interscience Inc., Tucson, AZ, 2005.
- J. C. Kaimal and J. J. Finnigan, *Atmospheric Boundary Layer Flows*, Oxford University Press, New York, NY, 1994.
- R. D. De Roo, *University of Florida C-band Radiometer Summary*, Space Physics Research Laboratory, University of Michigan, Ann Arbor, MI, March, 2002.
- R. D. D Roo, *TMR-3 Radiometer Tuning Procedures*, Space Physics Research Laboratory, University of Michigan, Ann Arbor, MI, March, 2003.
- P. Schotanus, F. T. M. Nieuwstadt, and H. A. R. DeBruin, "Temperature measurement with a sonic anemometer and its application to heat and moisture fluctuations," *Bound.-Layer Meteorol.*, vol. 26, pp. 81-93, 1983.
- A. van Dijk, W. Kohsiek, and H. A. R. DeBruin, "Oxygen sensitivity of krypton and Lyman-alpha hygrometer," *J. Atmos. Ocean. Tech.*, vol. 20, pp. 143-151., 2003.
- A. van Dijk, A. F. Moene, and H. A. R. DeBurin, *The Principles of Surface Flux Physics: Theory, Practice, and Description of the ECPACK Library*, <http://www.met.wau.nl/projects/jep/>, 2004.
- E. K. Webb, G. I. Pearman, and R. Leuning, "Correction of flux measurements for density effects due to heat and water vapor transfer," *Quart. J. Roy. Meteorol., Soc.*, vol. 106, pp. 85-100, 1980.
- J. M. Wilczak, S. P. Oncley, and S. A. Stage, "Sonic anemometer tilt correction algorithms," *Bound.-Layer Meteorol.*, vol. 99, pp. 127-150, 2001.

A. FIELD OBSERVATIONS

Figure Captions

Figure A-1. Brightness temperatures at vertical and horizontal polarizations	28
Figure A-2. Latent (LE) and sensible (H) heat fluxes	28
Figure A-3. Down- and up-welling solar radiation	29
Figure A-4. Down- and up-welling far infrared radiation	29
Figure A-5. Total net radiation	30
Figure A-6. Surface temperature	30
Figure A-7. Soil temperature at depth of: 2cm, 4cm Hydra probe, 8cm at Northwest station	31
Figure A-8. Soil temperature at depth of: 16cm, 32cm at Northwest station	31
Figure A-9. Soil temperature at depth of: 64cm, 120cm at Northwest station	32
Figure A-10. Soil temperature at depth of: 2cm, 4cm Hydra probe, 8cm at East station	32
Figure A-11. Soil temperature at depth of: 16cm, 32cm at East station	33
Figure A-12. Soil temperature at depth of: 64cm, 120cm at East station	33
Figure A-13. Soil temperature at depth of: 2cm, 4cm Hydra probe, 4cm at Southwest station.....	34
Figure A-14. Soil temperature at depth of: 8cm, 16cm, 32cm at Southwest station	34
Figure A-15. Soil temperature at depth of: 64cm, 120cm at Southwest station	35
Figure A-16. VSM at depth of: two measurements at 2cm and 4cm at Northwest station	35
Figure A-17. VSM at depth of: 4cm Hydra probe, 8cm, 16cm at Northwest station	36
Figure A-18. VSM at depth of: 32cm, 64cm, 120cm at Northwest station	36
Figure A-19. VSM at depth of: 1.7m near Northwest monitoring well at Northwest station	37
Figure A-20. VSM at depth of: 2cm, 2cm replicate, and 4cm at East station	37
Figure A-21. VSM at depth of: 4cm Hydra probe, 8cm, 16cm at East station	38
Figure A-22. VSM at depth of: 32cm, 64cm, 120cm at East station	38
Figure A-23. VSM at depth of: 2cm, 2cm replicate, and 4cm at Southwest station	39
Figure A-24. VSM at depth of: 4cm Hydra probe, 8cm, 16cm at Southwest station	39
Figure A-25. VSM at depth of: 32cm, 64cm, 120cm at Southwest station	40
Figure A-26. Soil heat flux at depth of: 2cm, 5cm at Northwest station	40
Figure A-27. Soil heat flux at depth of: 5cm at CSAT station	41
Figure A-28. Soil heat flux at depth of: 5cm at East station	41
Figure A-29. Soil heat flux at depth of: 5cm at Southwest station	42
Figure A-30. Rainfall from the raingauge at the east and west edge of footprint	42
Figure A-31. Rainfall from the raingauge at the east and west edge of the field	43
Figure A-32. Canopy temperature at 4 cm, 10 cm, 20 cm	43
Figure A-33. Canopy temperature at 50 cm, 75 cm, and 90 cm	44
Figure A-34. VSM at specific sampling points	44

Figure A-35. Soil temperature at depths of 2, 4, and 8cm (left to right) for each designated sampling point, July 29, 2004 (DoY 211)	45
Figure A-36. Soil temperature at depths of 2, 4, and 8cm (left to right) for each designated sampling point, Aug. 05, 2004 (DoY 218)	46
Figure A-37. Soil temperature at depths of 2, 4, and 8cm (left to right) for each designated sampling point, Aug. 12, 2004 (DoY 225)	47
Figure A-38. Soil temperature at depths of 2, 4, and 8cm (left to right) for each designated sampling point, Aug. 19, 2004 (DoY 232)	48
Figure A-39. Soil temperature at depths of 2, 4, and 8cm (left to right) for each designated sampling point, Aug. 24, 2004 (DoY 237)	49
Figure A-40. Soil temperature at depths of 2, 4, and 8cm (left to right) for each designated sampling point, Aug. 31, 2004 (DoY 244)	50
Figure A-41. Soil temperature at depths of 2, 4, and 8cm (left to right) for each designated sampling point, Sep. 14, 2004 (DoY 258)	51
Figure A-42. Soil temperature at depths of 2, 4, and 8cm (left to right) for each designated sampling point, Sep. 23, 2004 (DoY 267)	52
Figure A-43. Soil temperature at depths of 2, 4, and 8cm (left to right) for each designated sampling point, Sep. 28, 2004 (DoY 272)	53
Figure A-44. Soil temperature at depths of 2, 4, and 8cm (left to right) for each designated sampling point, Oct. 07, 2004 (DoY 281)	54
Figure A-45. Soil temperature at depths of 2, 4, and 8cm (left to right) for each designated sampling point, Oct. 14, 2004 (DoY 288)	55
Figure A-46. Soil temperature at depths of 2, 4, and 8cm (left to right) for each designated sampling point, Oct. 21, 2004 (DoY 295)	56
Figure A-47. Soil temperature at depths of 2, 4, and 8cm (left to right) for each designated sampling point, Oct. 28, 2004 (DoY 302)	57
Figure A-48. Soil temperature at depths of 2, 4, and 8cm (left to right) for each designated sampling point, Nov. 04, 2004 (DoY 309)	58
Figure A-49. Soil temperature at depths of 2, 4, and 8cm (left to right) for each designated sampling point, Nov. 11, 2004 (DoY 316)	59
Figure A-50. Soil temperature at depths of 2, 4, and 8cm (left to right) for each designated sampling point, Nov. 18, 2004 (DoY 323)	60
Figure A-51. Soil temperature at depths of 2, 4, and 8cm (left to right) for each designated sampling point, Nov. 28, 2004 (DoY 333)	61
Figure A-52. Soil temperature at depths of 2, 4, and 8cm (left to right) for each designated sampling point, Dec. 10, 2004 (DoY 345)	62

Figure A-53. Soil moisture at in-row; 1/4 row; 1/2 row (left to right) for each designated sampling point, July 29, 2004 (DoY 211)	63
Figure A-54. Soil moisture at in-row; 1/4 row; 1/2 row (left to right) for each designated sampling point, Aug. 05, 2004 (DoY 218)	64
Figure A-55. Soil moisture at in-row; 1/4 row; 1/2 row (left to right) for each designated sampling point, Aug. 12, 2004 (DoY 225)	65
Figure A-56. Soil moisture at in-row; 1/4 row; 1/2 row (left to right) for each designated sampling point, Aug. 19, 2004 (DoY 232)	66
Figure A-57. Soil moisture at in-row; 1/4 row; 1/2 row (left to right) for each designated sampling point, Aug. 24, 2004 (DoY 237)	67
Figure A-58. Soil moisture at in-row; 1/4 row; 1/2 row (left to right) for each designated sampling point, Aug. 31, 2004 (DoY 244)	68
Figure A-59. Soil moisture at in-row; 1/4 row; 1/2 row (left to right) for each designated sampling point, Sep. 14, 2004 (DoY 258)	69
Figure A-60. Soil moisture at in-row; 1/4 row; 1/2 row (left to right) for each designated sampling point, Sep. 23, 2004 (DoY 267)	70
Figure A-61. Soil moisture at in-row; 1/4 row; 1/2 row (left to right) for each designated sampling point, Sep. 28, 2004 (DoY 272)	71
Figure A-62. Soil moisture at in-row; 1/4 row; 1/2 row (left to right) for each designated sampling point, Oct. 07, 2004 (DoY 281)	72
Figure A-63. Soil moisture at in-row; 1/4 row; 1/2 row (left to right) for each designated sampling point, Oct. 14, 2004 (DoY 288)	73
Figure A-64. Soil moisture at in-row; 1/4 row; 1/2 row (left to right) for each designated sampling point, Oct. 21, 2004 (DoY 295)	74
Figure A-65. Soil moisture at in-row; 1/4 row; 1/2 row (left to right) for each designated sampling point, Oct. 28, 2004 (DoY 302)	75
Figure A-66. Soil moisture at in-row; 1/4 row; 1/2 row (left to right) for each designated sampling point, Nov. 04, 2004 (DoY 309)	76
Figure A-67. Soil moisture at in-row; 1/4 row; 1/2 row (left to right) for each designated sampling point, Nov. 11, 2004 (DoY 316)	77
Figure A-68. Soil moisture at in-row; 1/4 row; 1/2 row (left to right) for each designated sampling point, Nov. 18, 2004 (DoY 323)	78
Figure A-69. Soil moisture at in-row; 1/4 row; 1/2 row (left to right) for each designated sampling point, Nov. 28, 2004 (DoY 333)	79
Figure A-70. Soil moisture at in-row; 1/4 row; 1/2 row (left to right) for each designated sampling point, Dec. 10, 2004 (DoY 345)	80

Figure A-71. Average crop heights at vegetation sampling areas	81
Figure A-72. Average crop widths at vegetation sampling areas	82
Figure A-73. LAI at vegetation sampling areas	83
Figure A-74. Wet biomass and dry biomass at vegetation sampling areas	84
Figure A-75. Total root length at different depths at each vegetation sampling area	85
Figure A-76. Dry root mass at different depths at each vegetation sampling area	86
Figure A-77. NO ₄ concentration at the monitoring wells	87
Figure A-78. Ground water level below surface and ground water level above sea level	88
Figure A-79. Surface roughness at the east side of the footprint: along the row	89
Figure A-80. Surface roughness at the east side of the footprint: across the row	89
Figure A-81. Surface roughness at the south side of the footprint: along the row	90
Figure A-82. Surface roughness at the south side of the footprint: across the row	90
Figure A-83. Surface roughness at the west side of the footprint: along the row	91
Figure A-84. Surface roughness at the west side of the footprint: across the row	91

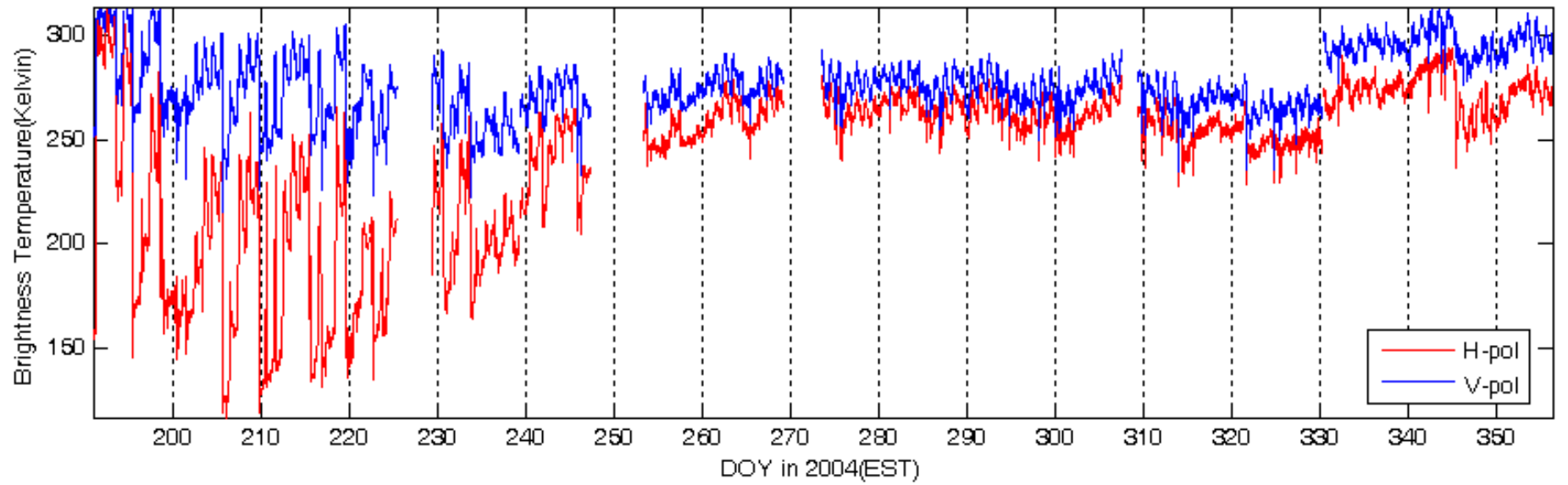


Figure A-1. Brightness temperatures at vertically and horizontally polarizations

28

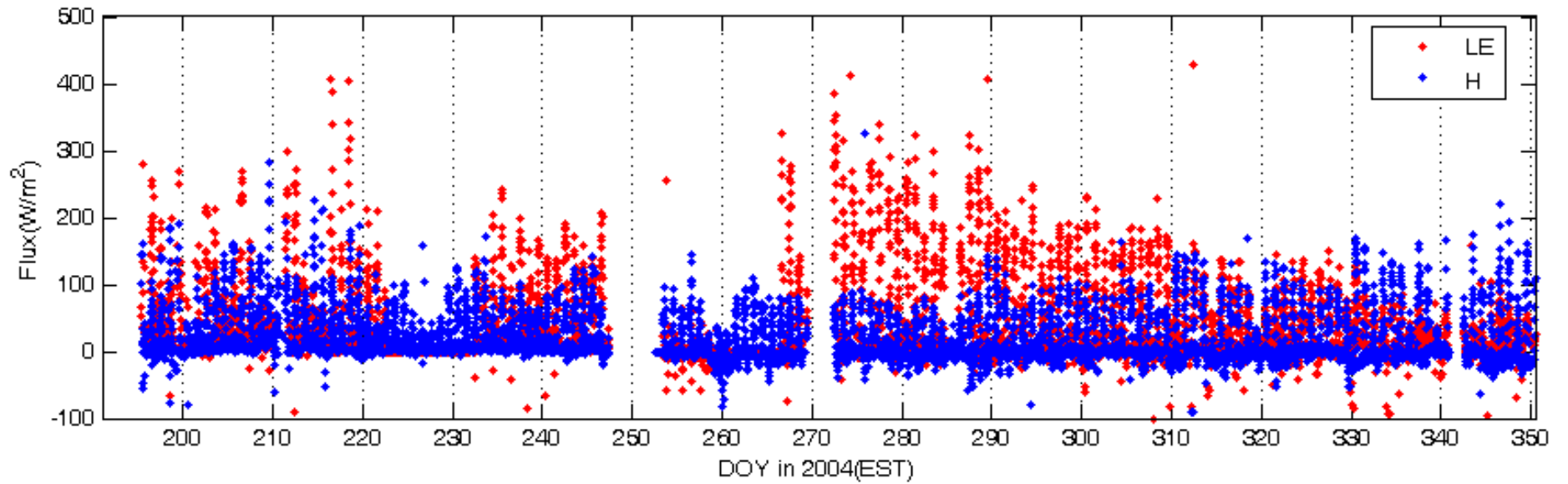


Figure A-2 Latent (LE) and sensible (H) heat fluxes

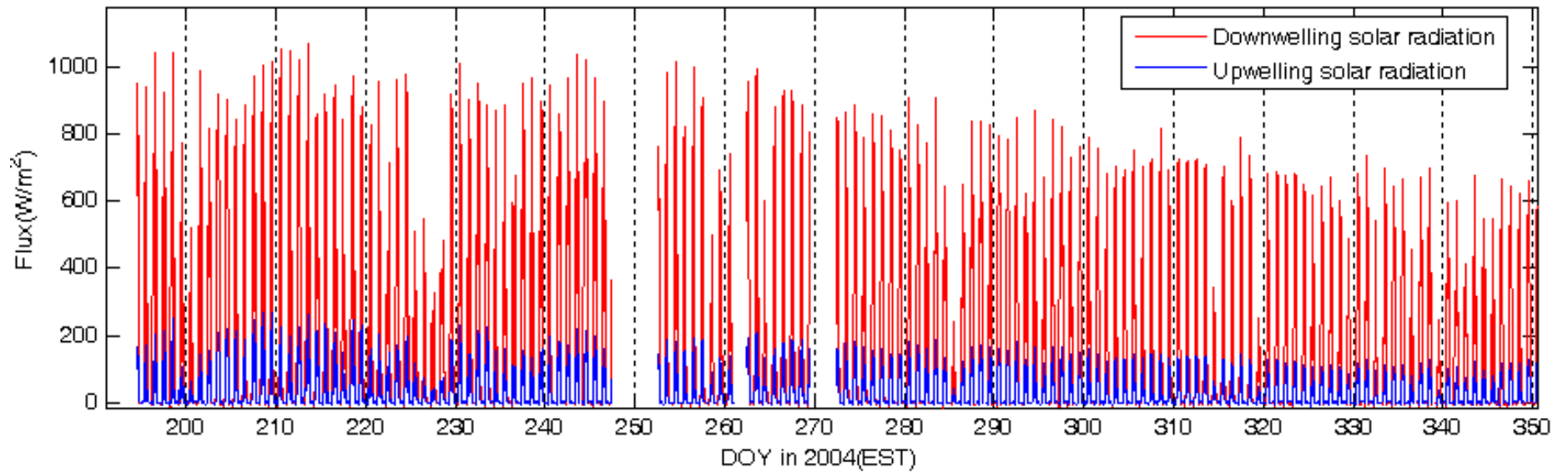


Figure A-3. Down- and up-welling solar radiation

29

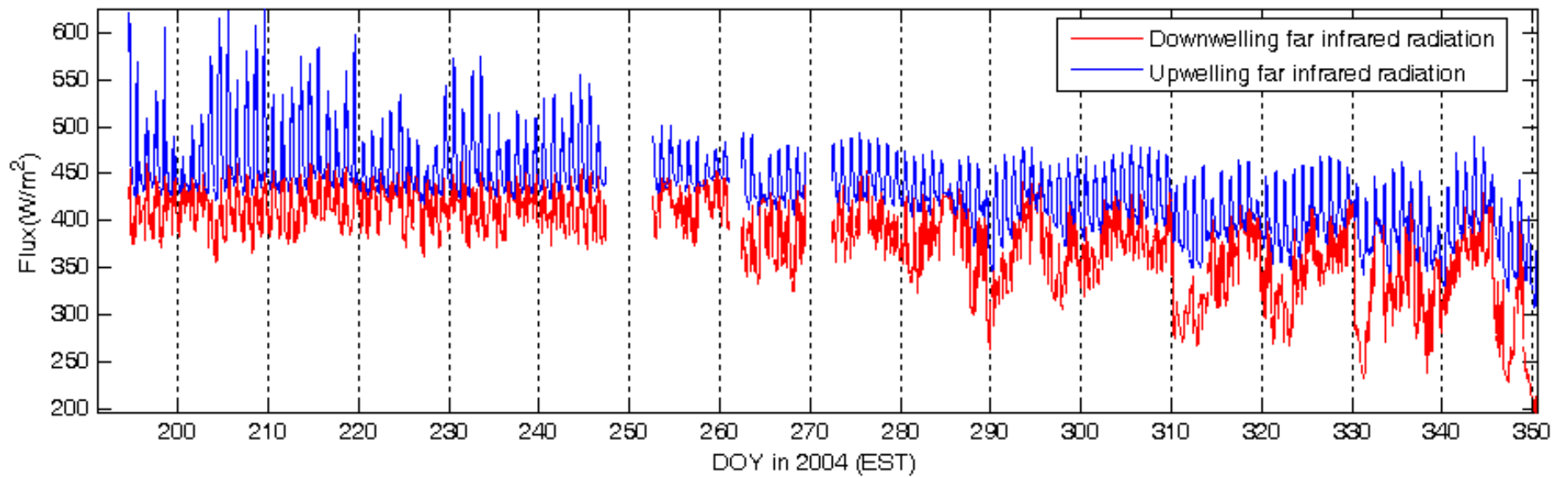


Figure A-4. Down- and up-welling far infrared radiation

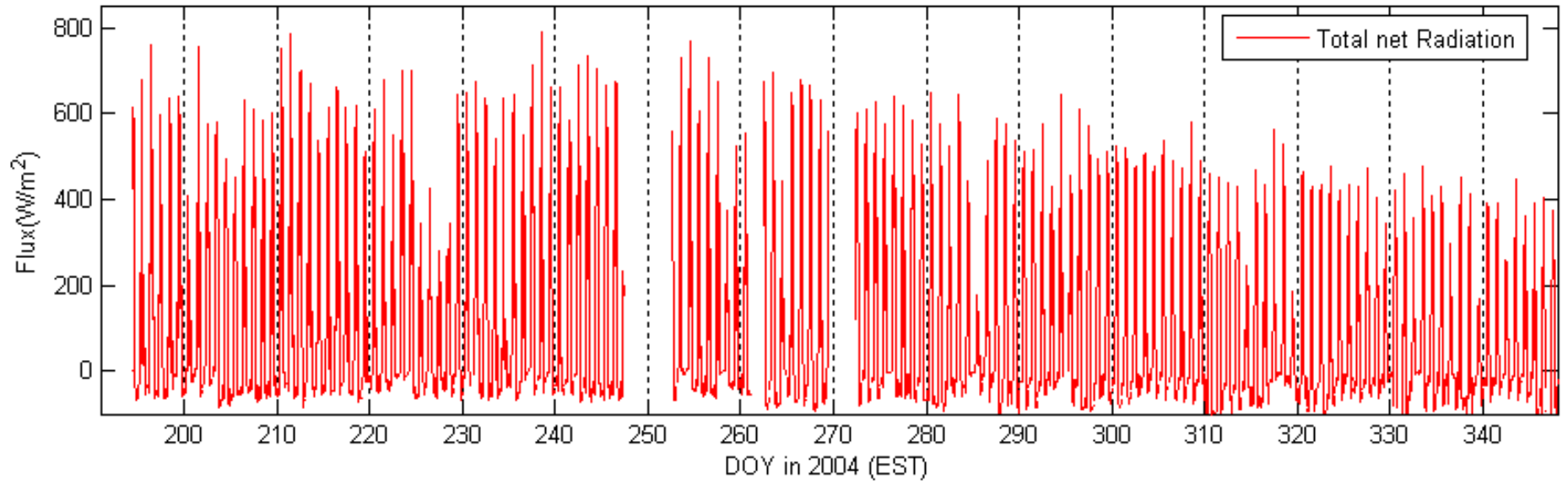


Figure A-5. Total net radiation

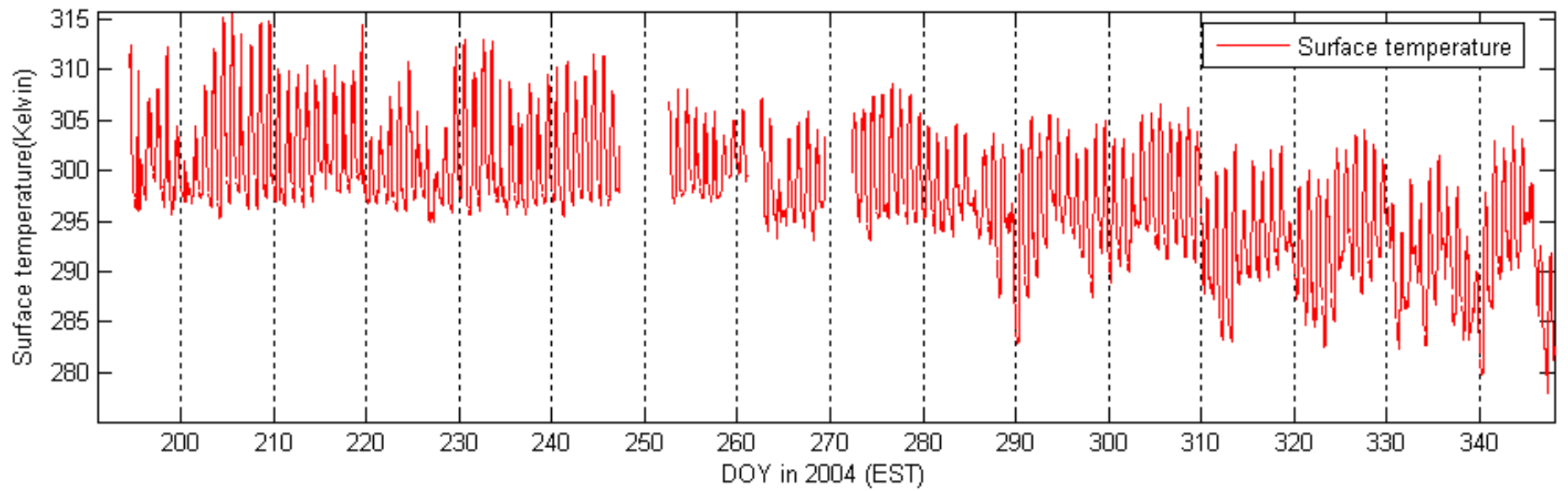


Figure A-6. Surface temperature

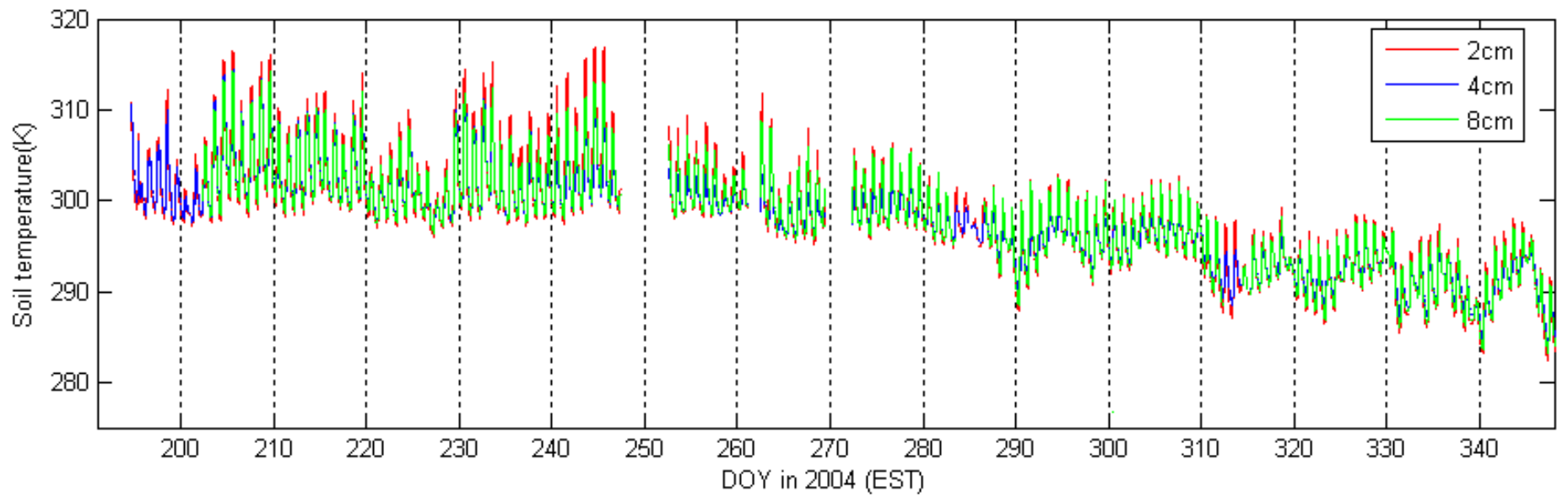


Figure A-7. Soil temperature at depth of: 2cm, 4cm Hydra probe, 8cm at Northwest station

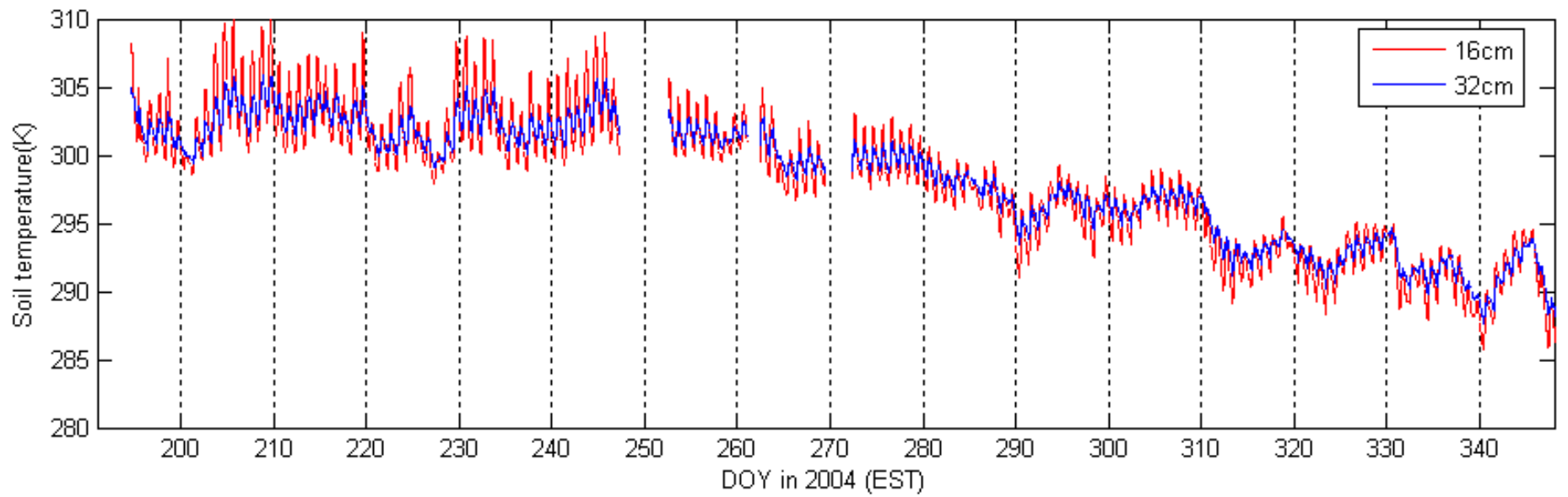


Figure A-8. Soil temperature at depth of: 16cm, 32cm at Northwest station

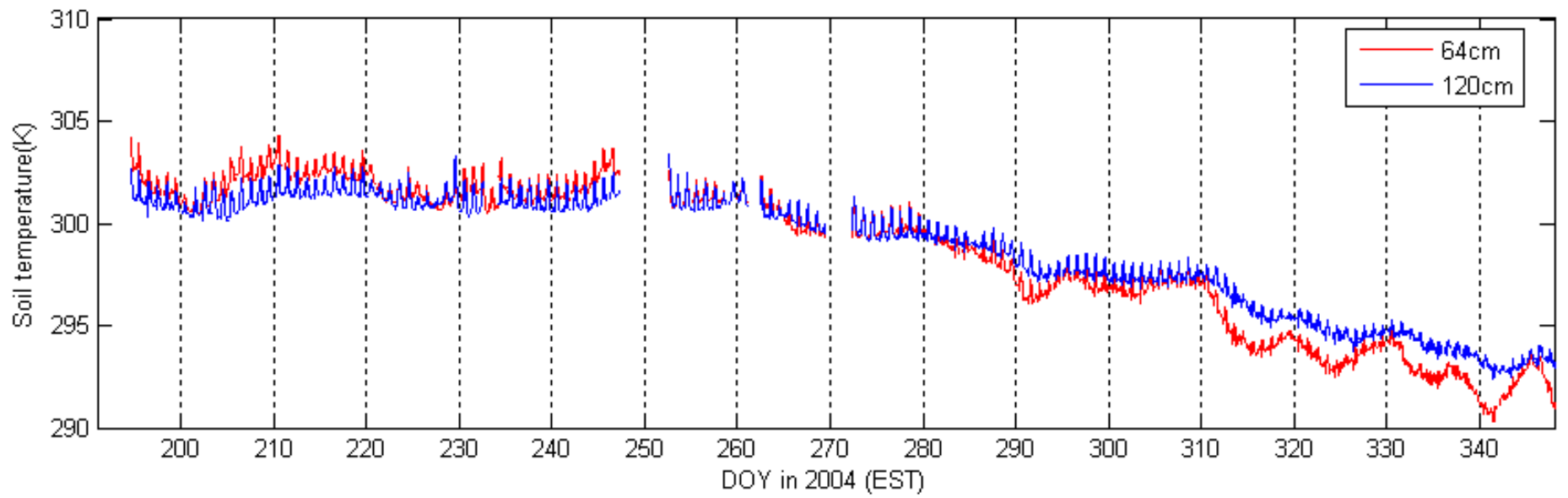


Figure A-9. Soil temperature at depth of: 64cm, 120cm at Northwest station

32

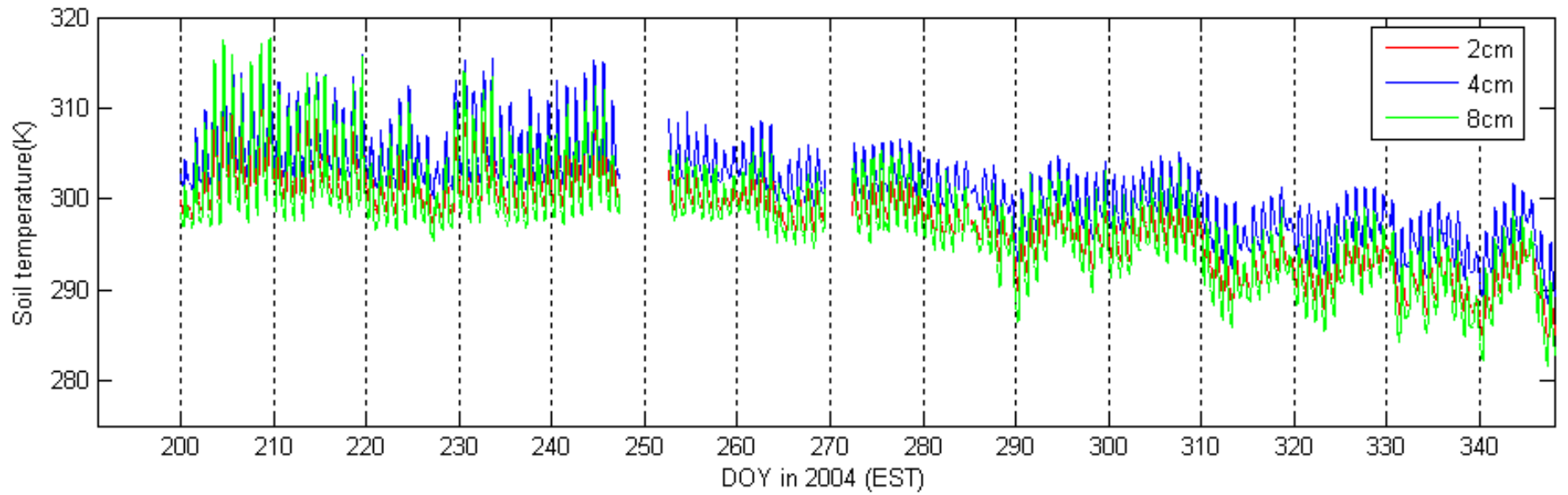


Figure A-10. Soil temperature at depth of: 2cm, 4cm Hydra probe, 8cm at East station

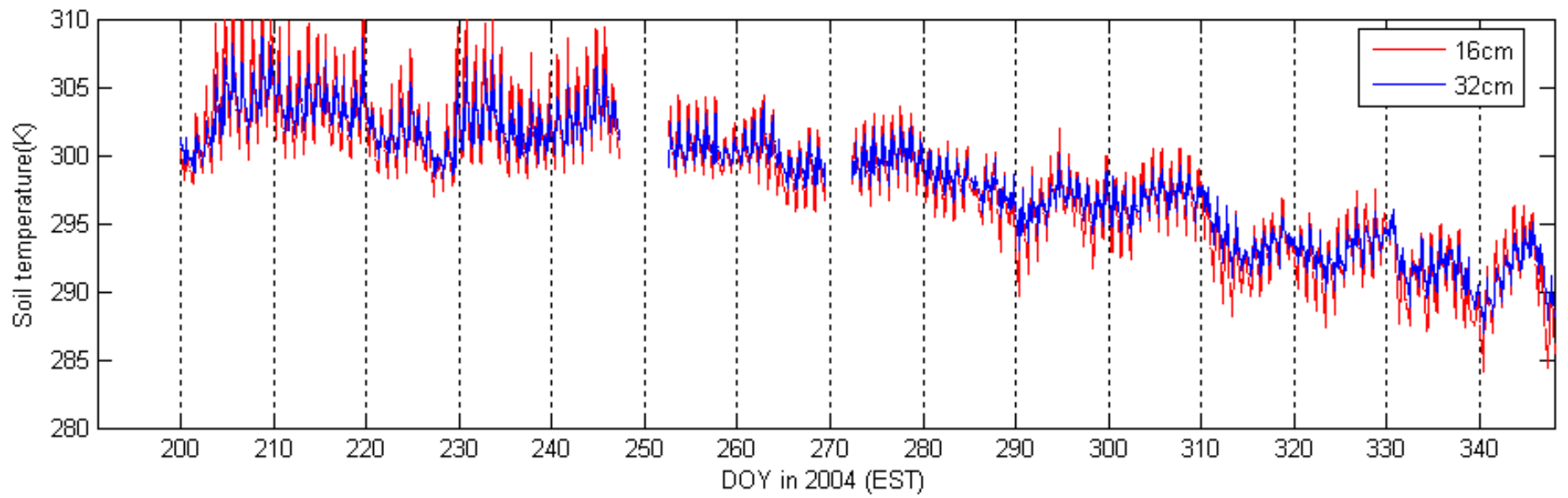


Figure A-11. Soil temperature at depth of: 16cm, 32cm at East station

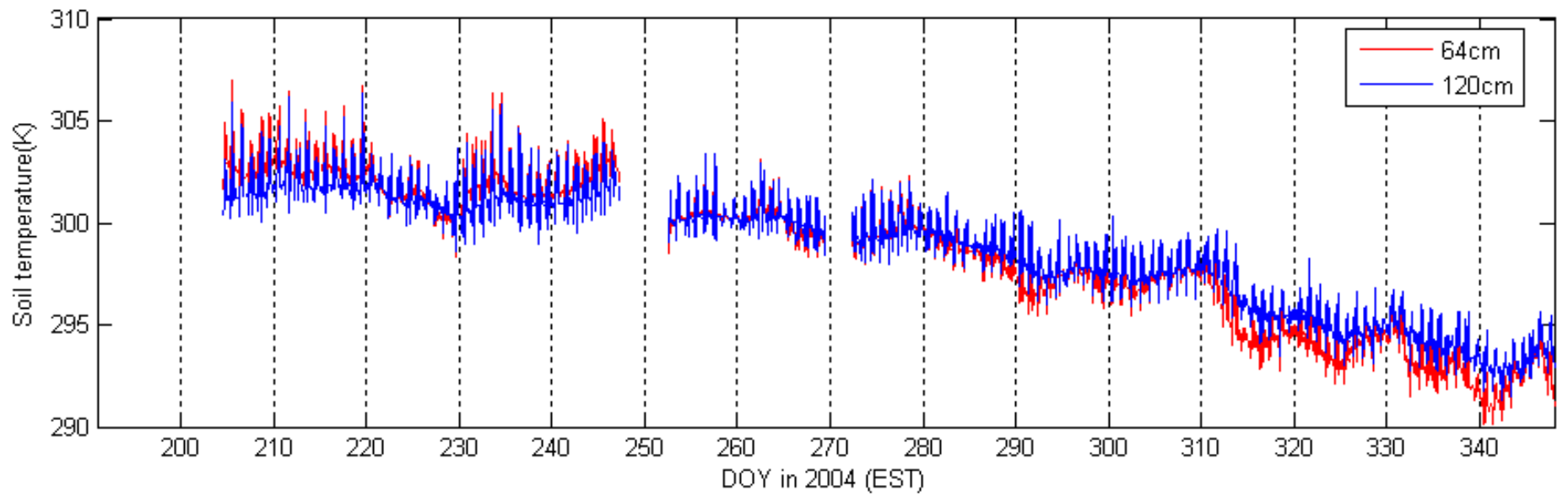


Figure A-12. Soil temperature at depth of: 64cm, 120cm at East station

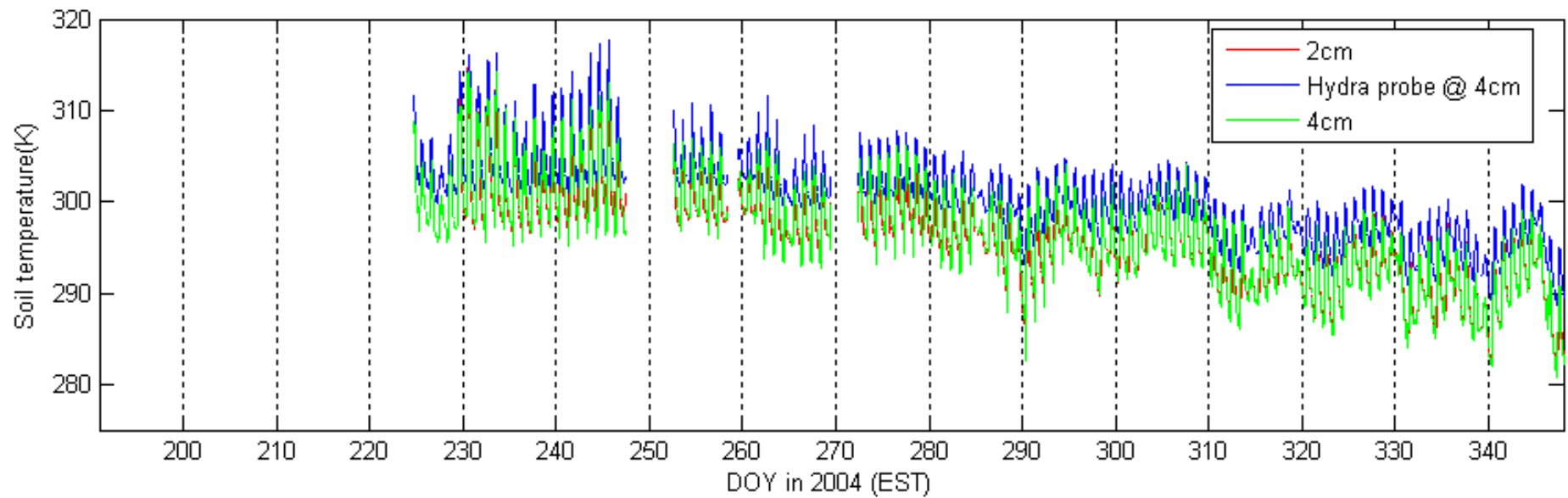


Figure A-13. Soil temperature at depth of: 2cm, 4cm Hydra probe, 4cm at Southwest station

34

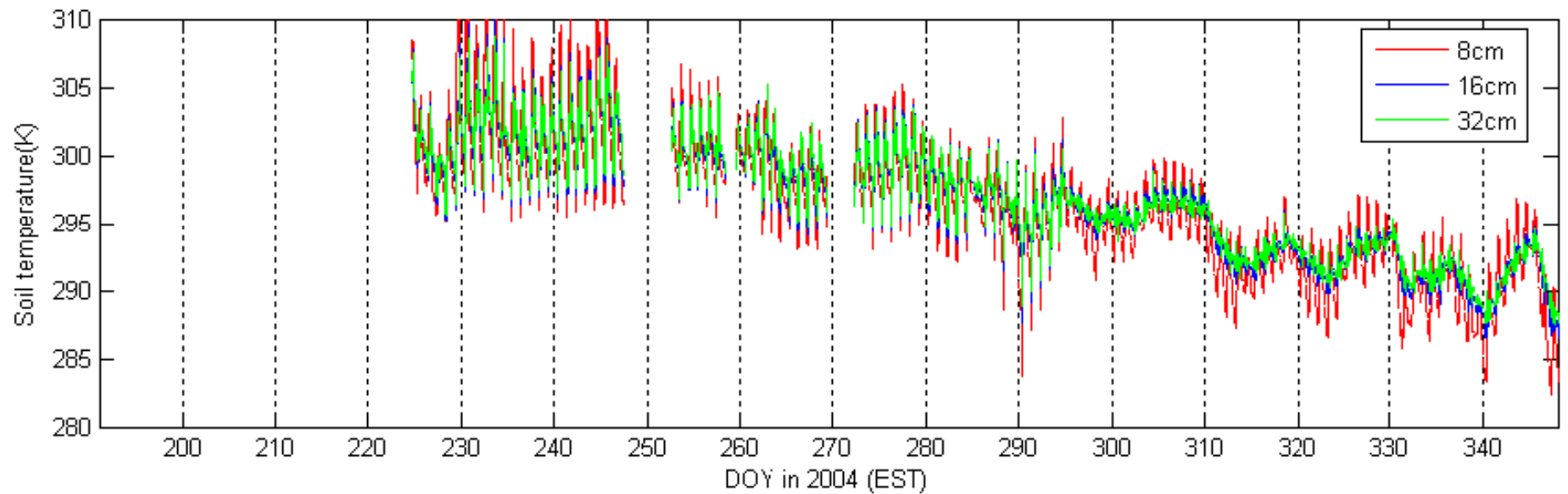


Figure A-14. Soil temperature at depth of: 8cm, 16cm, 32cm at Southwest station

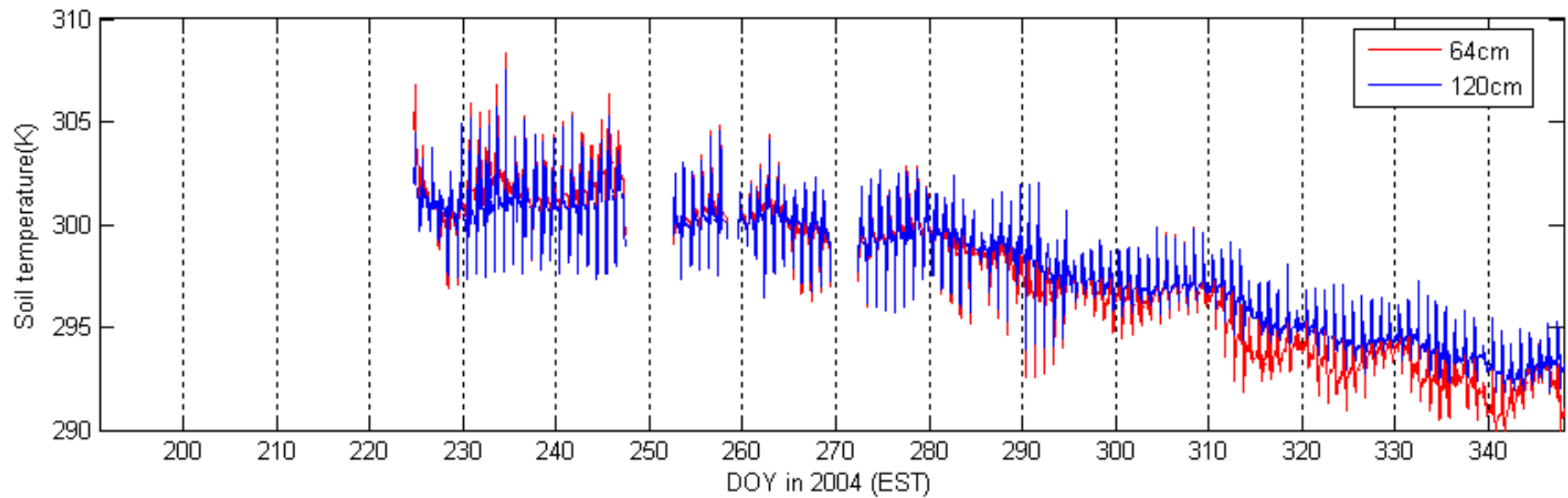


Figure A-15. Soil temperature at depth of: 64cm, 120cm at Southwest station

35

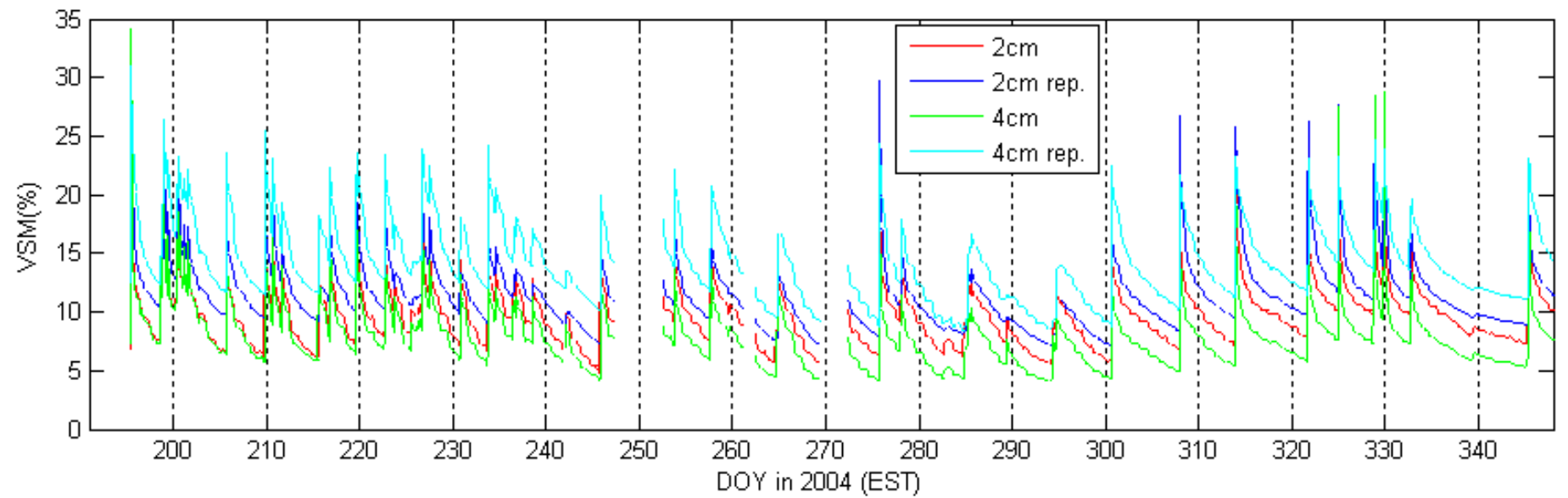


Figure A-16. VSM at depth of: two measurements at 2cm and 4cm at Northwest station

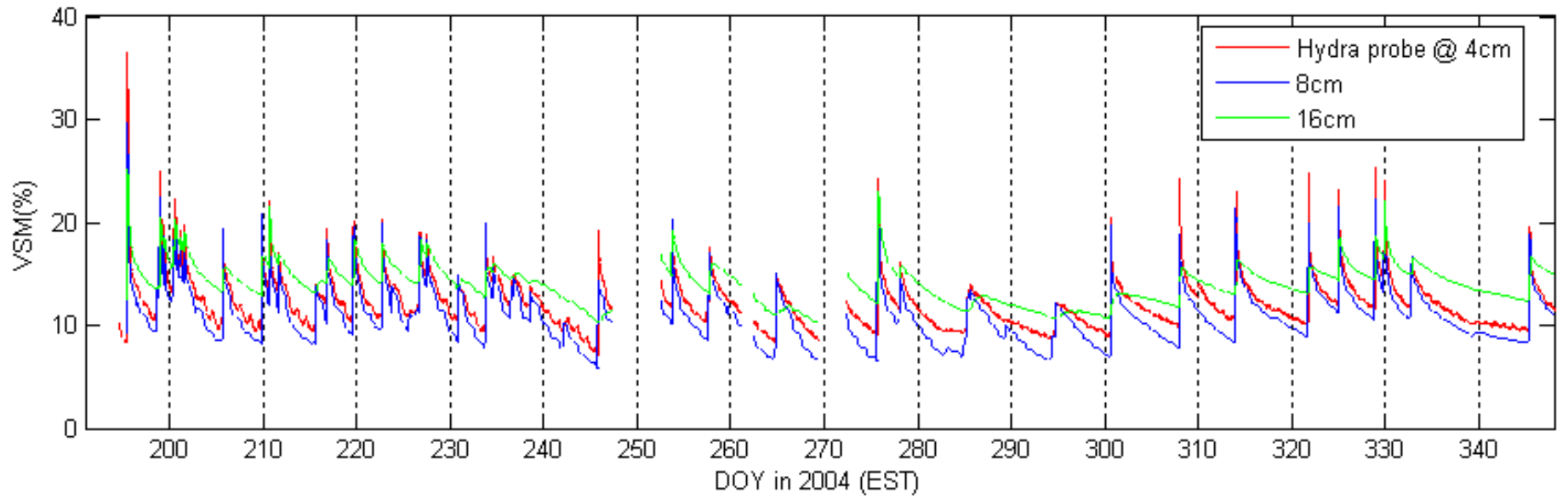


Figure A-17. VSM at depth of: 4cm Hydra probe, 8cm, 16cm at Northwest station

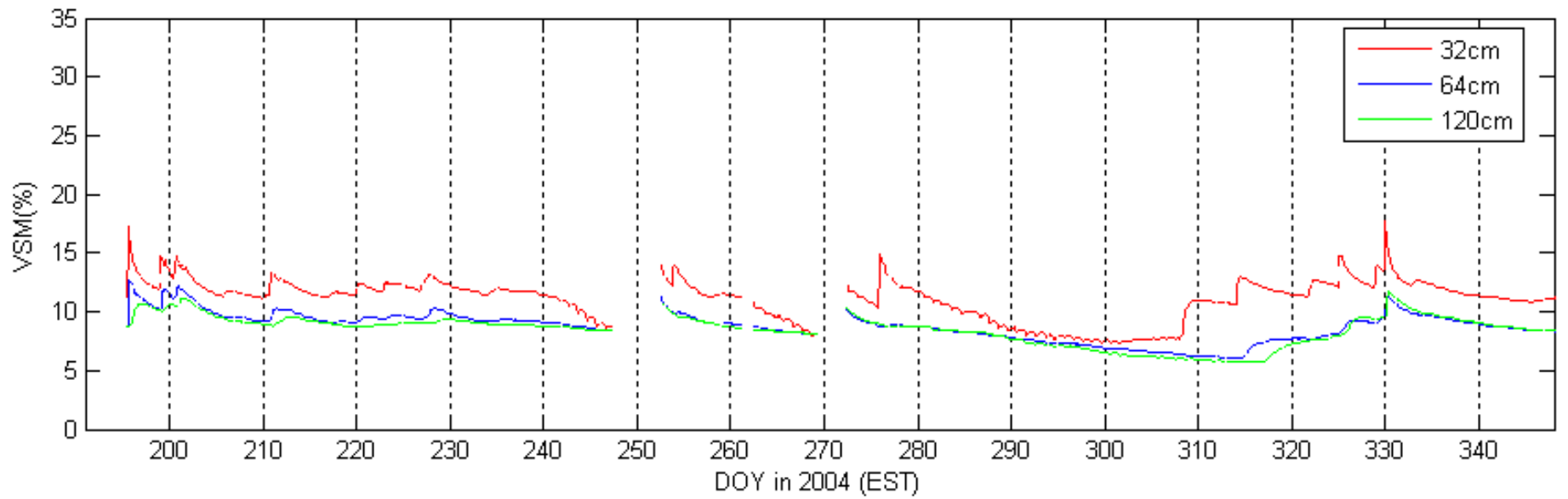


Figure A-18. VSM at depth of: 32cm, 64cm, 120cm at Northwest station

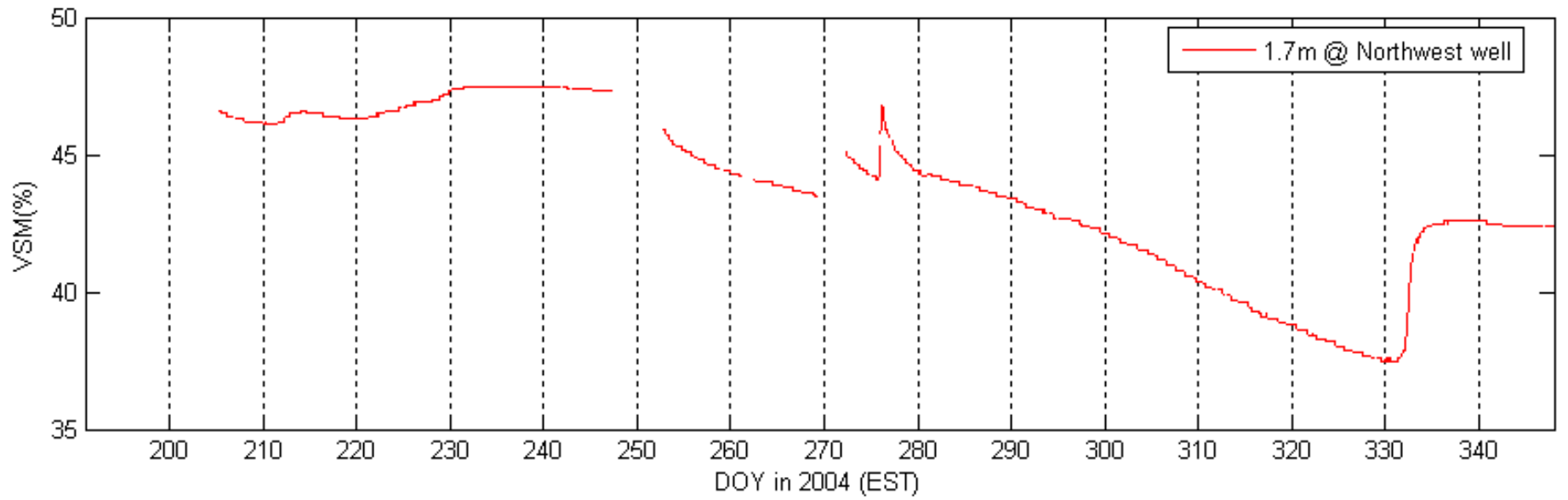


Figure A-19. VSM at depth of: 1.7m near Northwest monitoring well at Northwest station

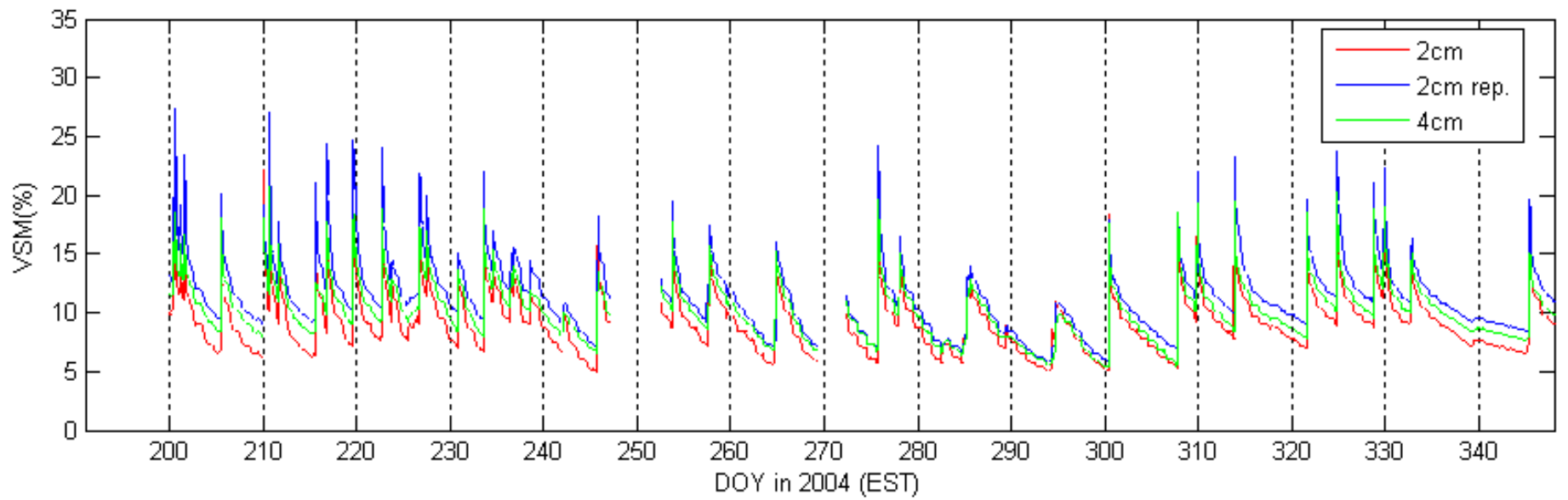


Figure A-20. VSM at depth of: 2cm, 2cm replicate, and 4cm at East station

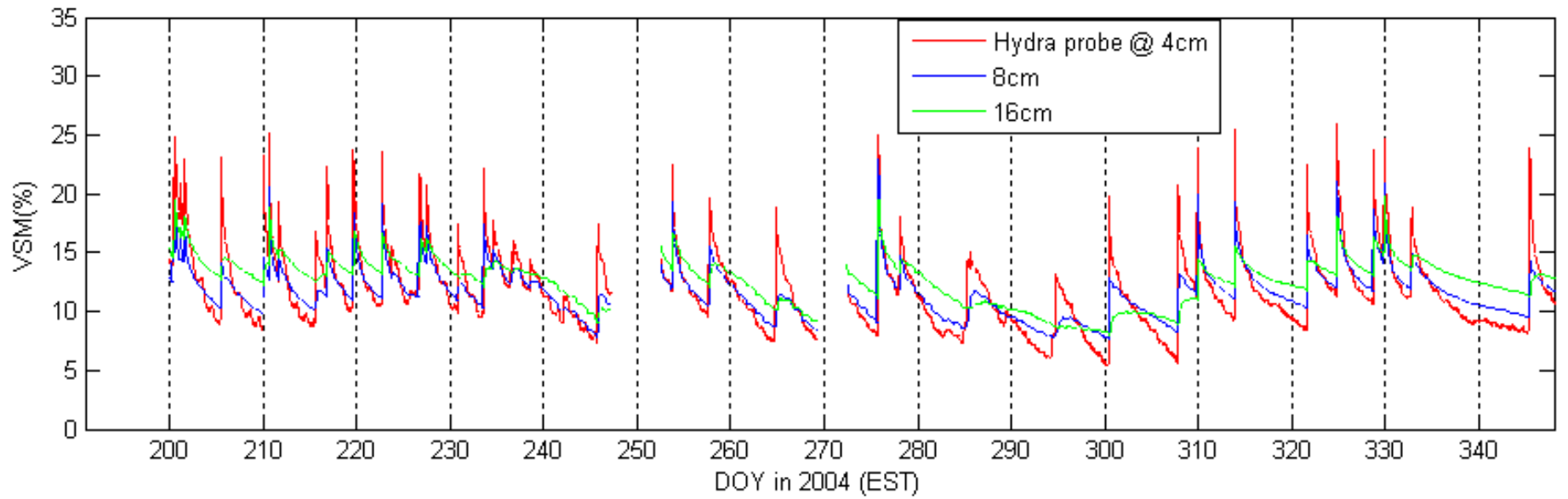


Figure A-21. VSM at depth of: 4cm Hydra probe, 8cm, 16cm at East station

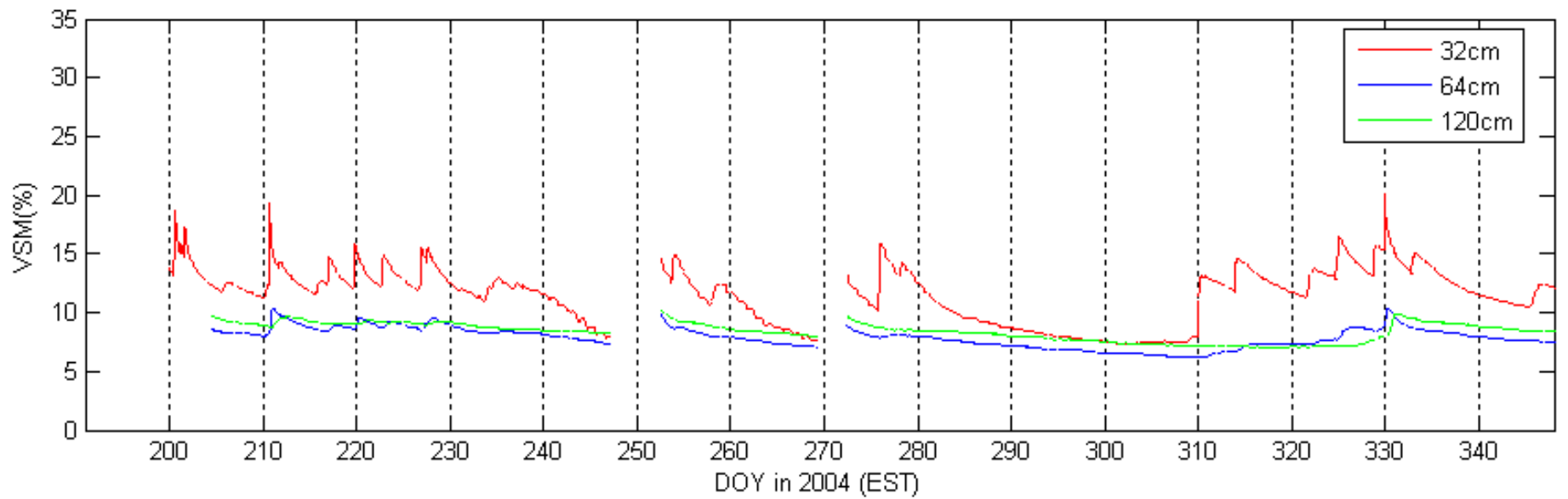


Figure A-22. VSM at depth of: 32cm, 64cm, 120cm at East station

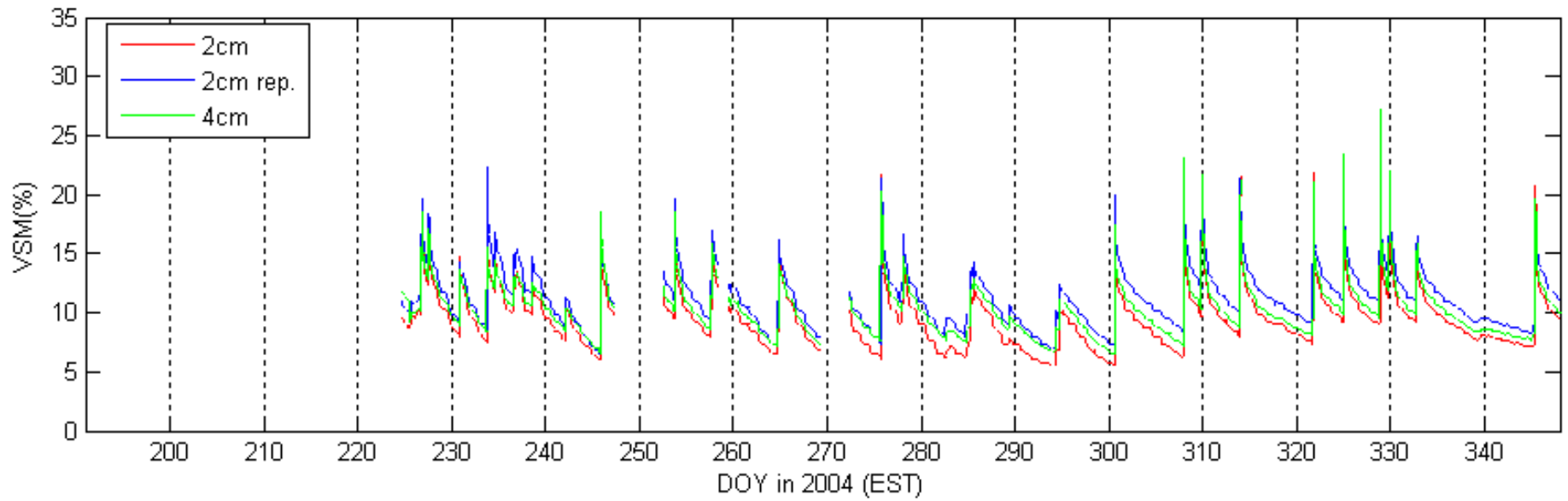


Figure A-23. VSM at depth of: 2cm, 2cm replicate, and 4cm at Southwest station

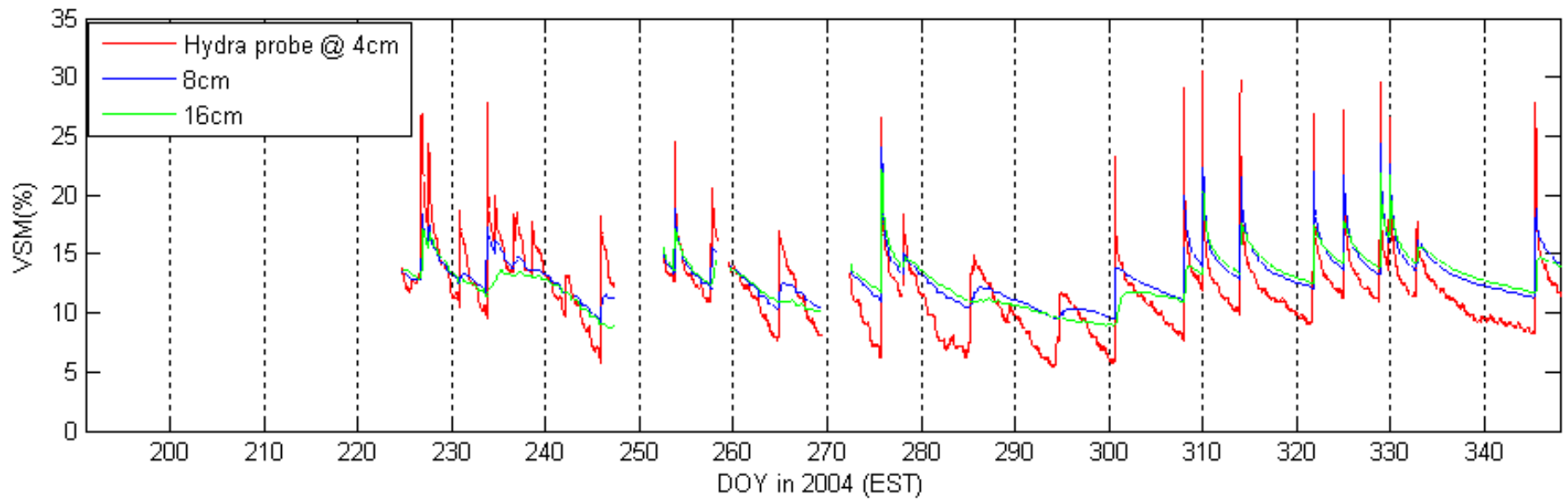


Figure A-24. VSM at depth of: 4cm Hydra probe, 8cm, 16cm at Southwest station

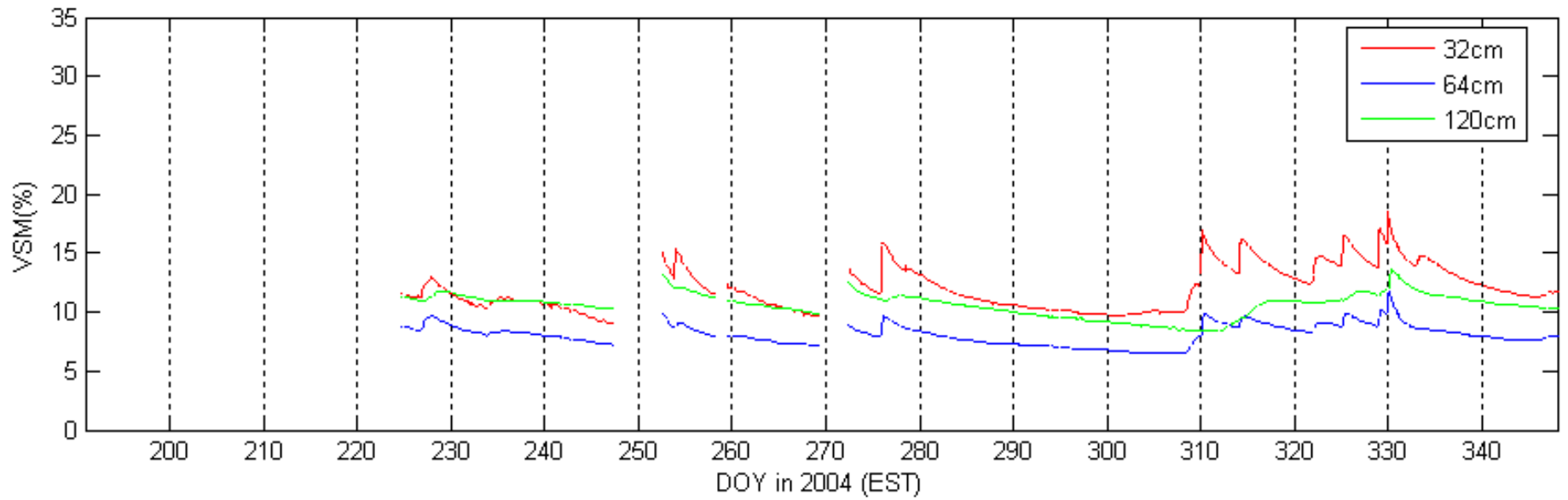


Figure A-25. VSM at depth of: 32cm, 64cm, 120cm at Southwest station

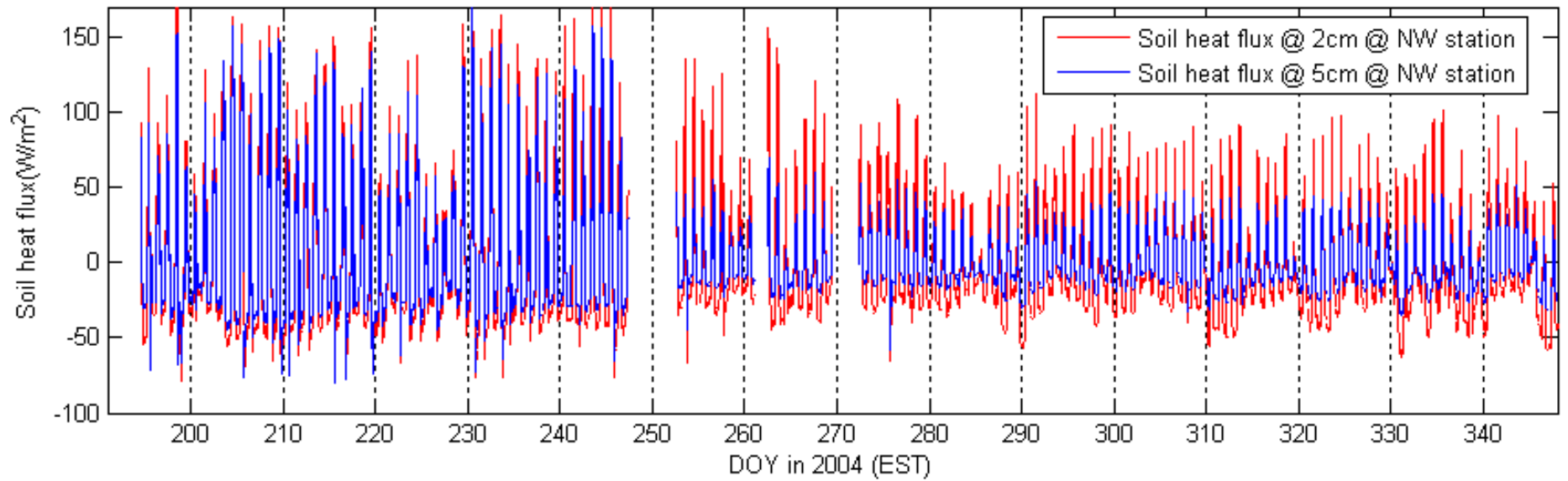


Figure A-26. Soil heat flux at depth of: 2cm, 5cm at Northwest station

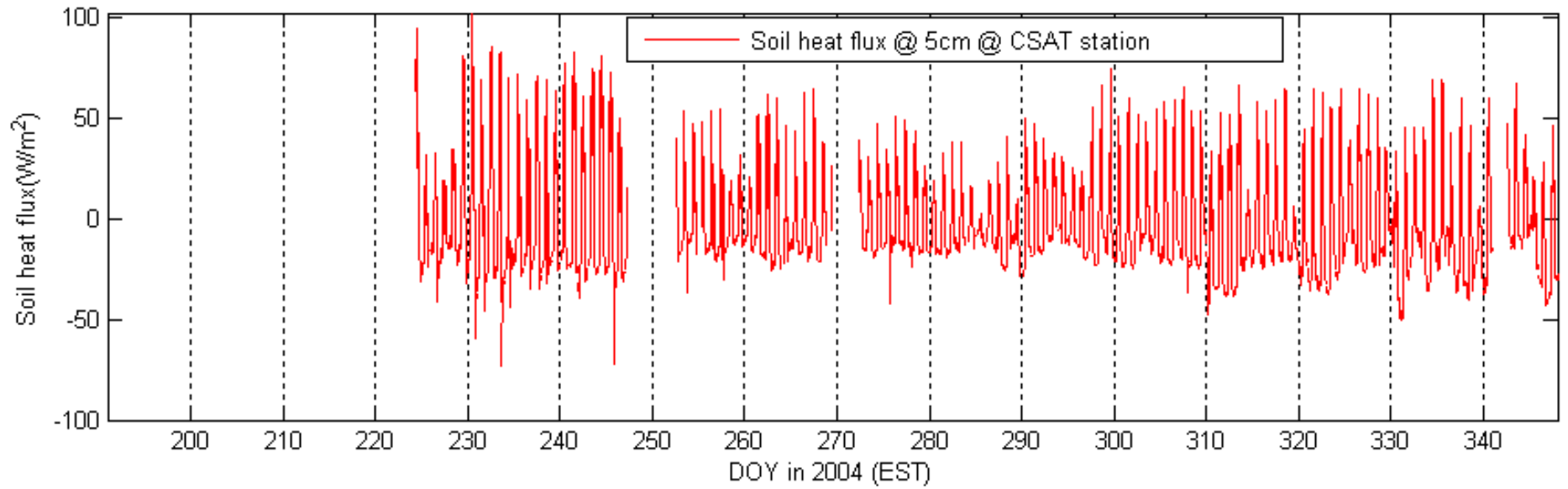


Figure A-27. Soil heat flux at depth of: 5cm at CSAT station

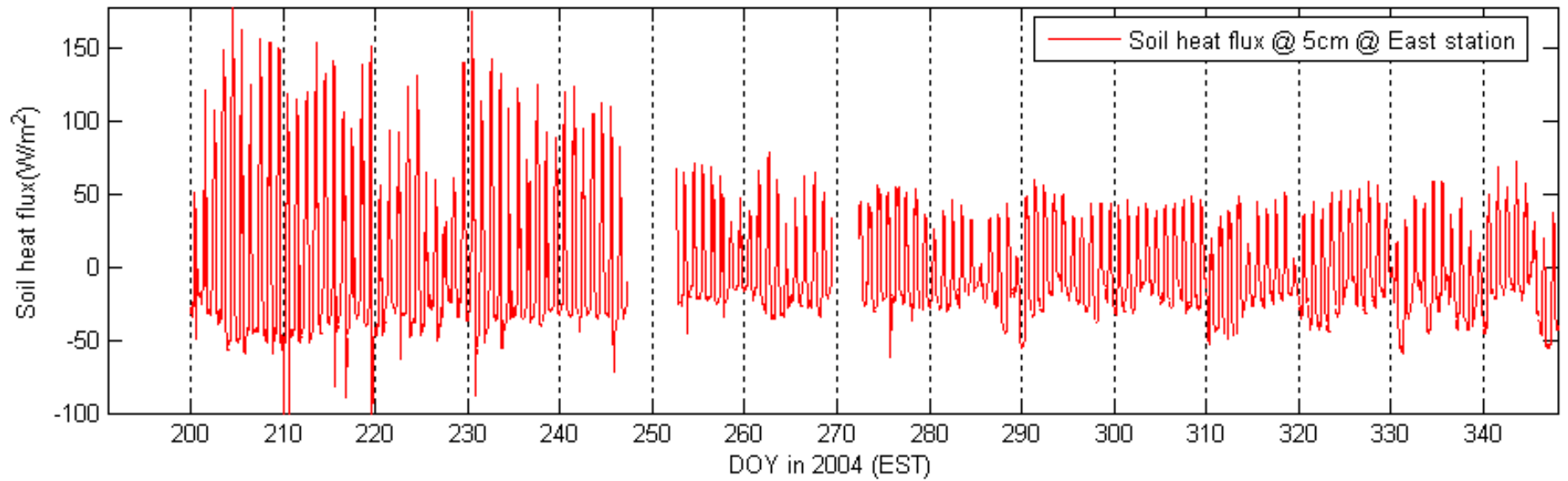


Figure A-28. Soil heat flux at depth of: 5cm at East station

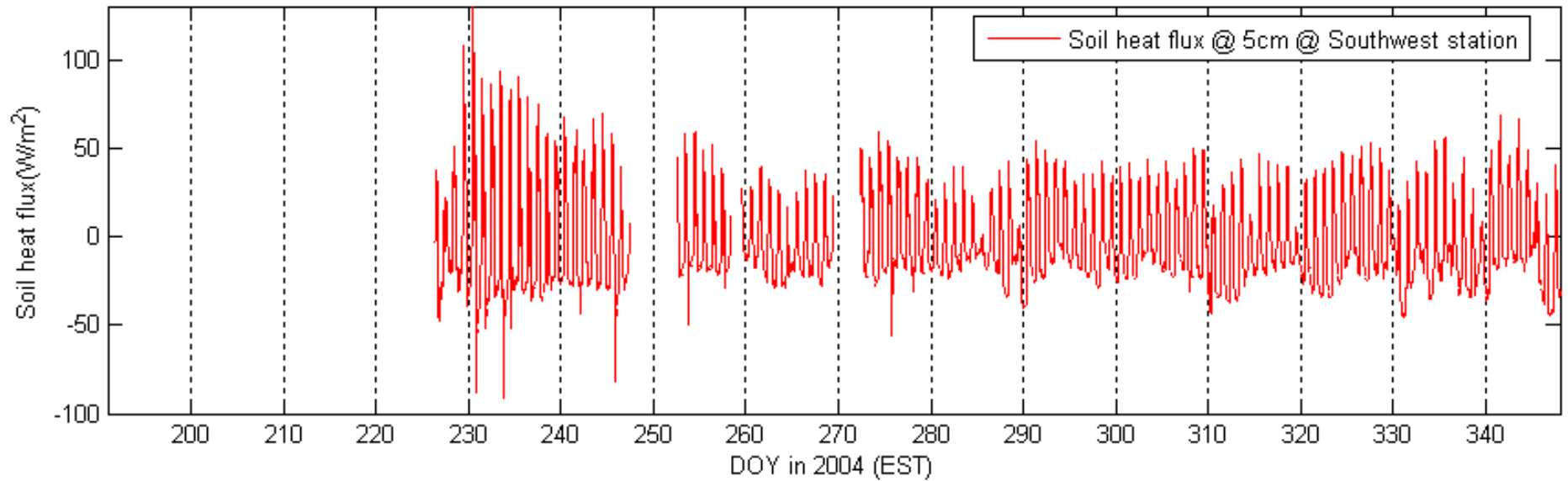


Figure A-29. Soil heat flux at depth of: 5cm at Southwest station

42

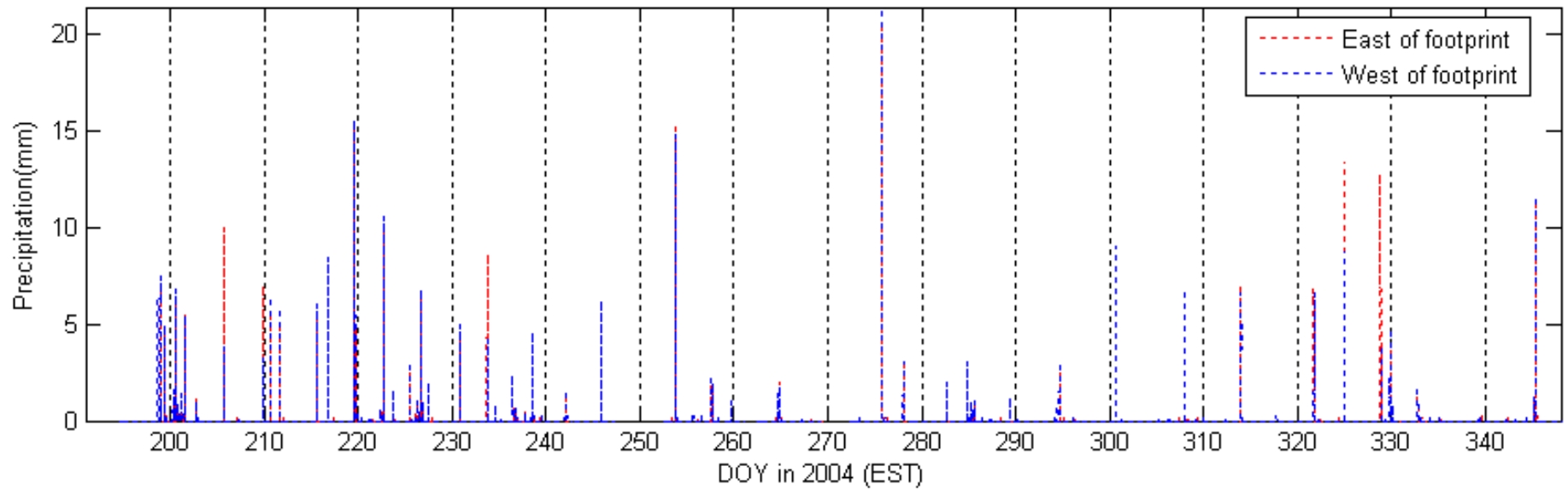


Figure A-30. Rainfall from the raingauge at the east and west edge of footprint

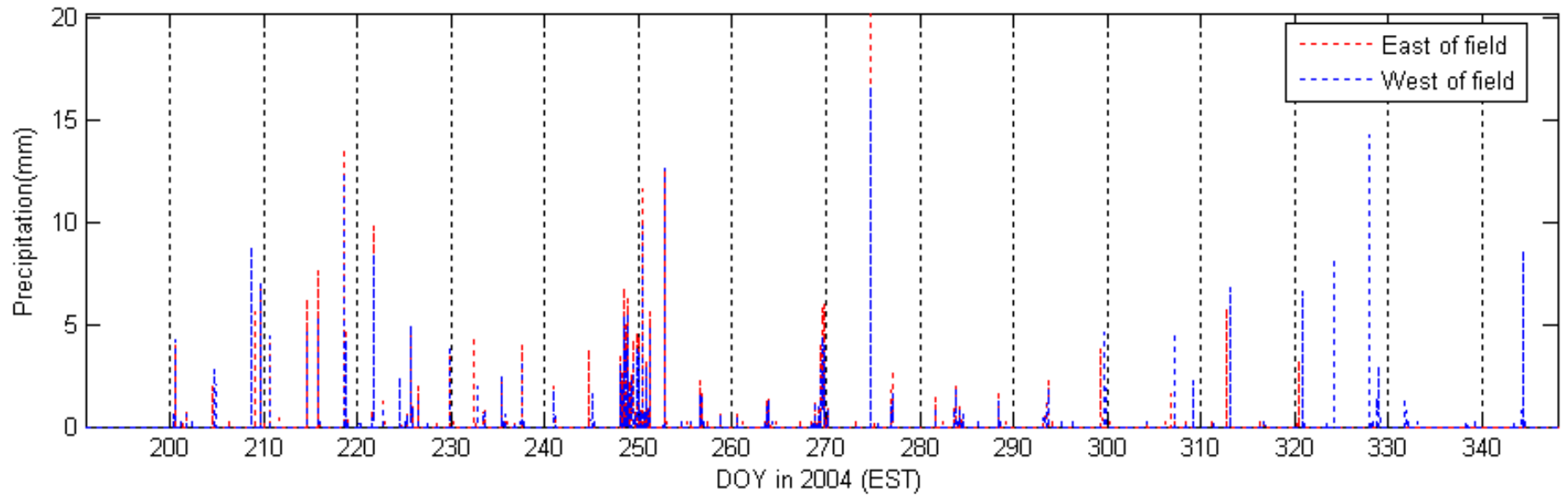


Figure A-31. Rainfall from the raingauge at the east and west edge of the field

43

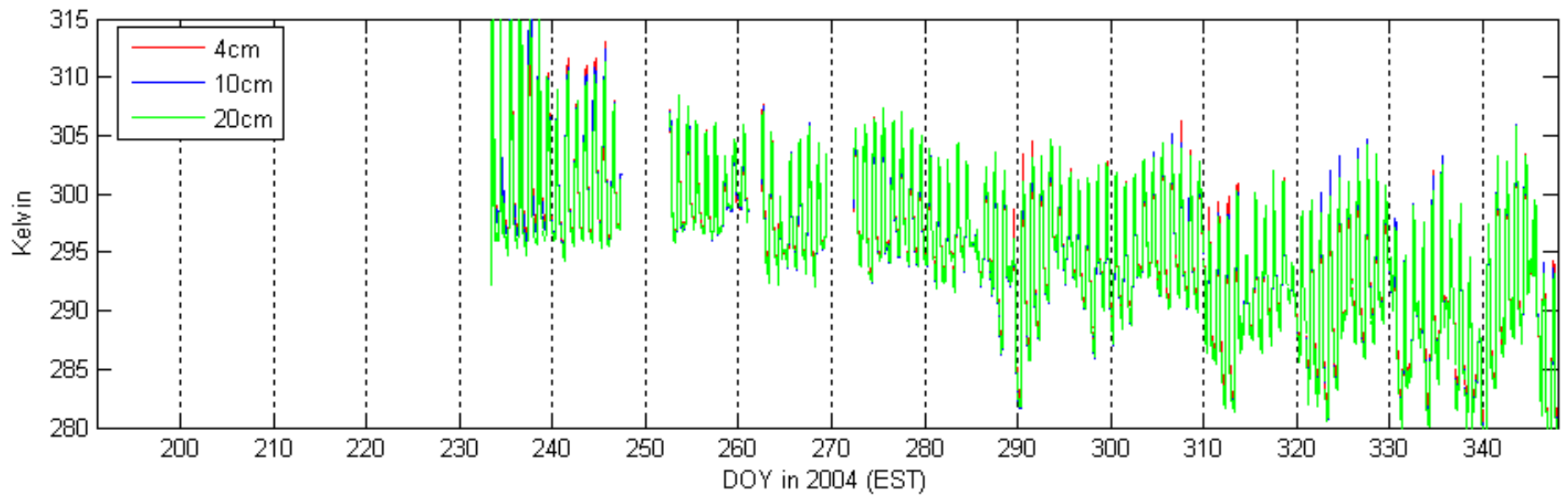


Figure A-32. Canopy temperature at 4 cm, 10 cm, 20 cm

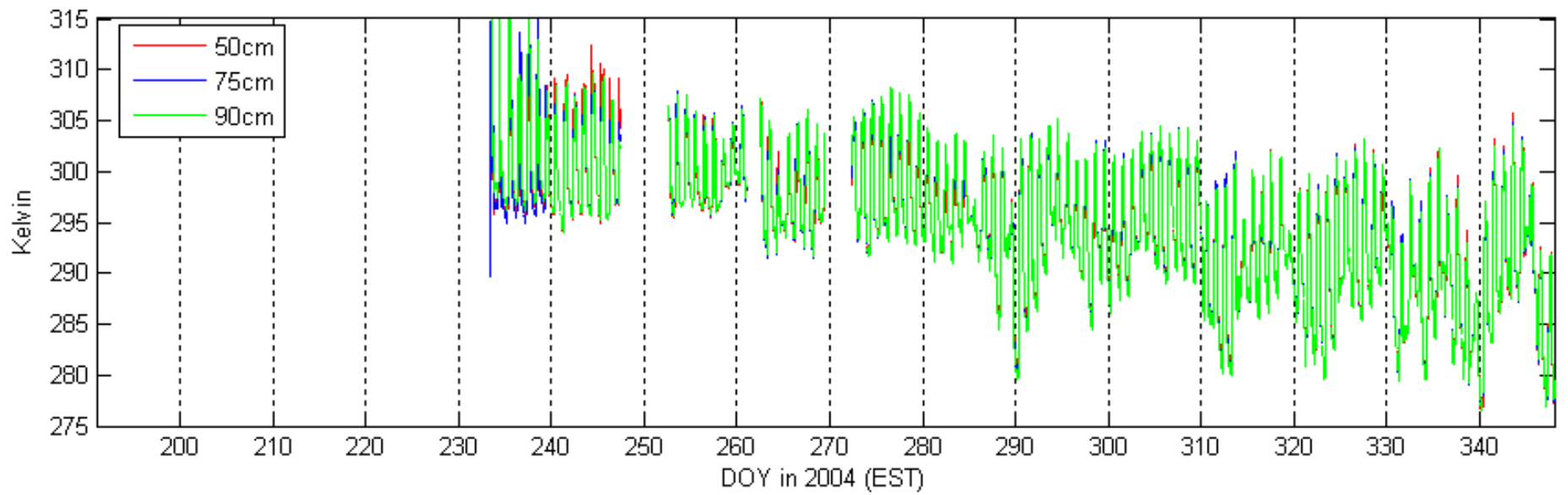


Figure A-33. Canopy temperature at 50 cm, 75 cm, and 90 cm

44

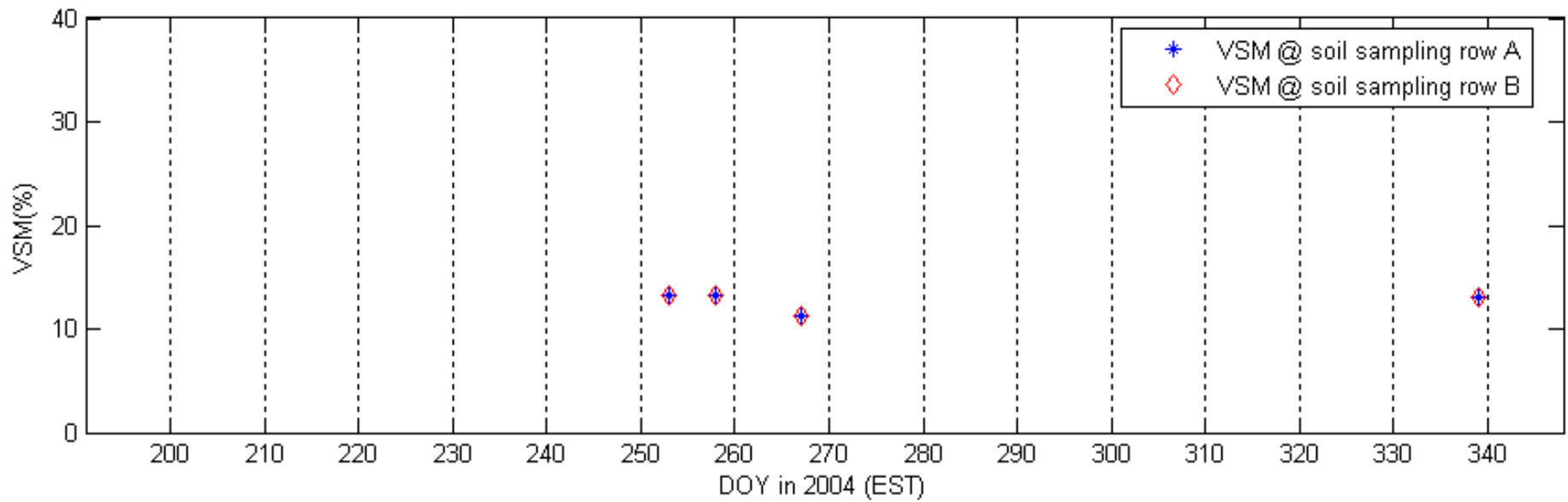


Figure A-34. VSM at specific sampling points in Row A and Row B

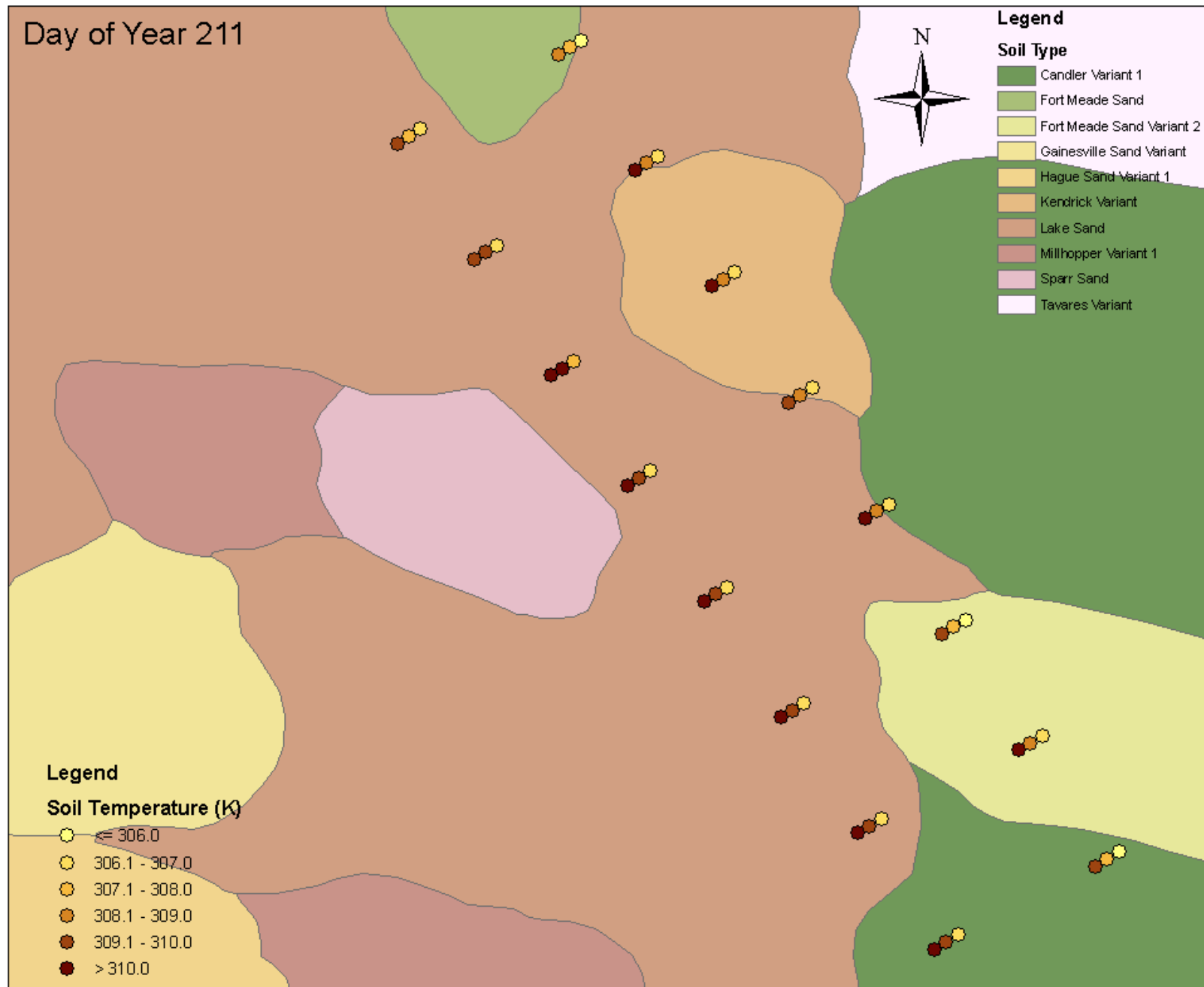


Figure A-35. Soil temperature at depths of 2, 4, and 8cm (left to right) for each designated sampling point, July 29, 2004 (DoY 211)

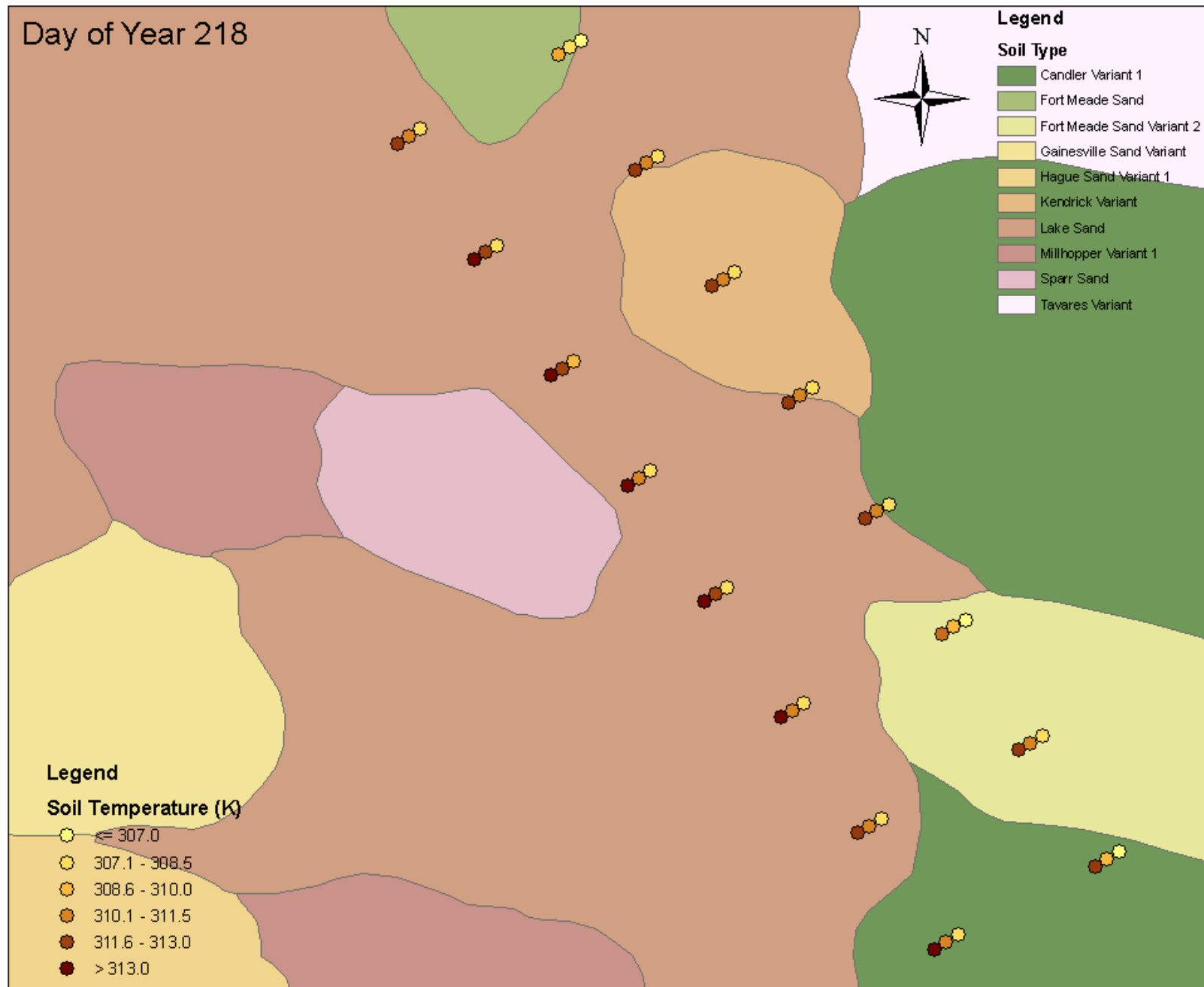


Figure A-36. Soil temperature at depths of 2, 4, and 8cm (left to right) for each designated sampling point, Aug. 05, 2004 (DoY 218)

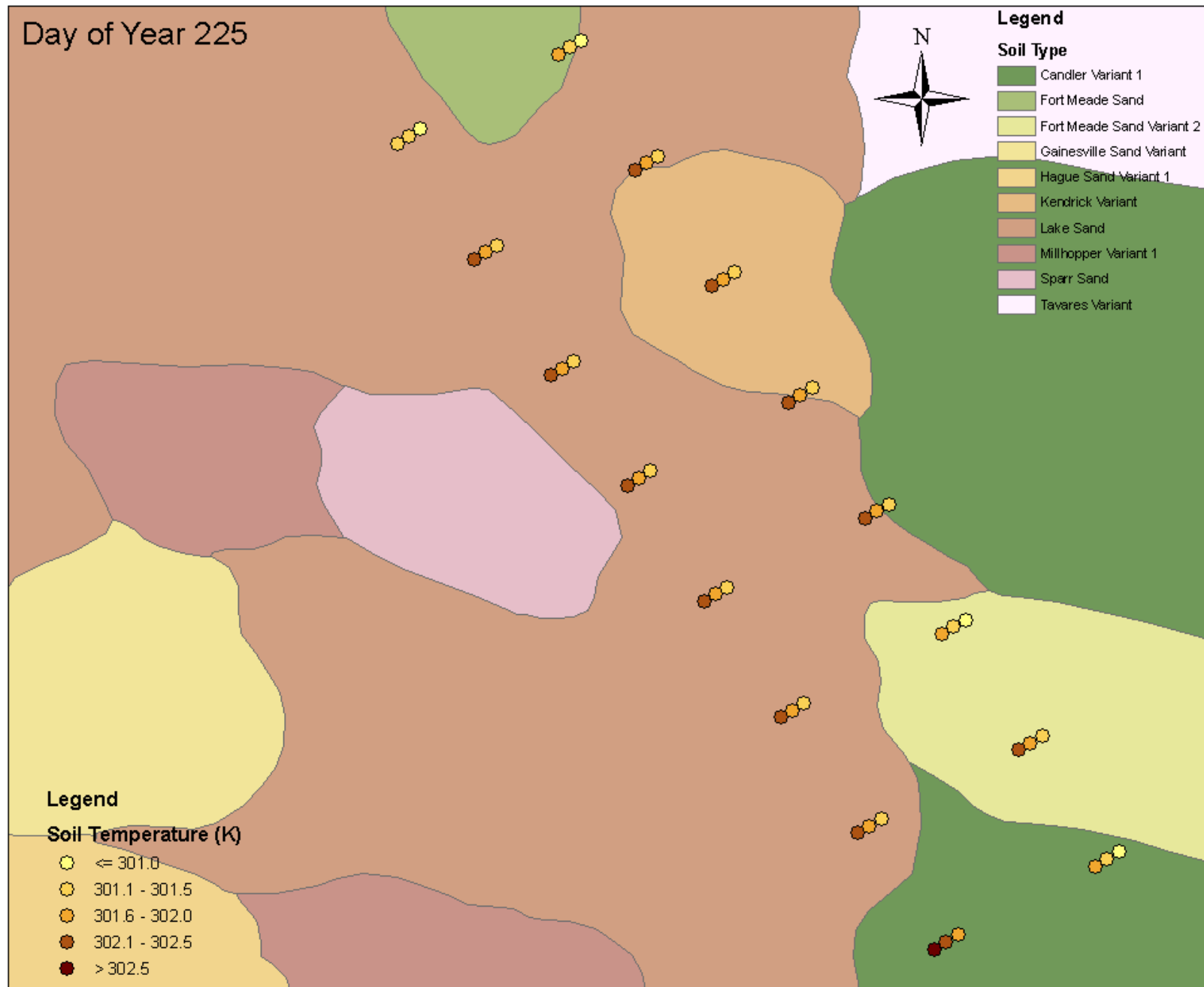


Figure A-37. Soil temperature at depths of 2, 4, and 8cm (left to right) for each designated sampling point, Aug. 12, 2004 (DoY 225)

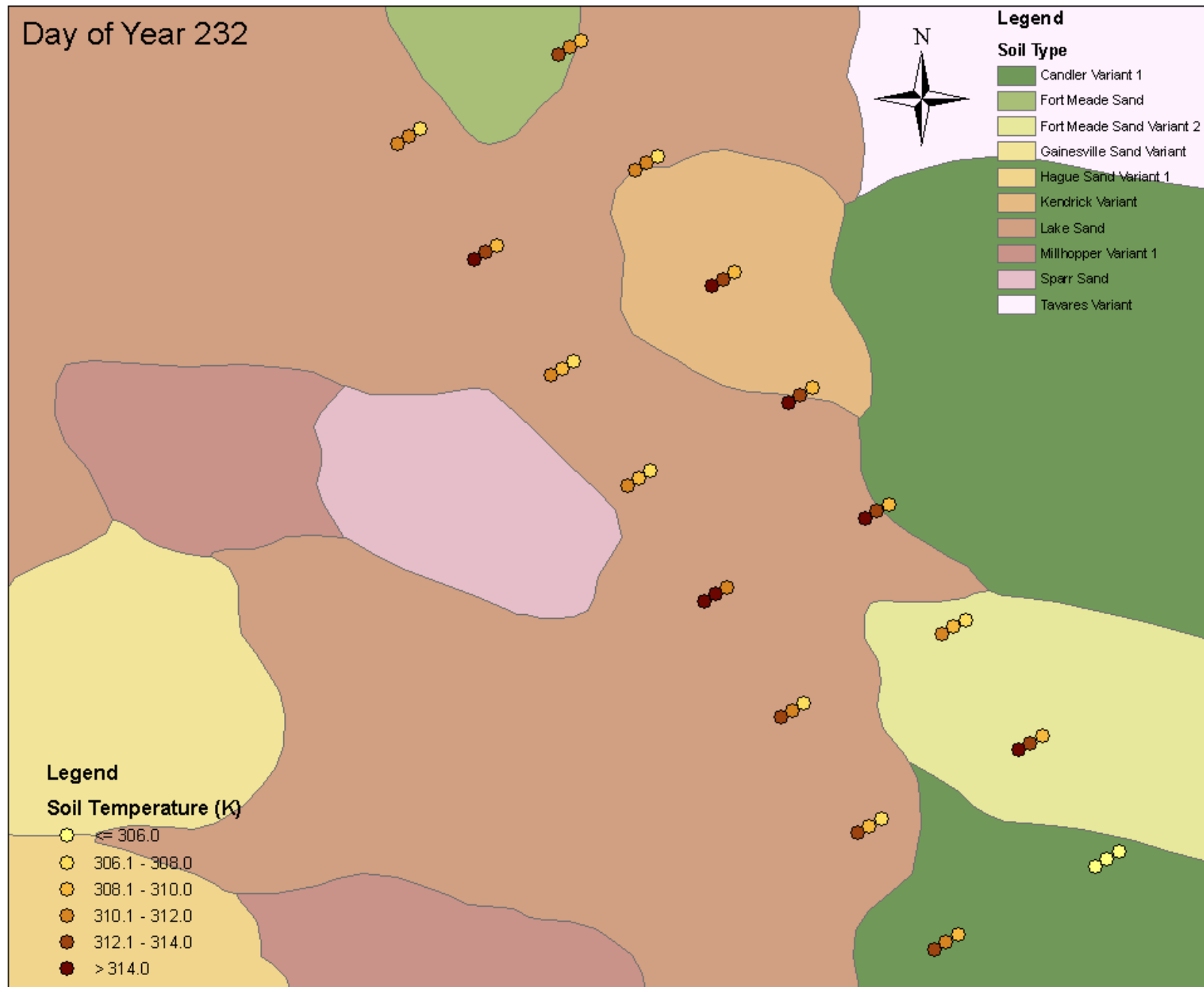


Figure A-38. Soil temperature at depths of 2, 4, and 8cm (left to right) for each designated sampling point, Aug. 19, 2004 (DoY 232)

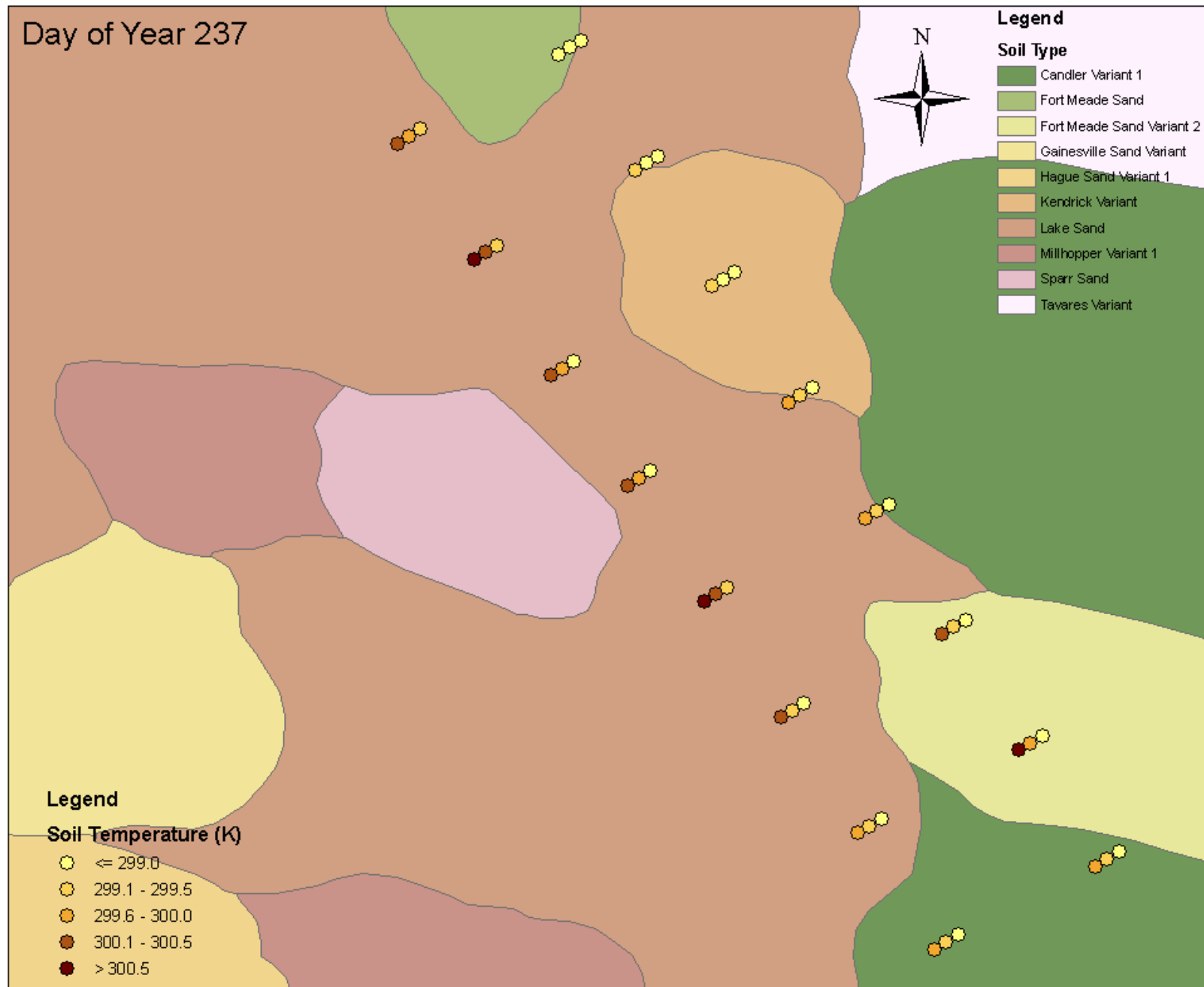


Figure A-39. Soil temperature at depths of 2, 4, and 8cm (left to right) for each designated sampling point, Aug. 24, 2004 (DoY 237)

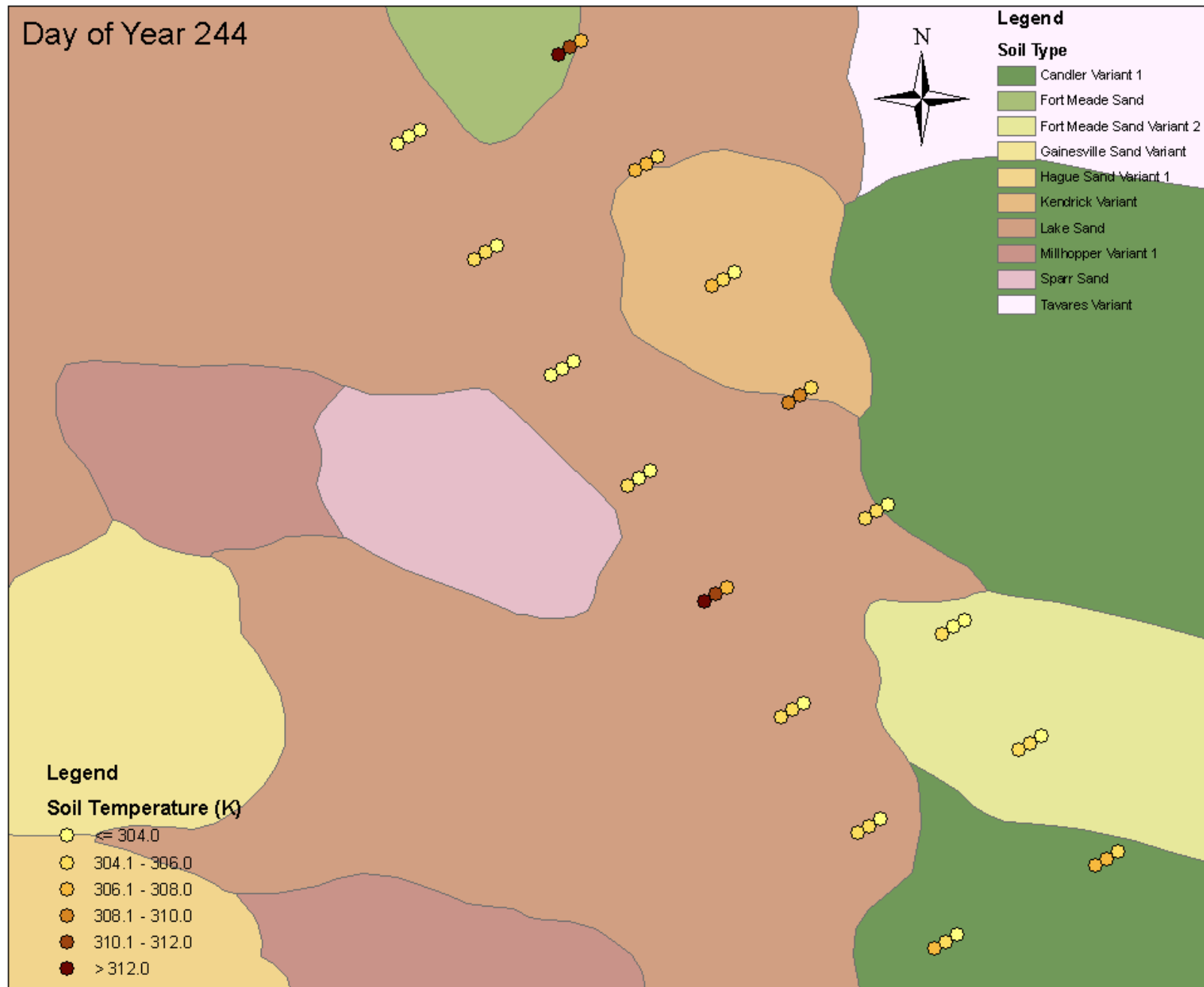


Figure A-40. Soil temperature at depths of 2, 4, and 8cm (left to right) for each designated sampling point, Aug. 31, 2004 (DoY 244)

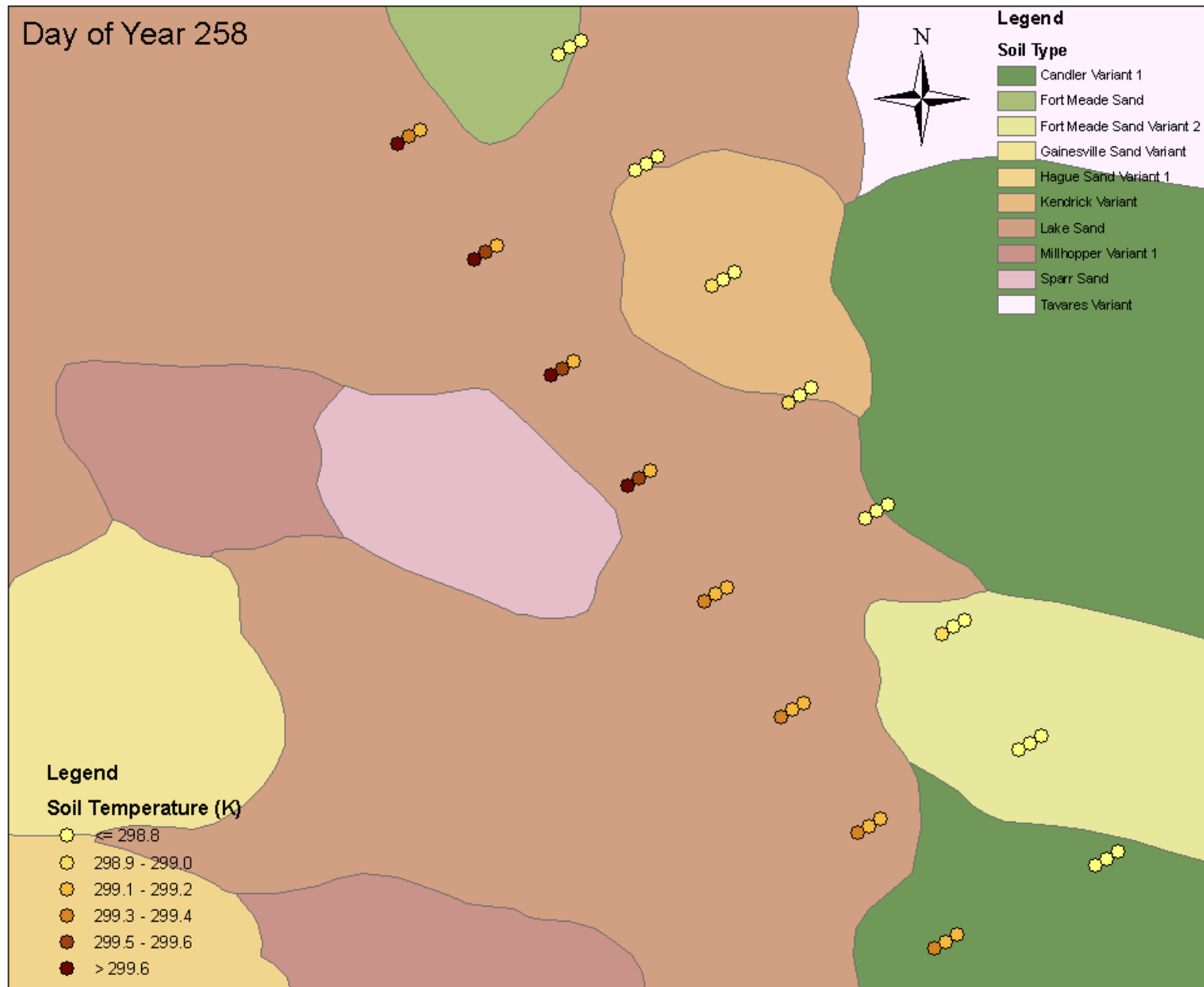


Figure A-41. Soil temperature at depths of 2, 4, and 8cm (left to right) for each designated sampling point, Sep. 14, 2004 (DoY 258)

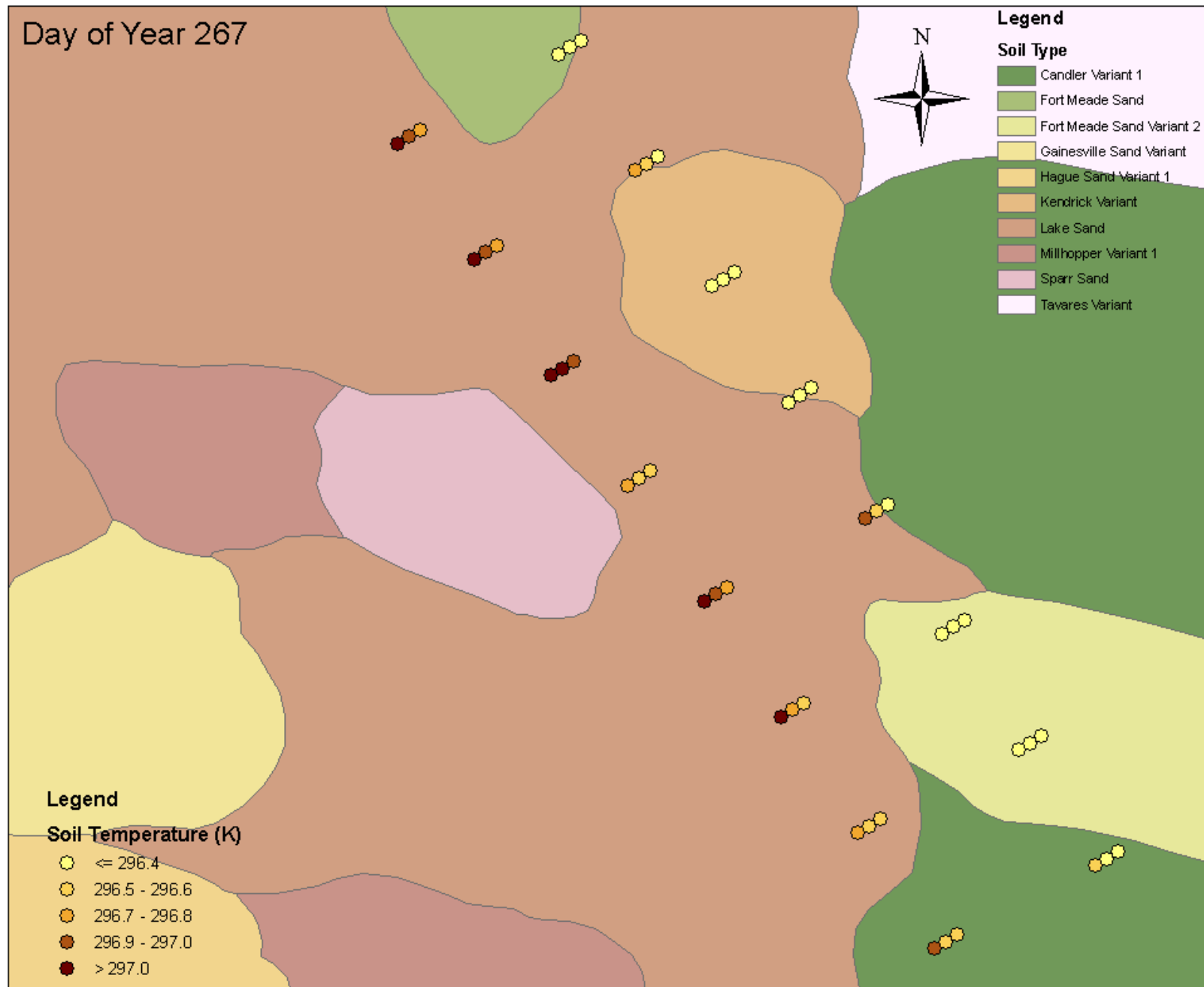


Figure A-42. Soil temperature at depths of 2, 4, and 8cm (left to right) for each designated sampling point, Sep. 23, 2004 (DoY 267)

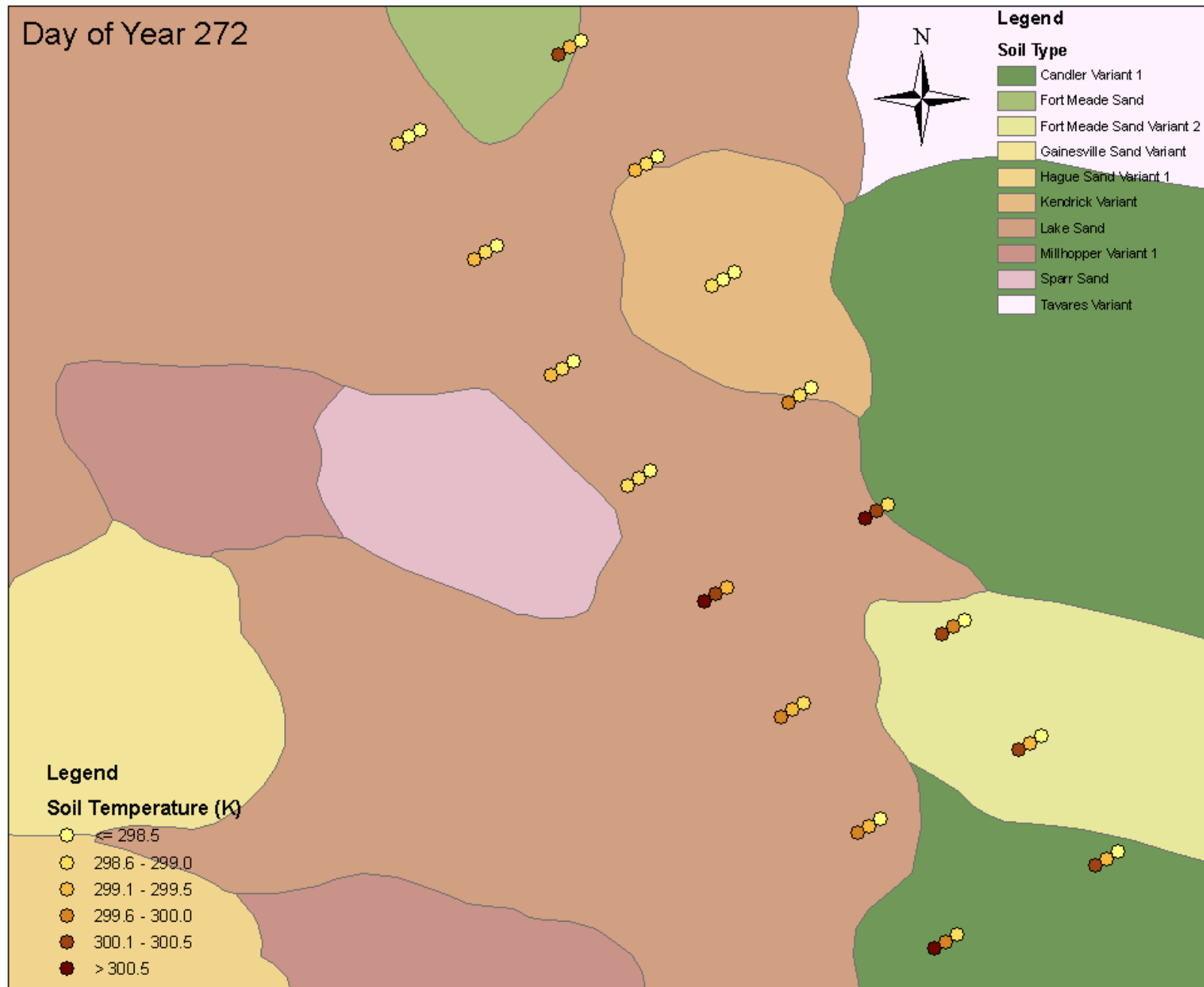


Figure A-43. Soil temperature at depths of 2, 4, and 8cm (left to right) for each designated sampling point, Sep. 28, 2004 (DoY 272)

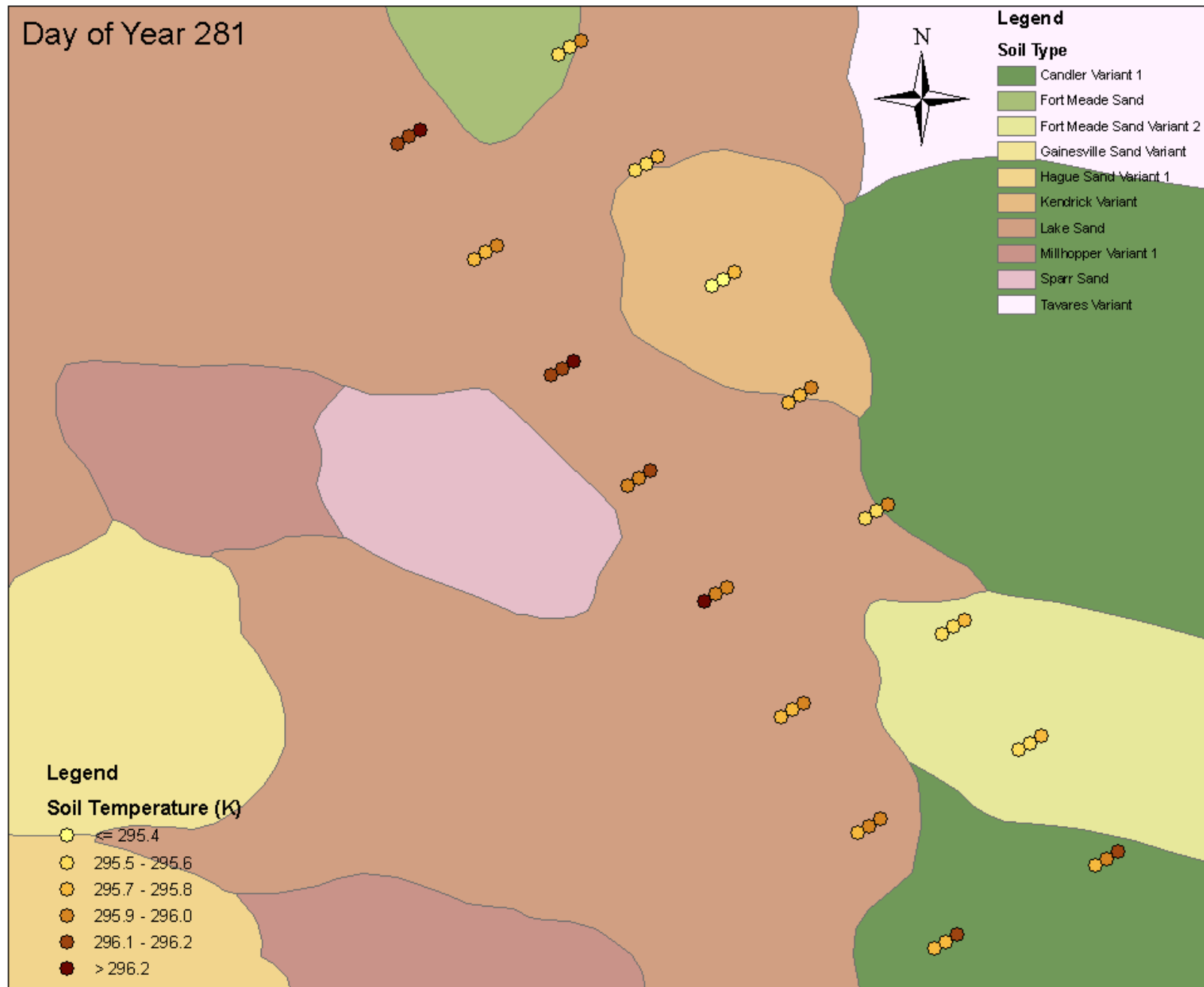


Figure A-44. Soil temperature at depths of 2, 4, and 8cm (left to right) for each designated sampling point, Oct. 07, 2004 (DoY 281)

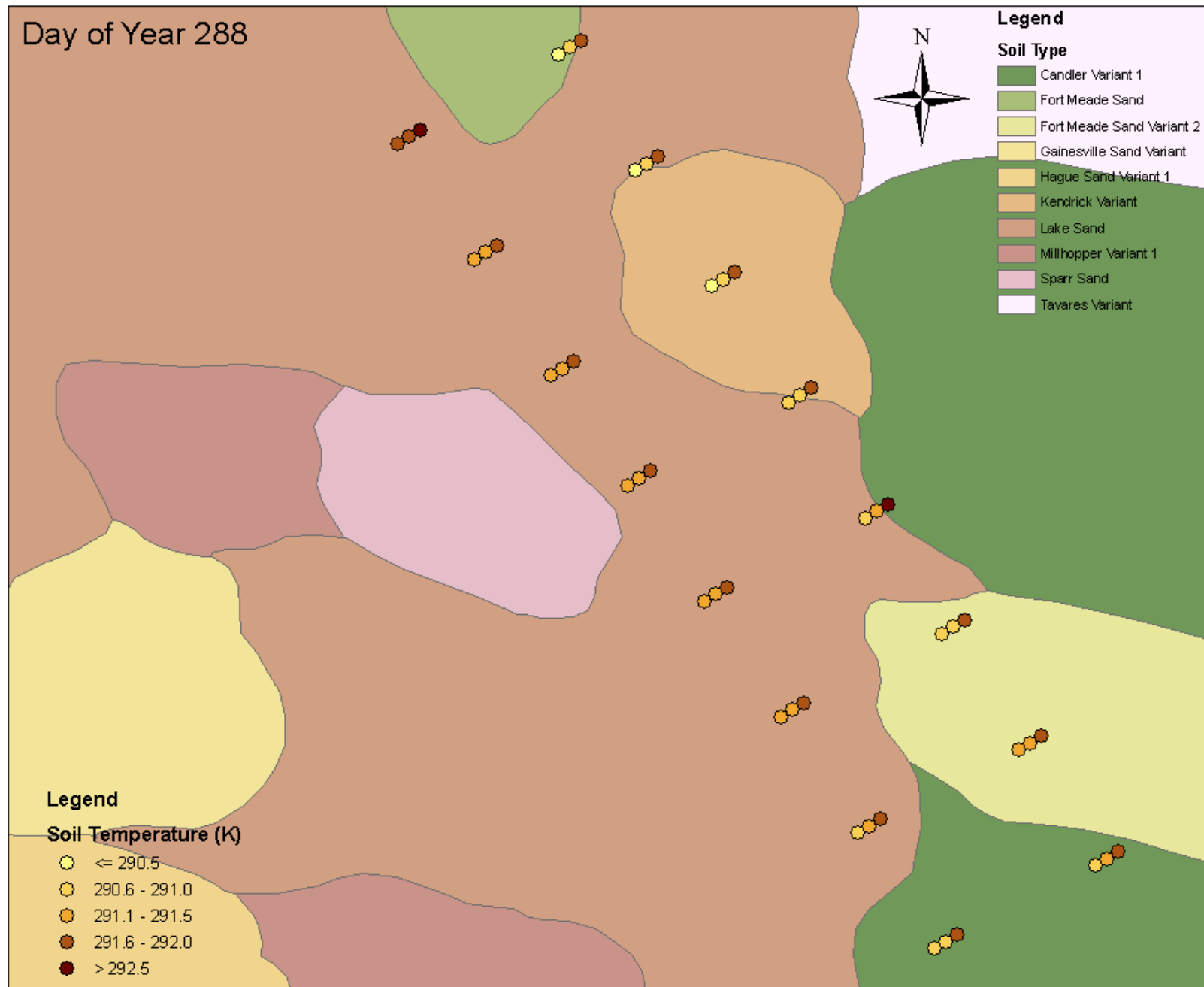


Figure A-45. Soil temperature at depths of 2, 4, and 8cm (left to right) for each designated sampling point, Oct. 14, 2004 (DoY 288)

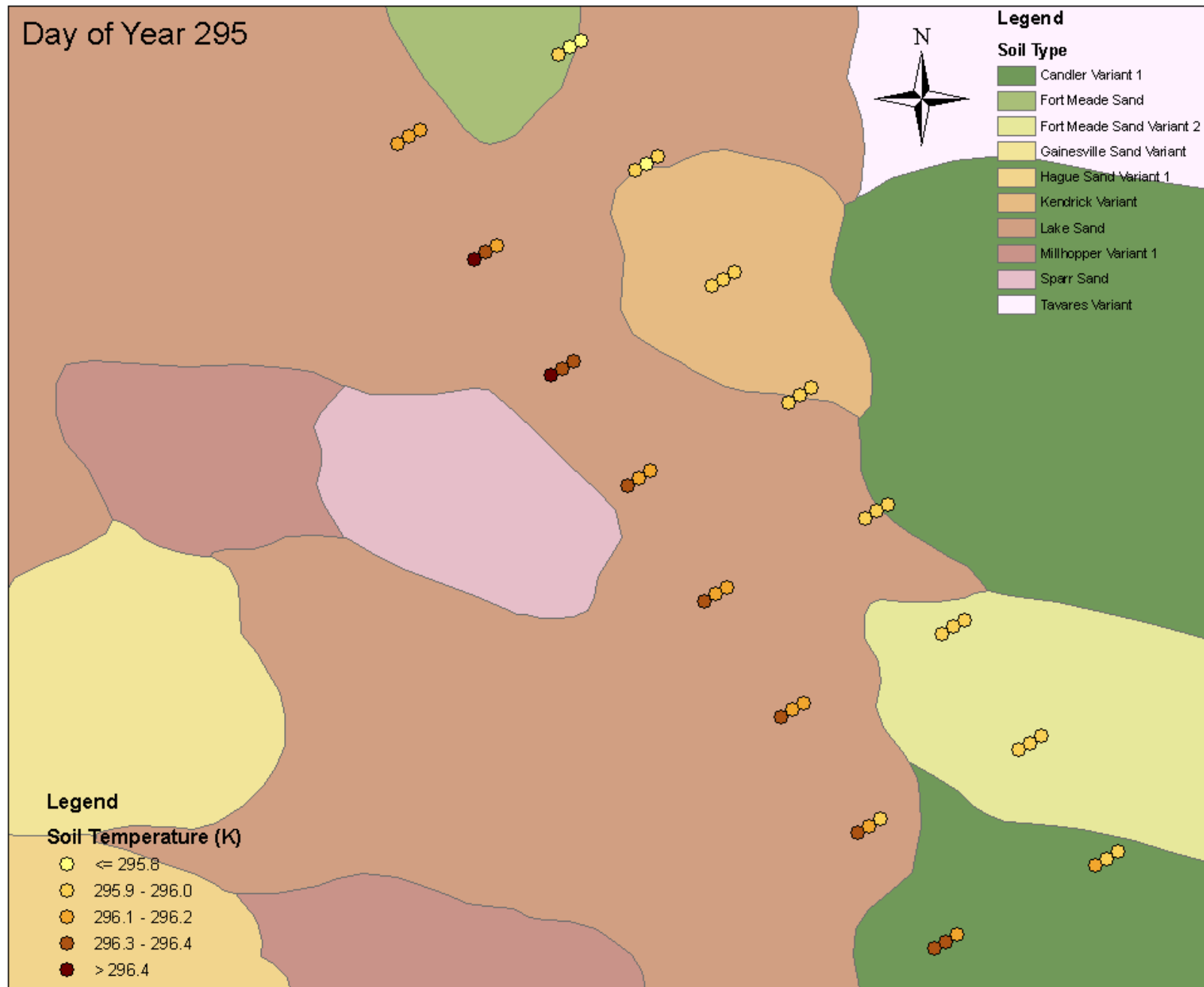


Figure A-46. Soil temperature at depths of 2, 4, and 8cm (left to right) for each designated sampling point, Oct. 21, 2004 (DoY 295)

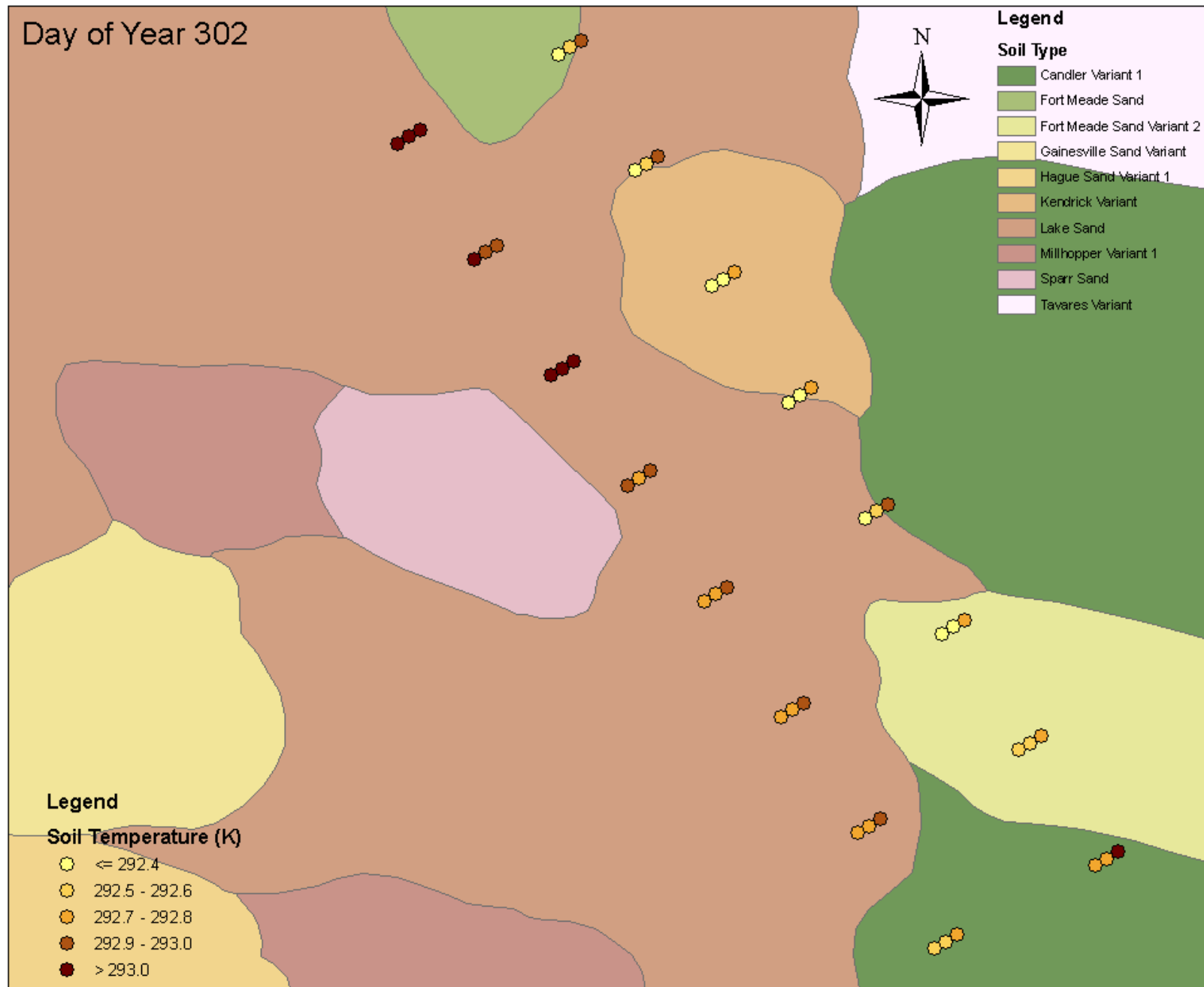


Figure A-47. Soil temperature at depths of 2, 4, and 8cm (left to right) for each designated sampling point, Oct. 28, 2004 (DoY 302)

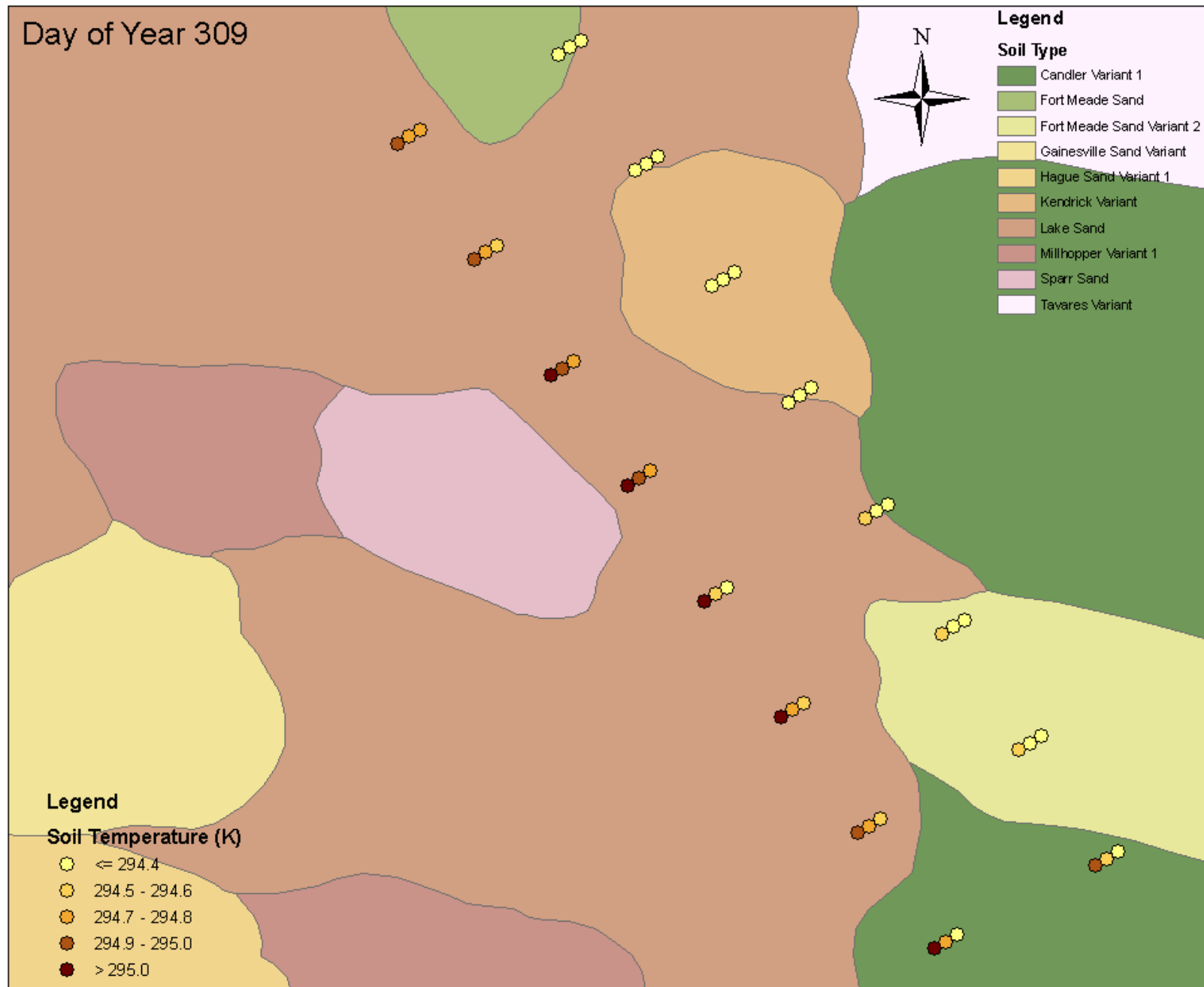


Figure A-48. Soil temperature at depths of 2, 4, and 8cm (left to right) for each designated sampling point, Nov. 04, 2004 (DoY 309)

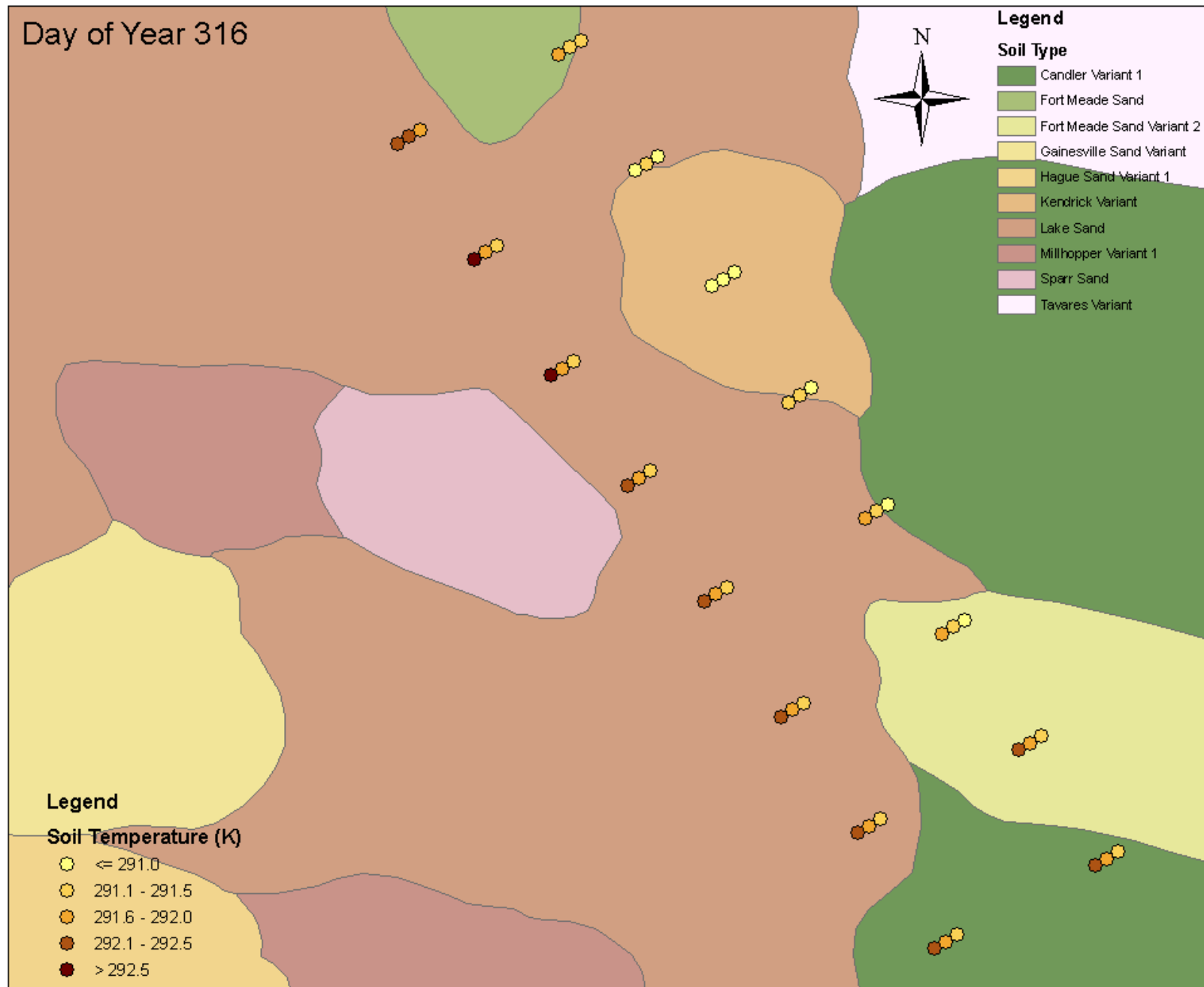


Figure A-49. Soil temperature at depths of 2, 4, and 8cm (left to right) for each designated sampling point, Nov. 11, 2004 (DoY 316)

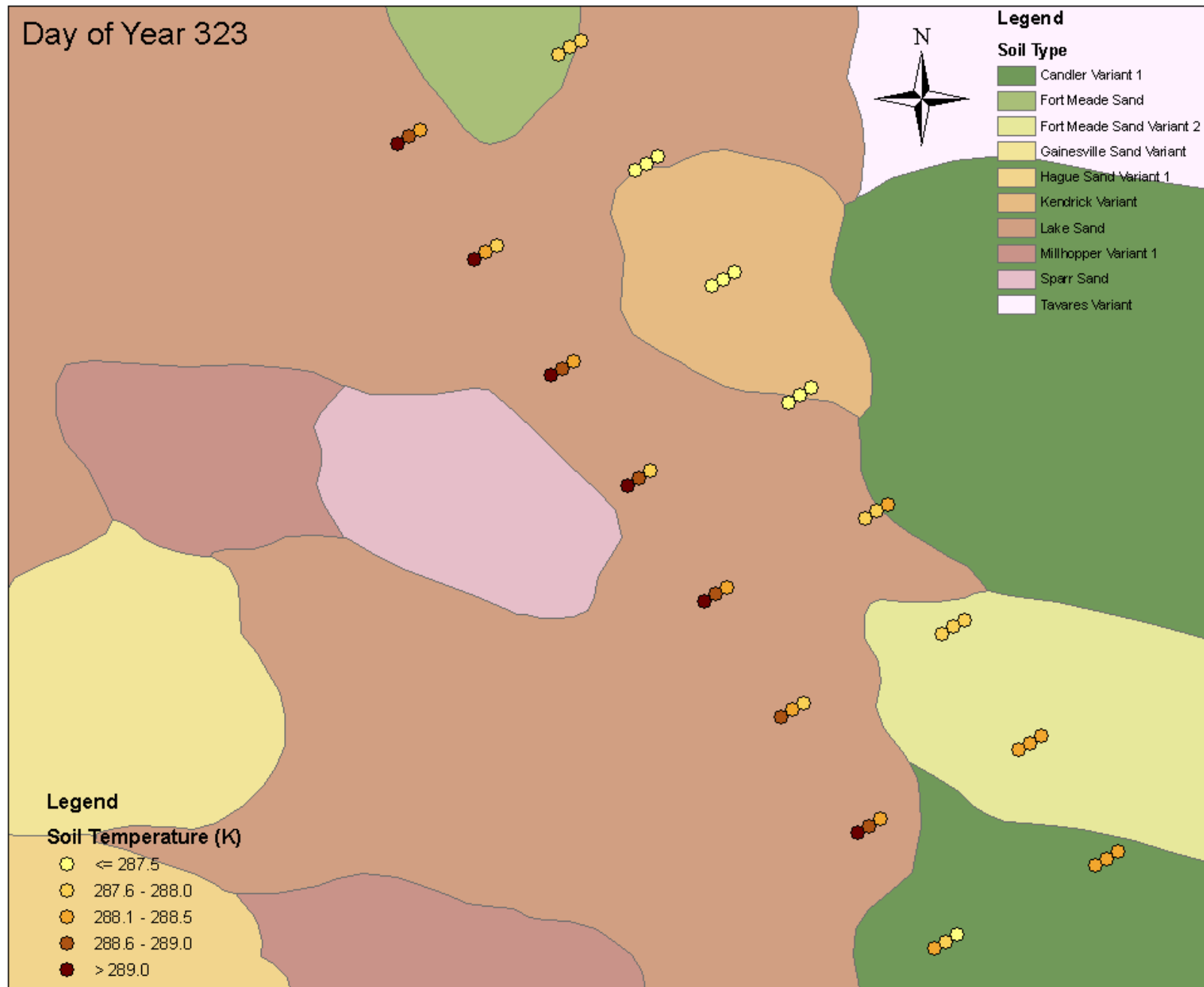


Figure A-50. Soil temperature at depths of 2, 4, and 8cm (left to right) for each designated sampling point, Nov. 18, 2004 (DoY 323)

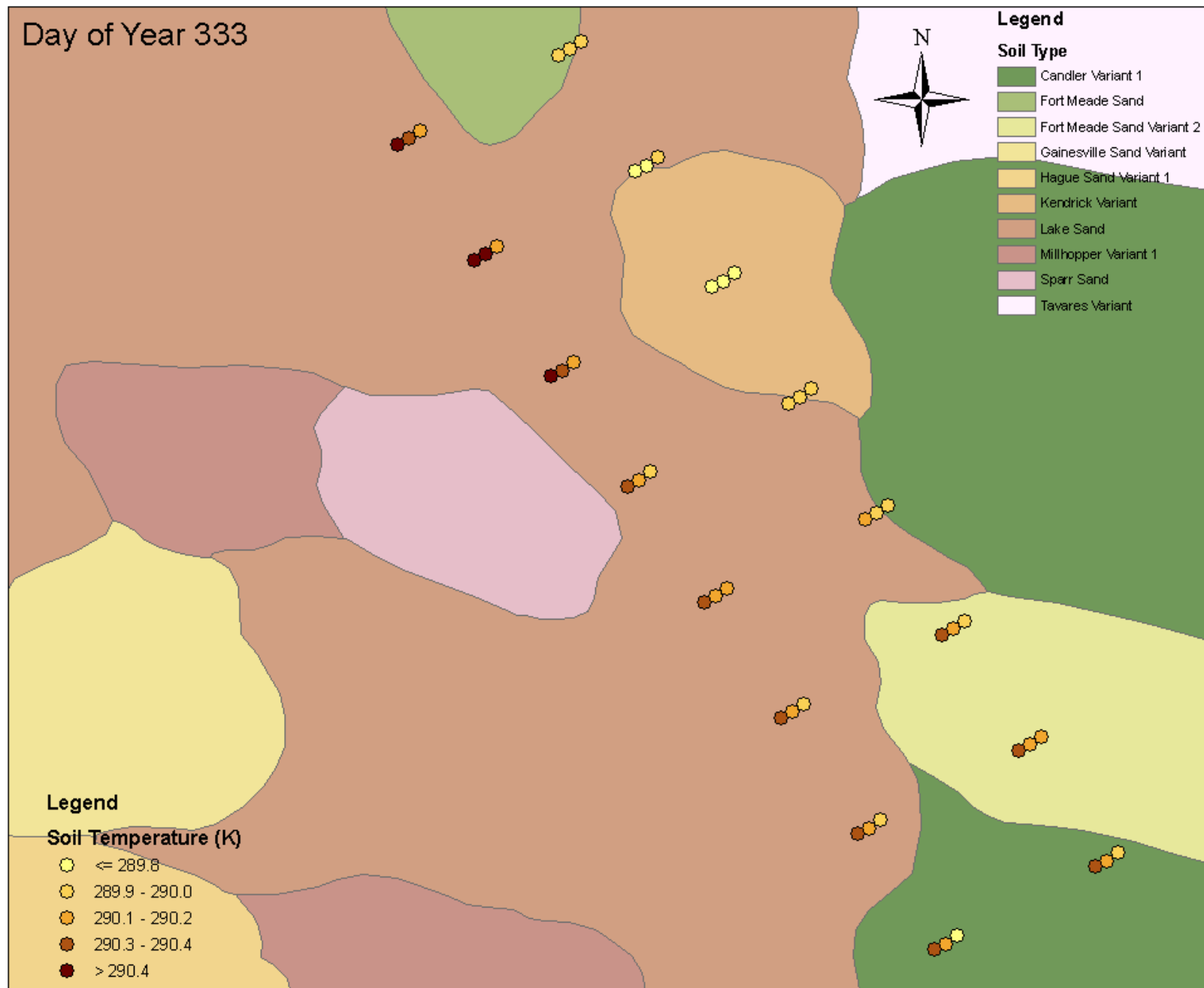


Figure A-51. Soil temperature at depths of 2, 4, and 8cm (left to right) for each designated sampling point, Nov. 28, 2004 (DoY 333)

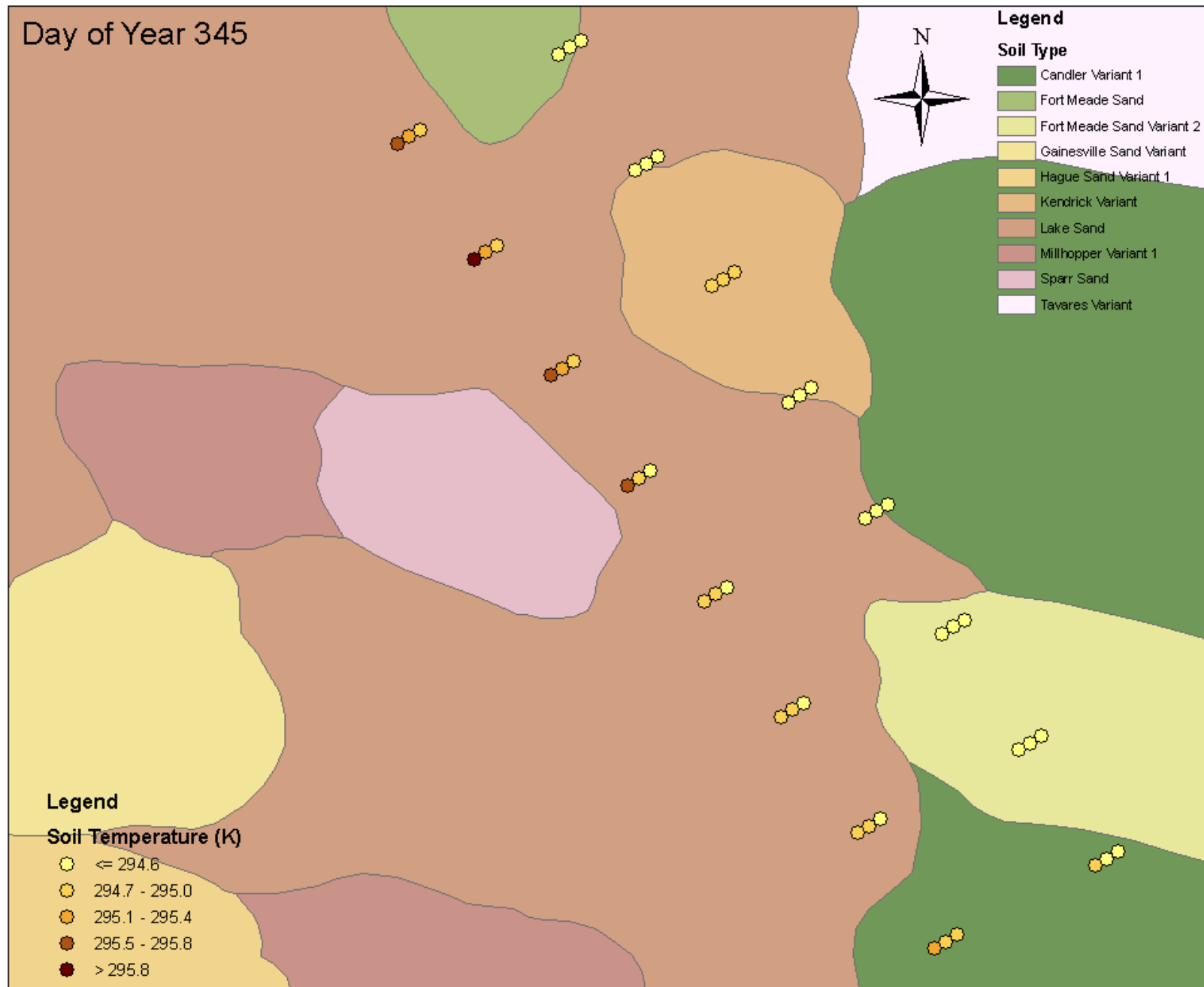


Figure A-52. Soil temperature at depths of 2, 4, and 8cm (left to right) for each designated sampling point, Dec. 10, 2004 (DoY 345)

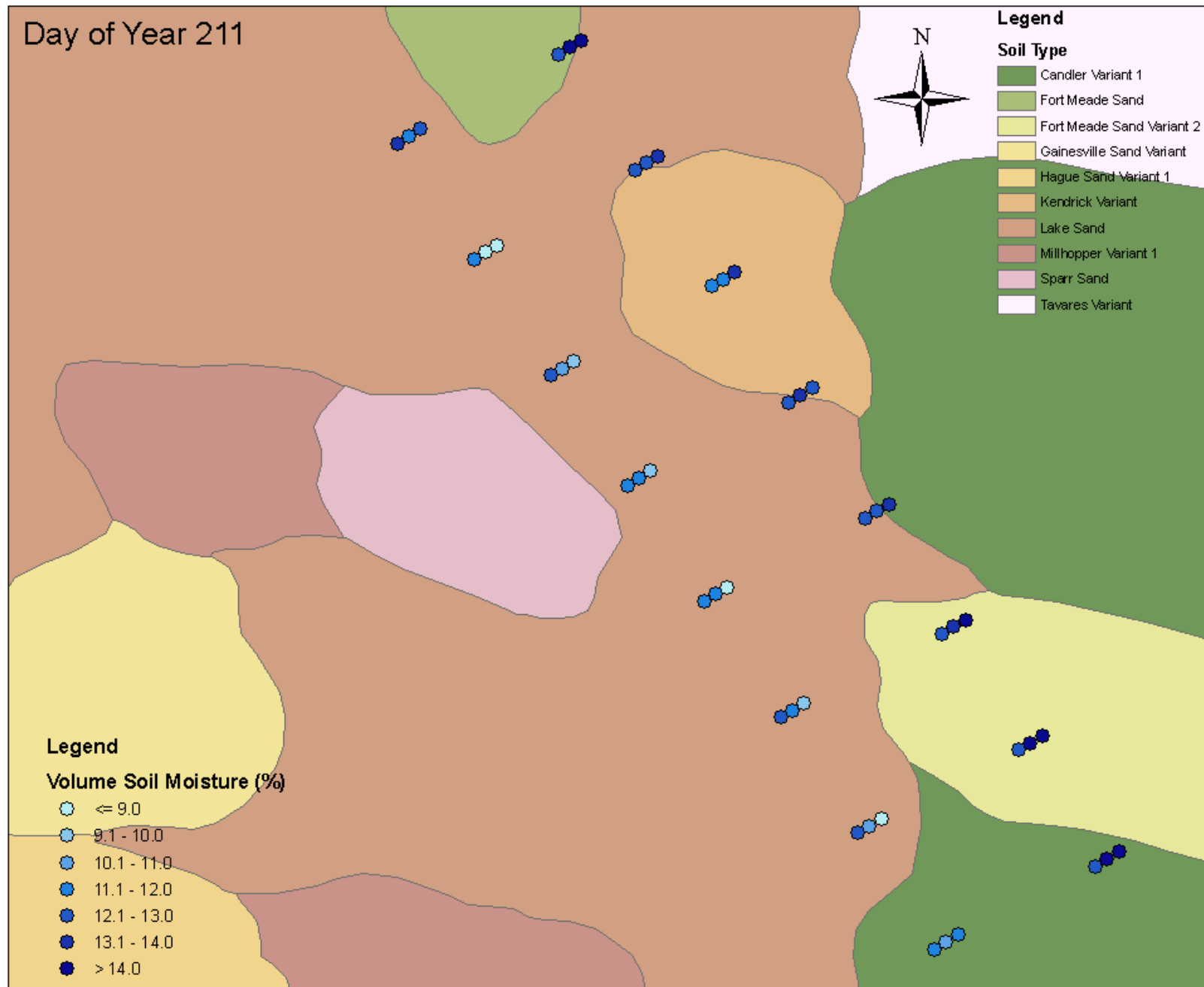


Figure A-53. Soil moisture at in-row; 1/4 row; 1/2 row (left to right) for each designated sampling point, July 29, 2004 (DoY 211)

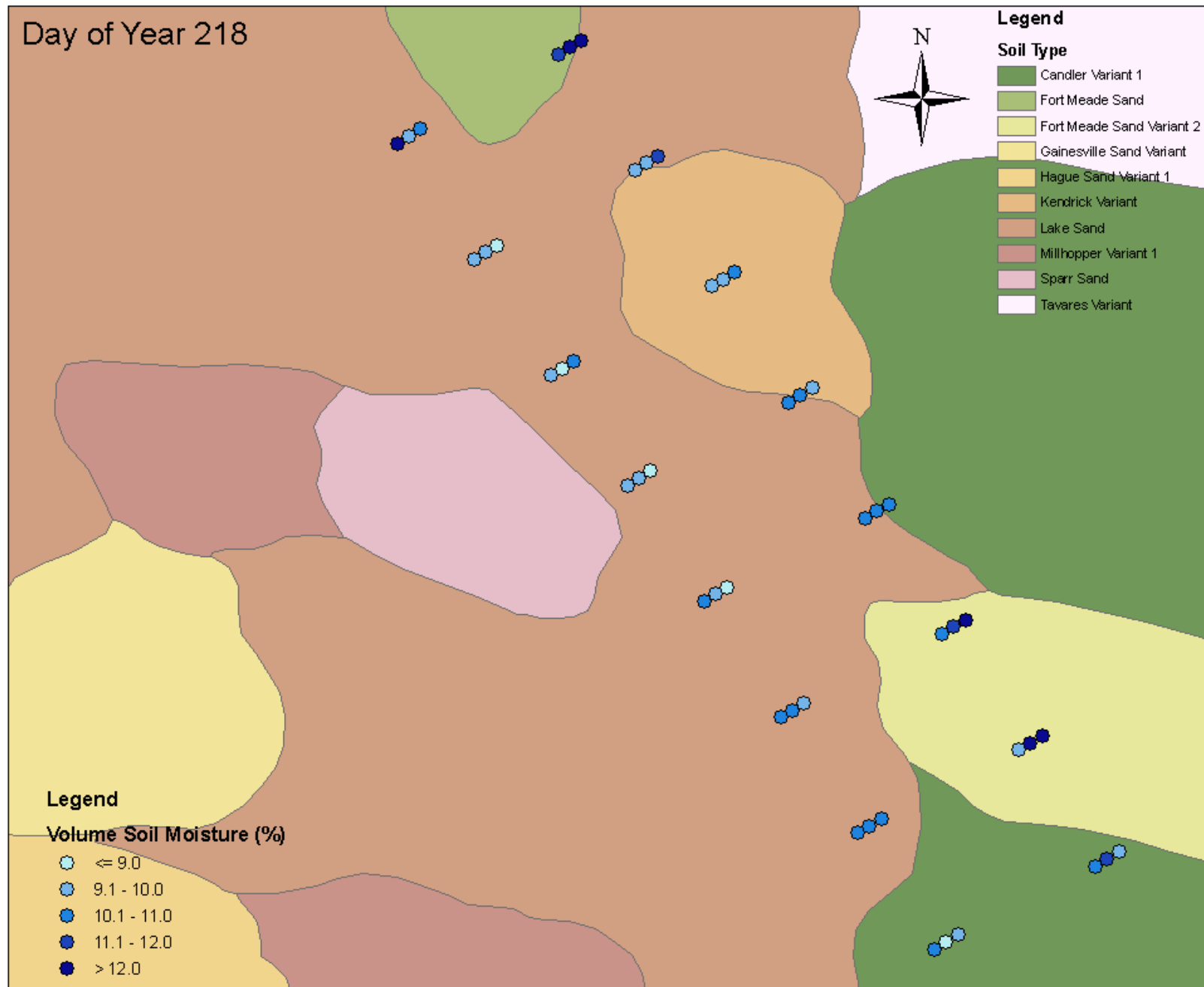


Figure A-54. Soil moisture at in-row; 1/4 row; 1/2 row (left to right) for each designated sampling point, Aug. 05, 2004 (DoY 218)

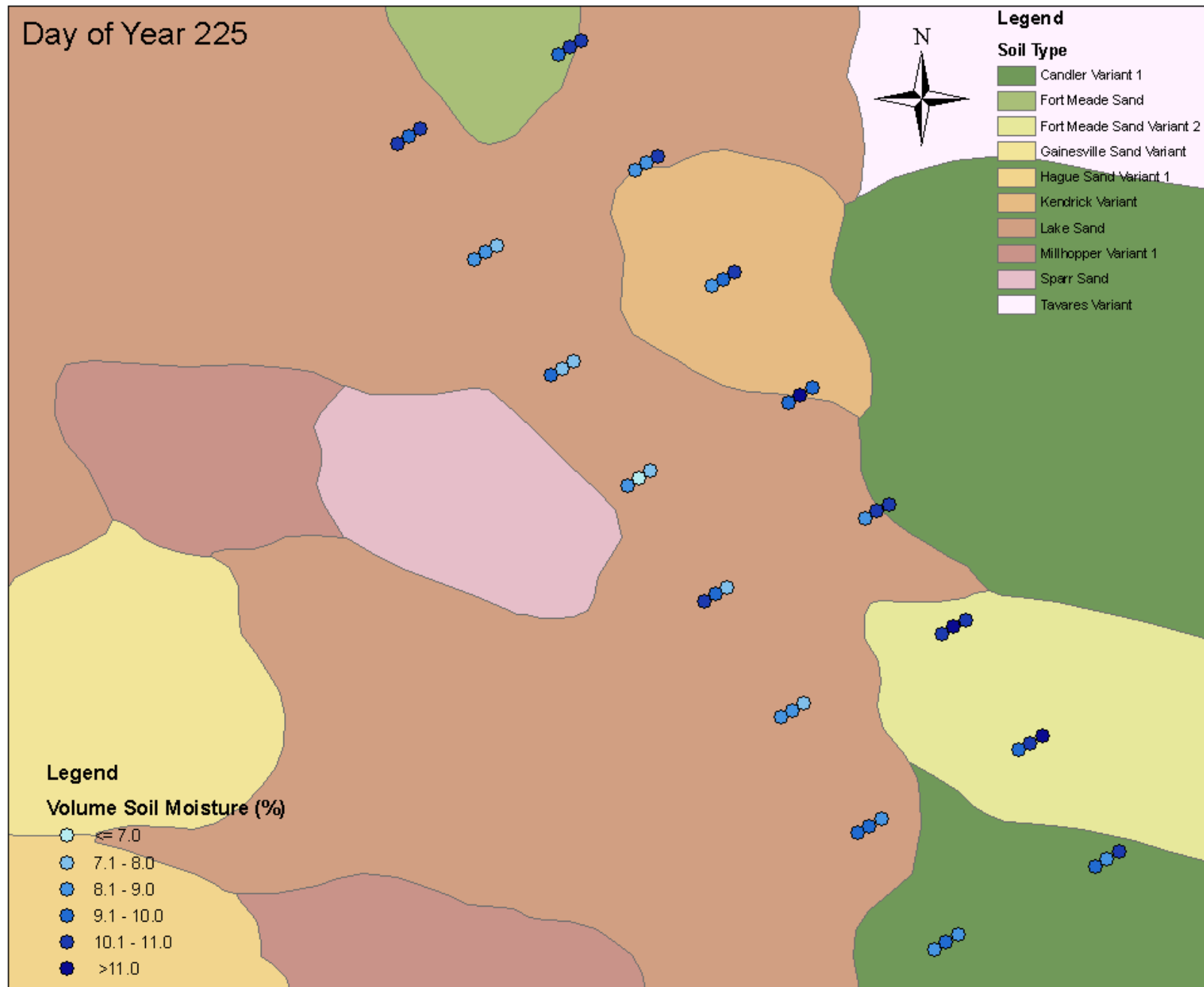


Figure A-55. Soil moisture at in-row; 1/4 row; 1/2 row (left to right) for each designated sampling point, Aug. 12, 2004 (DoY 225)

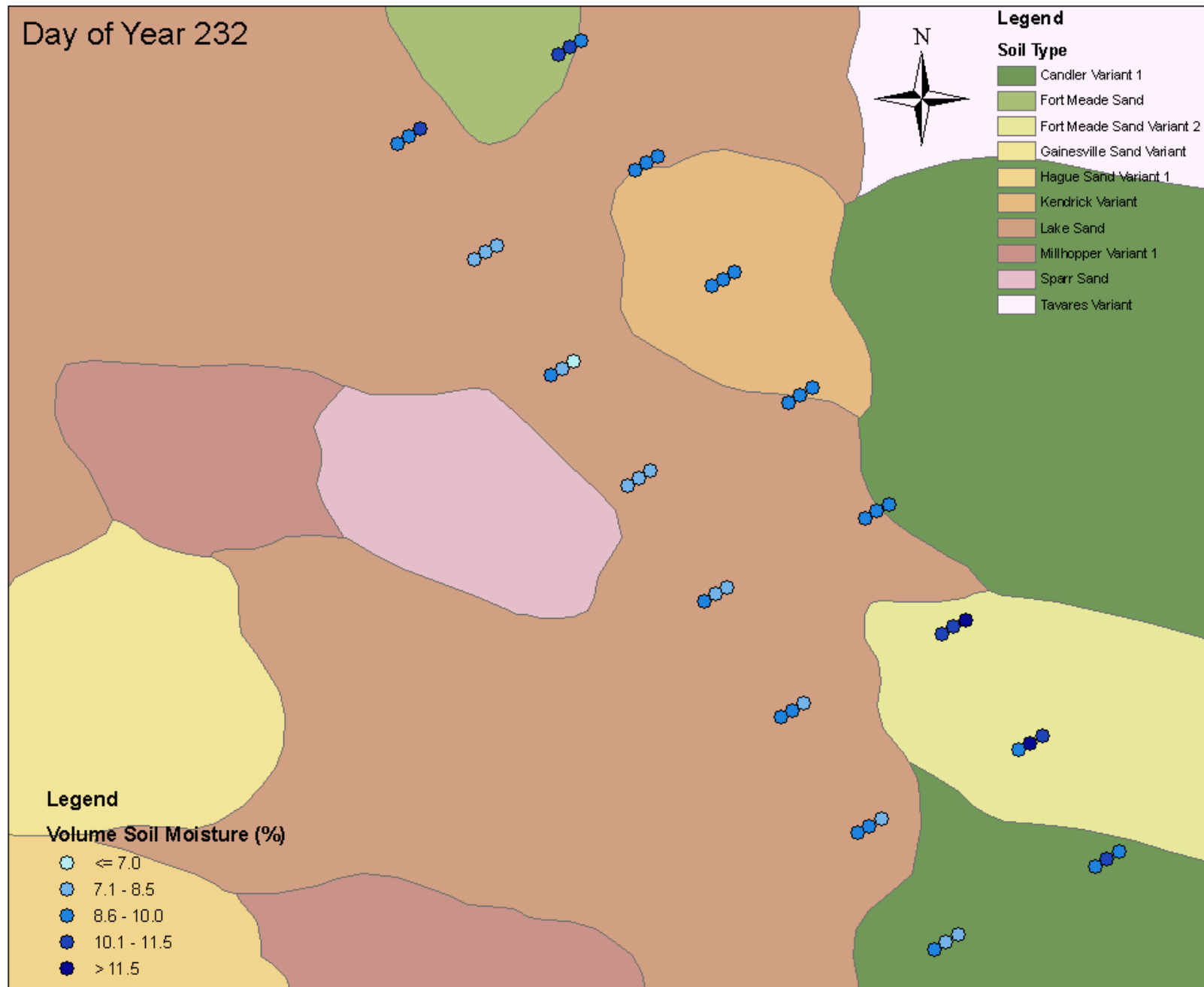


Figure A-56. Soil moisture at in-row; 1/4 row; 1/2 row (left to right) for each designated sampling point, Aug. 19, 2004 (DoY 232)

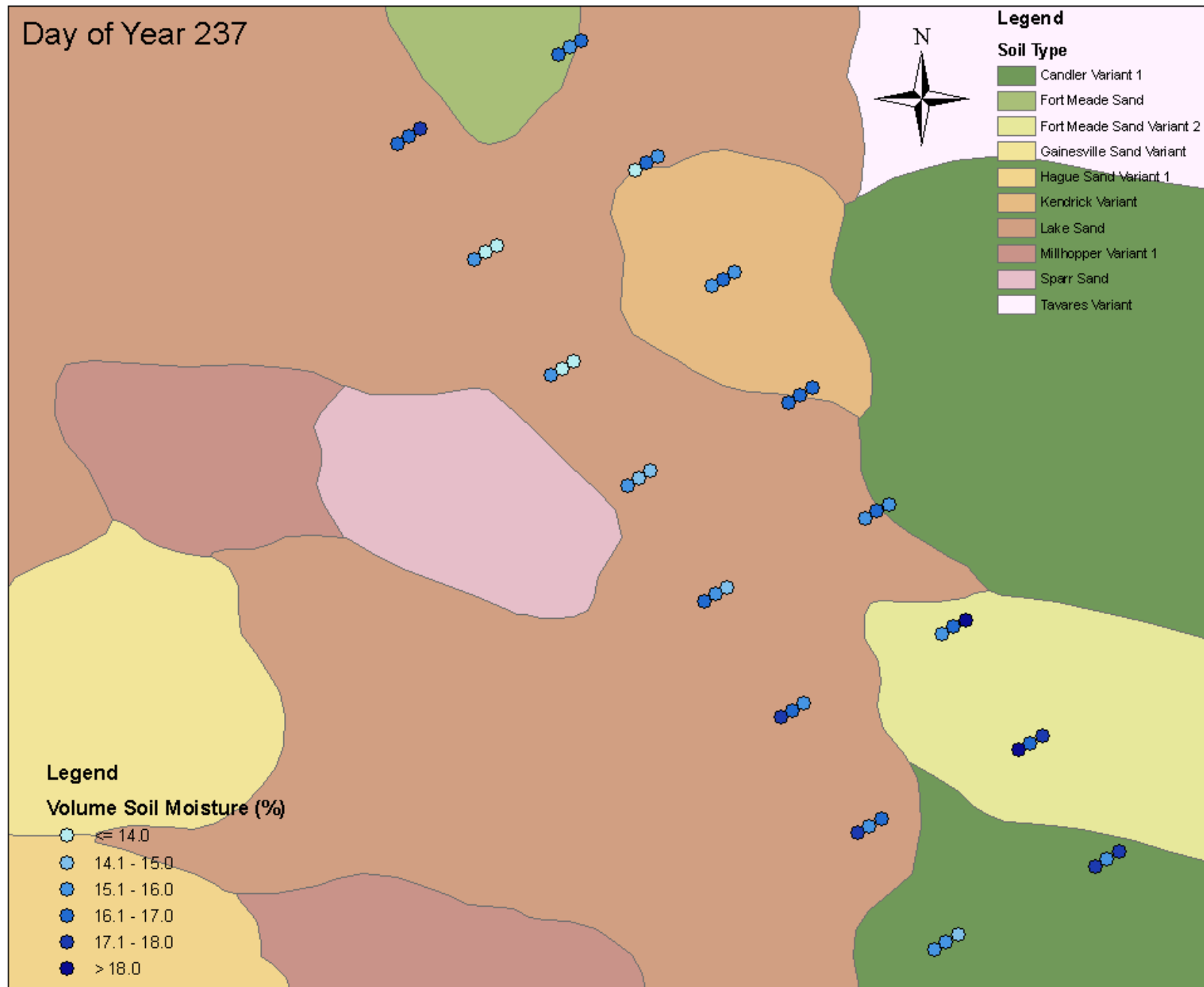


Figure A-57. Soil moisture at in-row; 1/4 row; 1/2 row (left to right) for each designated sampling point, Aug. 24, 2004 (DoY 237)

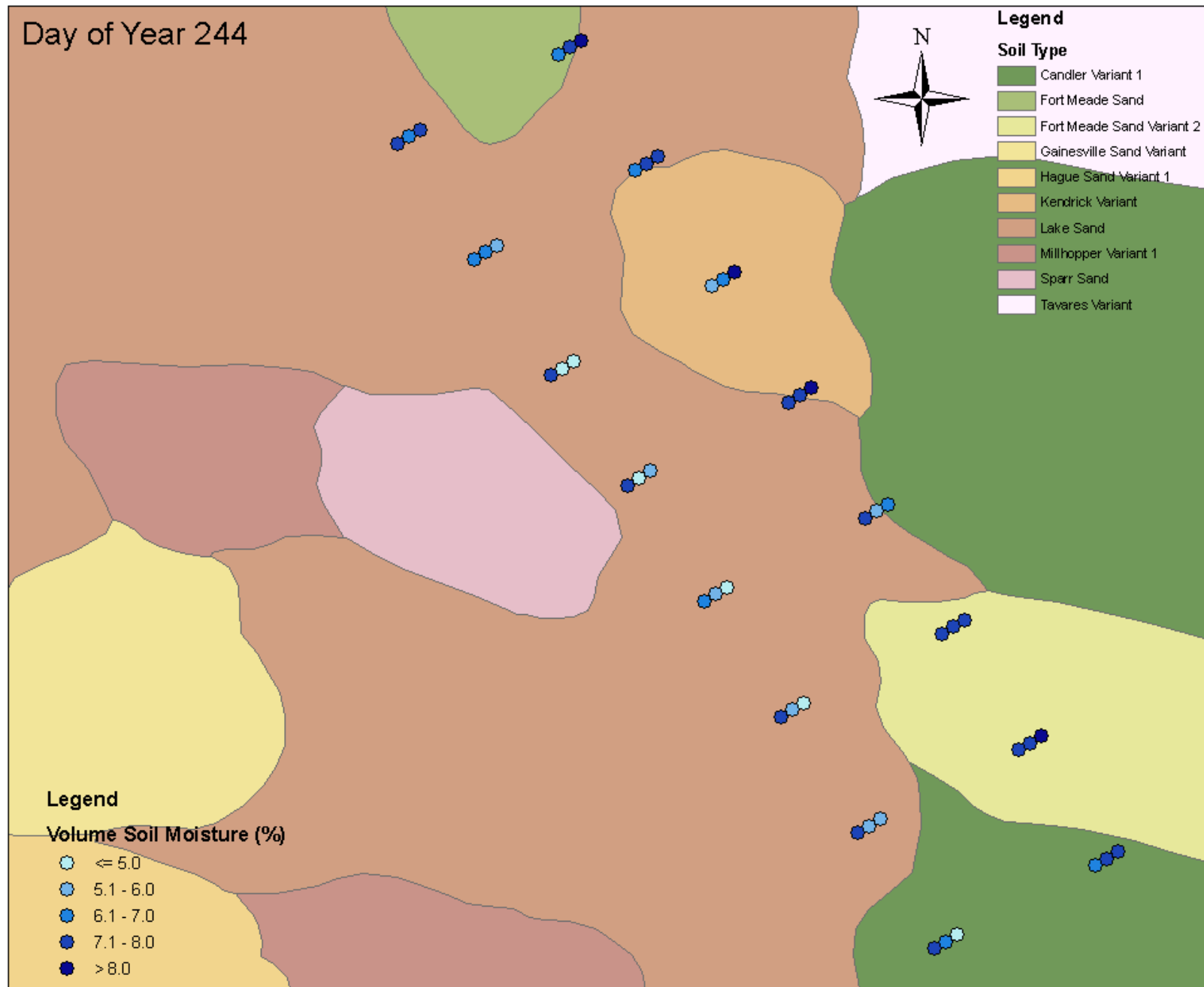


Figure A-58. Soil moisture at in-row; 1/4 row; 1/2 row (left to right) for each designated sampling point, Aug. 31, 2004 (DoY 244)

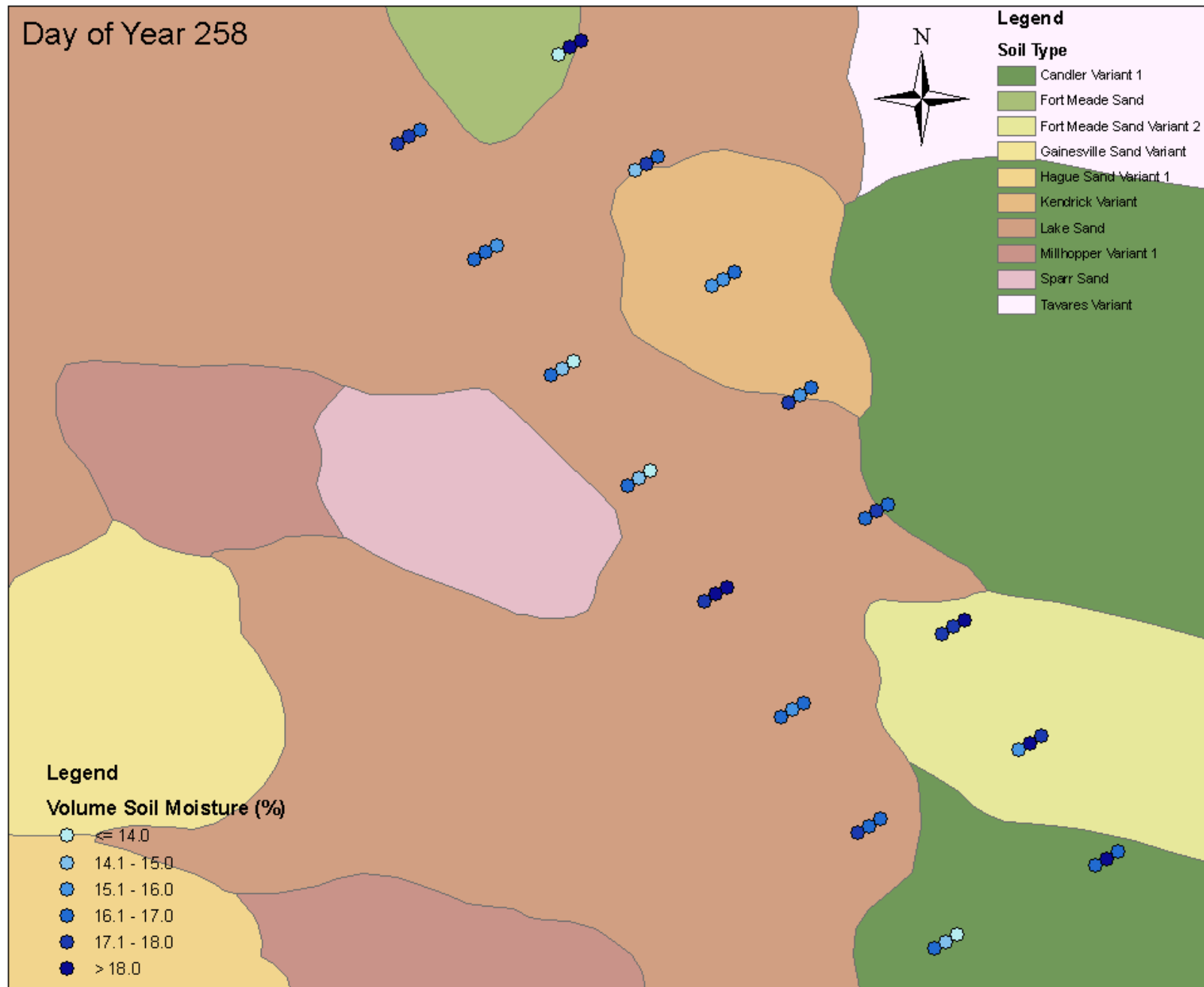


Figure A-59. Soil moisture at in-row; 1/4 row; 1/2 row (left to right) for each designated sampling point, Sep. 14, 2004 (DoY 258)

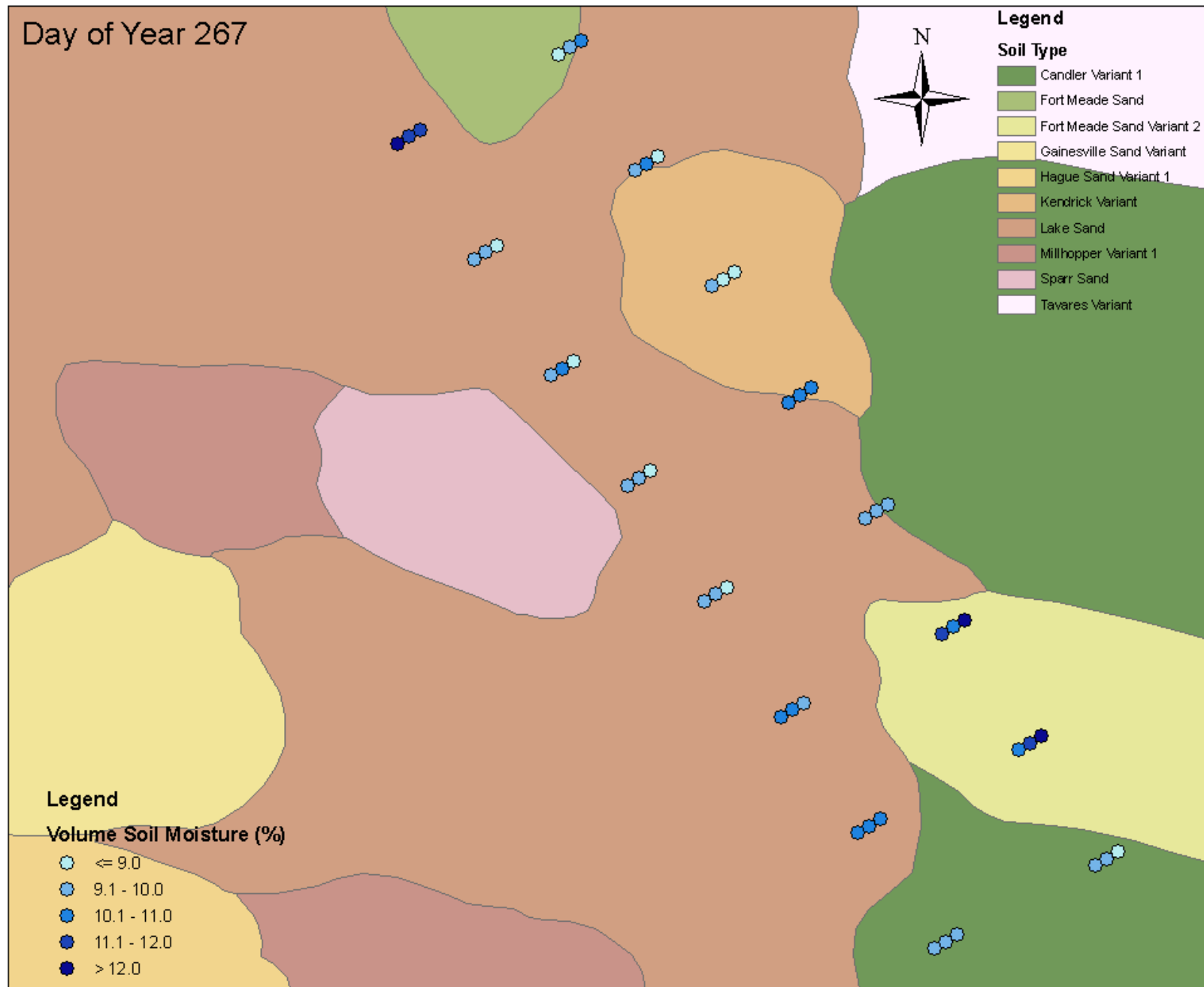


Figure A-60. Soil moisture at in-row; 1/4 row; 1/2 row (left to right) for each designated sampling point, Sep. 23, 2004 (DoY 267)

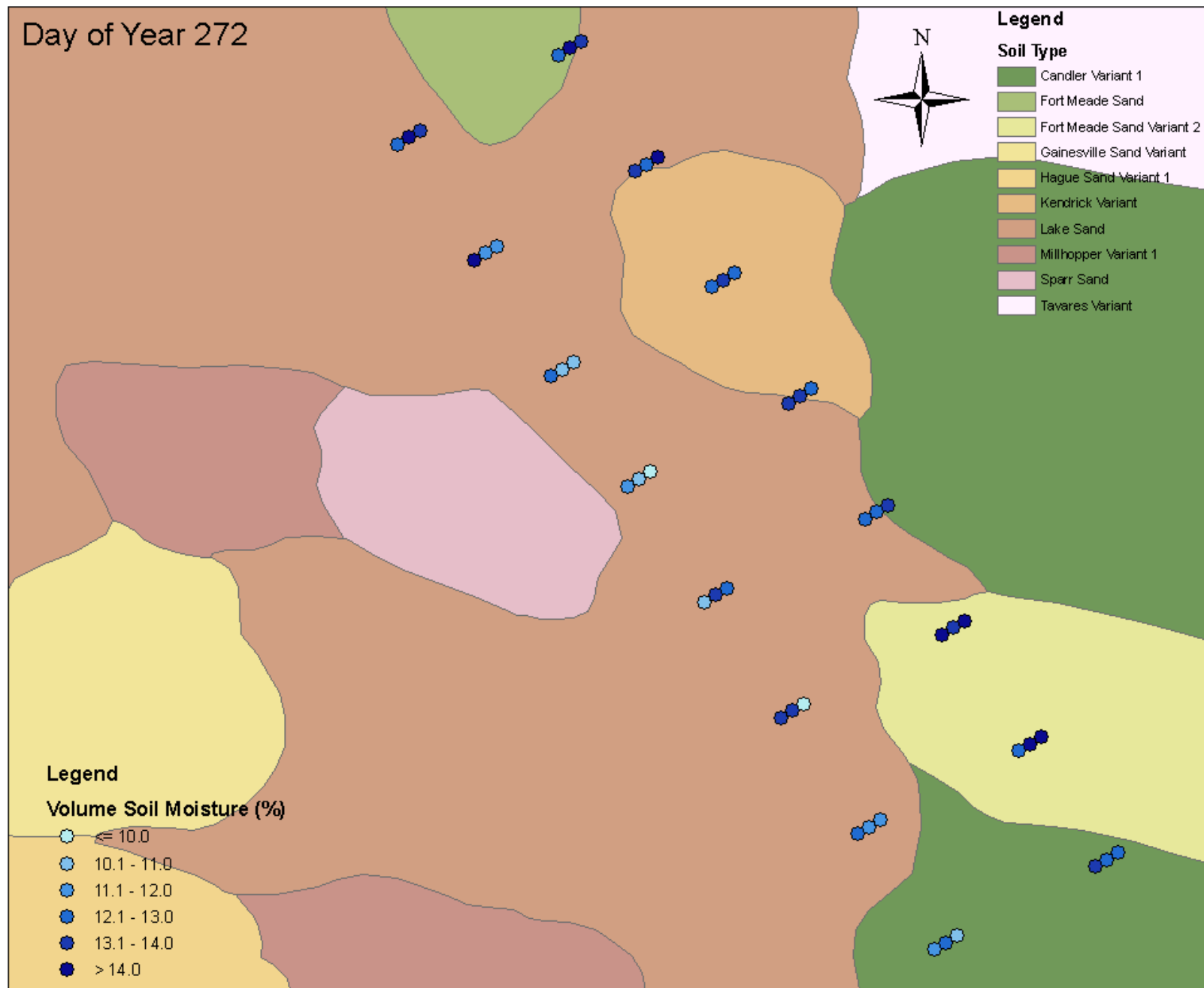


Figure A-61. Soil moisture at in-row; 1/4 row; 1/2 row (left to right) for each designated sampling point, Sep. 28, 2004 (DoY 272)

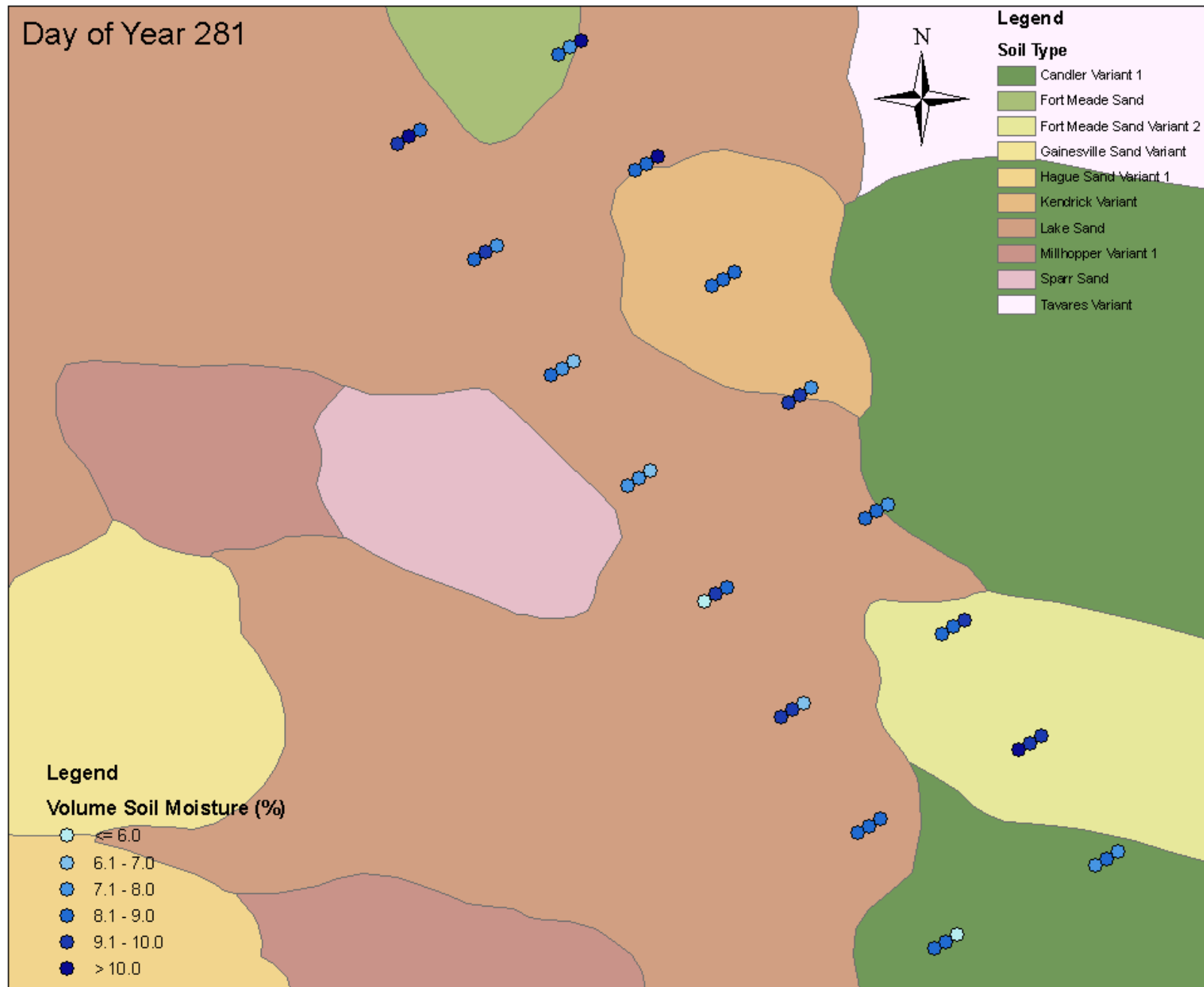


Figure A-62. Soil moisture at in-row; 1/4 row; 1/2 row (left to right) for each designated sampling point, Oct. 07, 2004 (DoY 281)

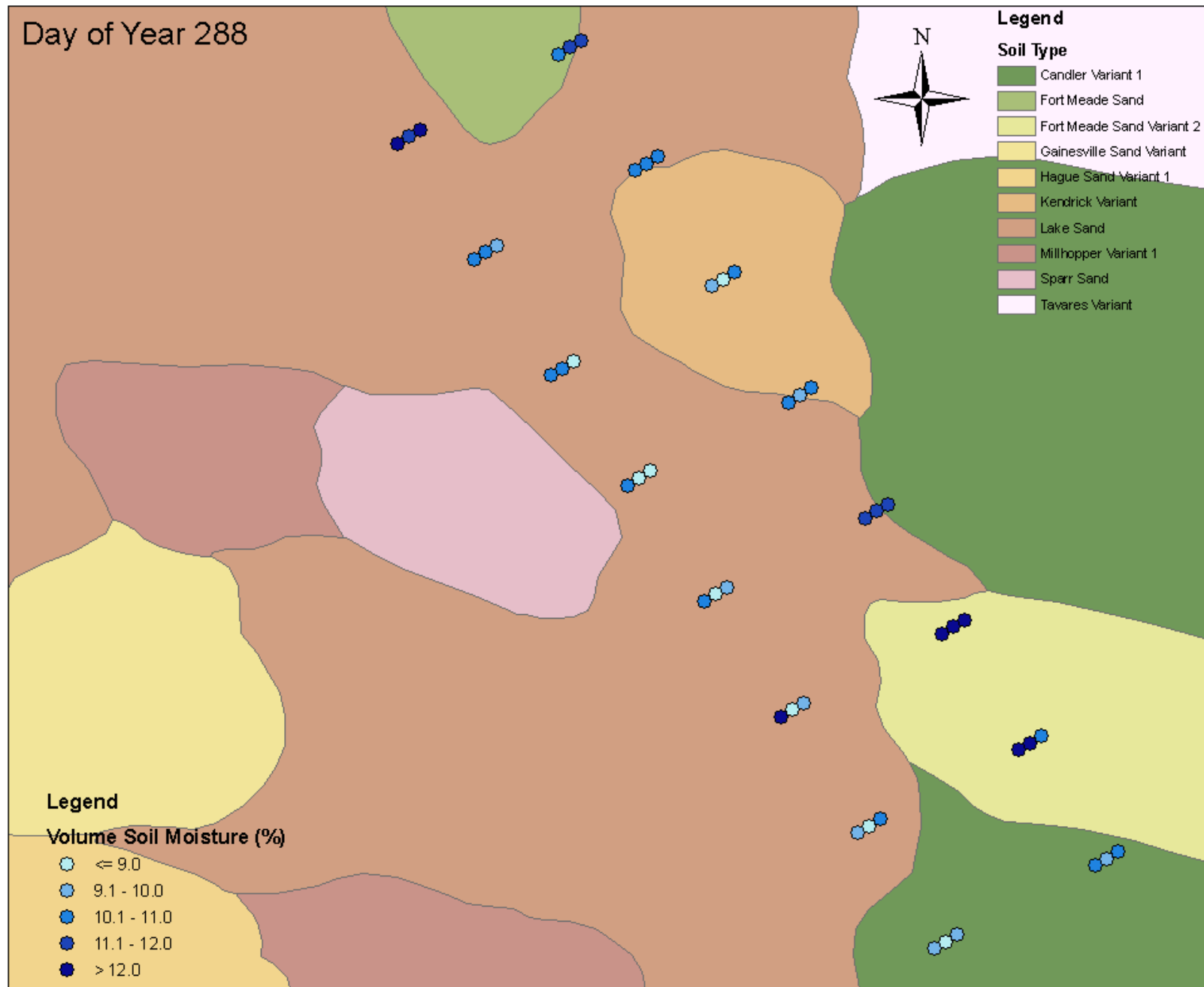


Figure A-63. Soil moisture at in-row; 1/4 row; 1/2 row (left to right) for each designated sampling point, Oct. 14, 2004 (DoY 288)

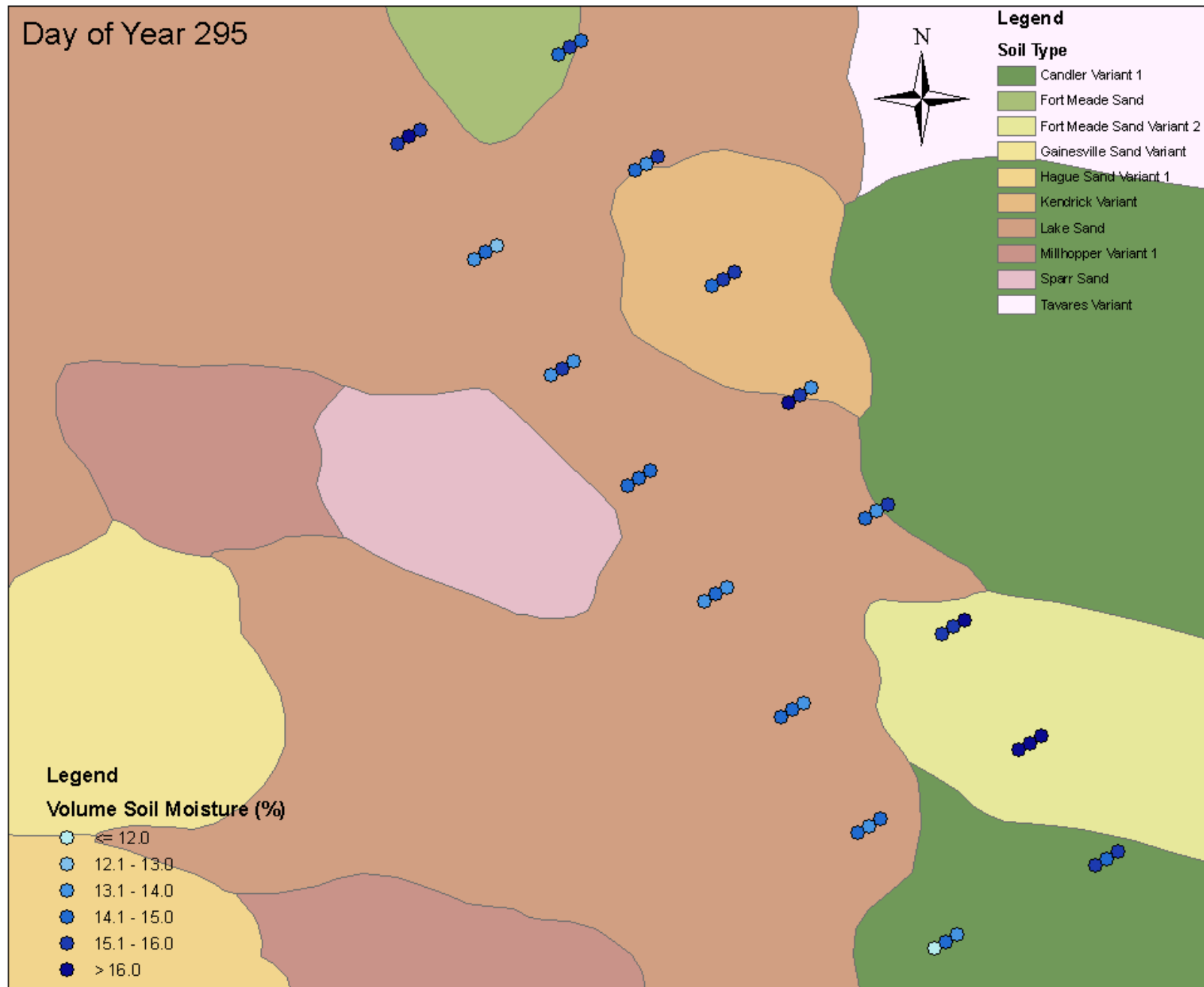


Figure A-64. Soil moisture at in-row; 1/4 row; 1/2 row (left to right) for each designated sampling point, Oct. 21, 2004 (DoY 295)

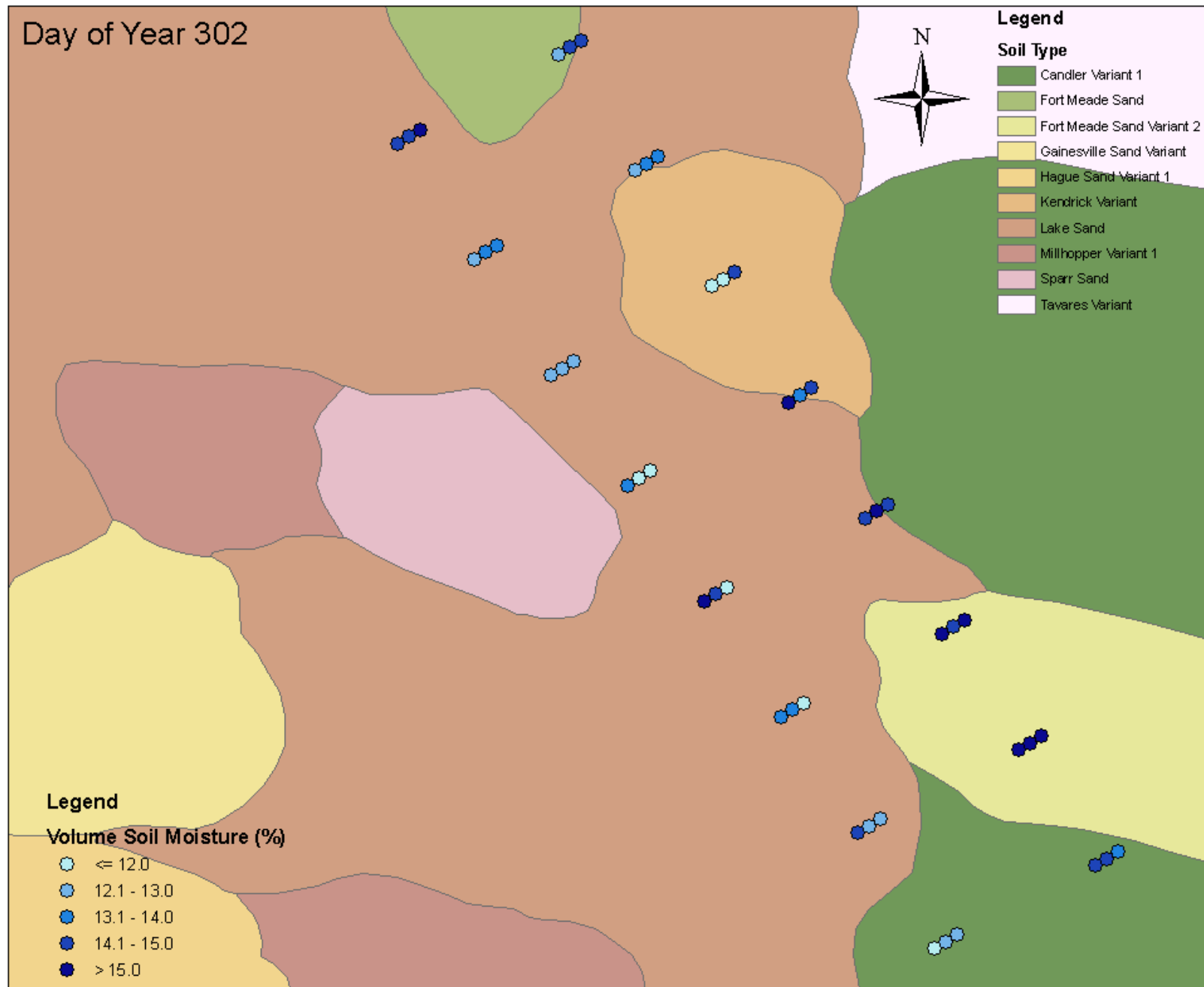


Figure A-65. Soil moisture at in-row; 1/4 row; 1/2 row (left to right) for each designated sampling point, Oct. 28, 2004 (DoY 302)

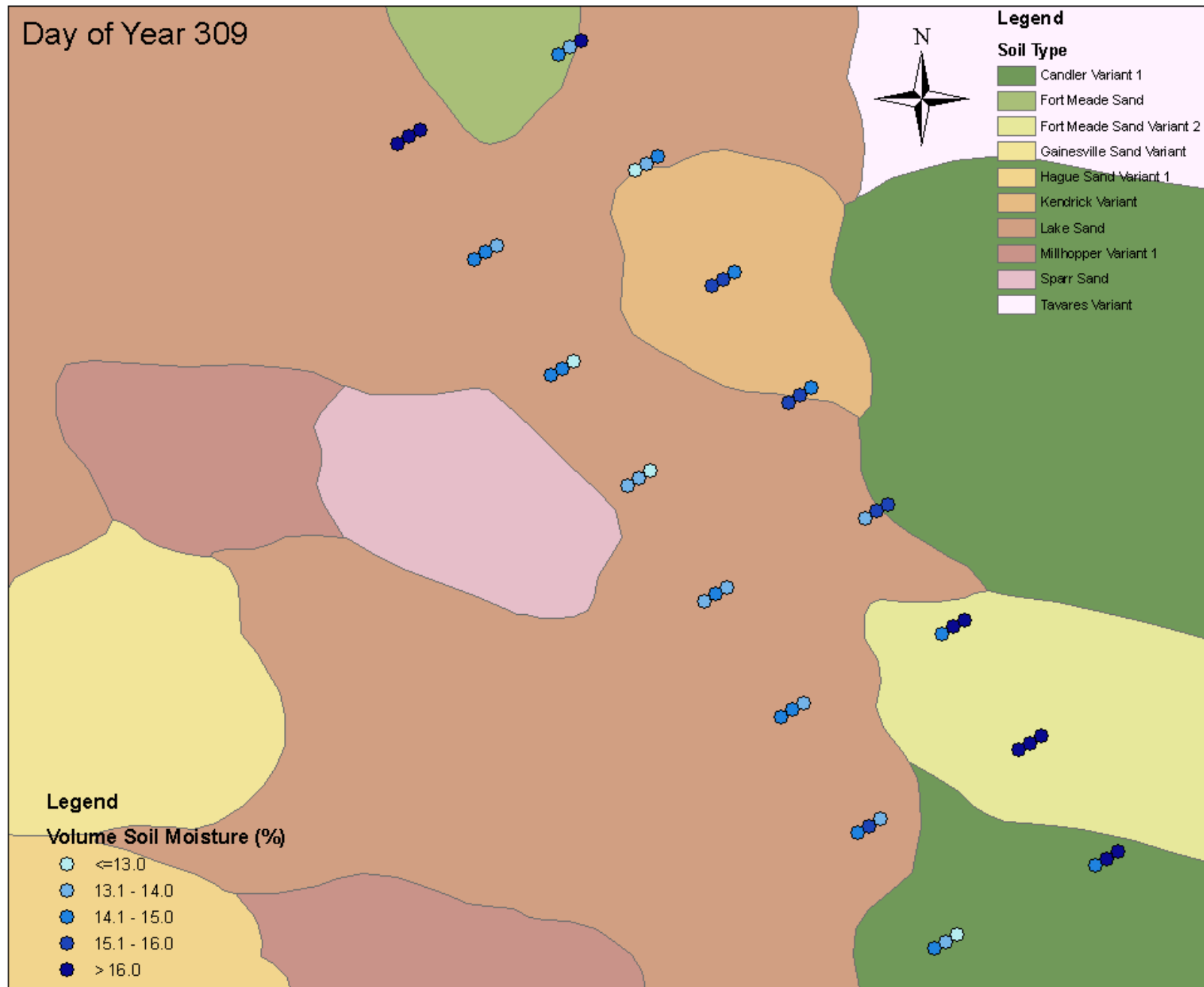


Figure A-66. Soil moisture at in-row; 1/4 row; 1/2 row (left to right) for each designated sampling point, Nov. 04, 2004 (DoY 309)

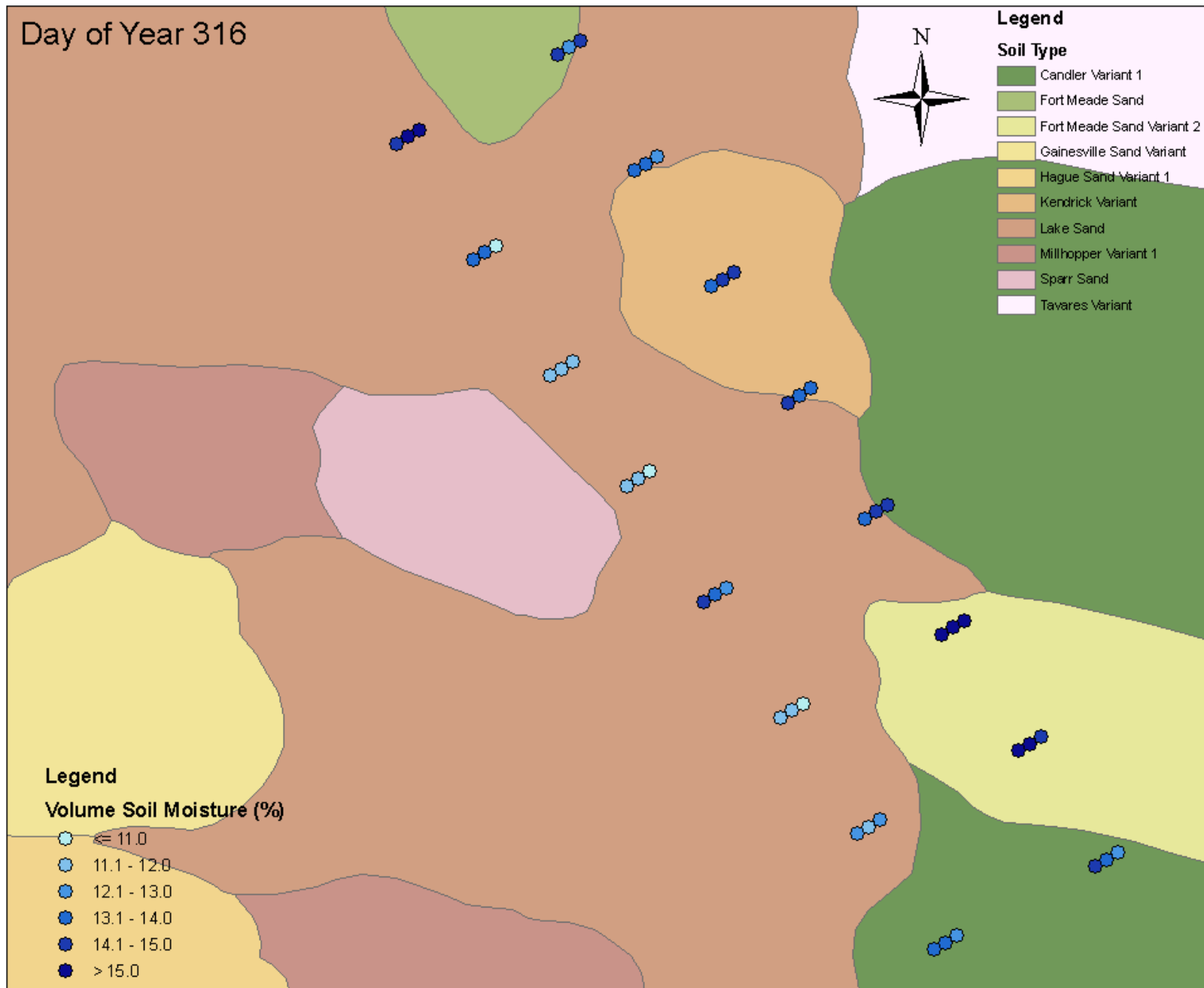


Figure A-67. Soil moisture at in-row; 1/4 row; 1/2 row (left to right) for each designated sampling point, Nov. 11, 2004 (DoY 316)

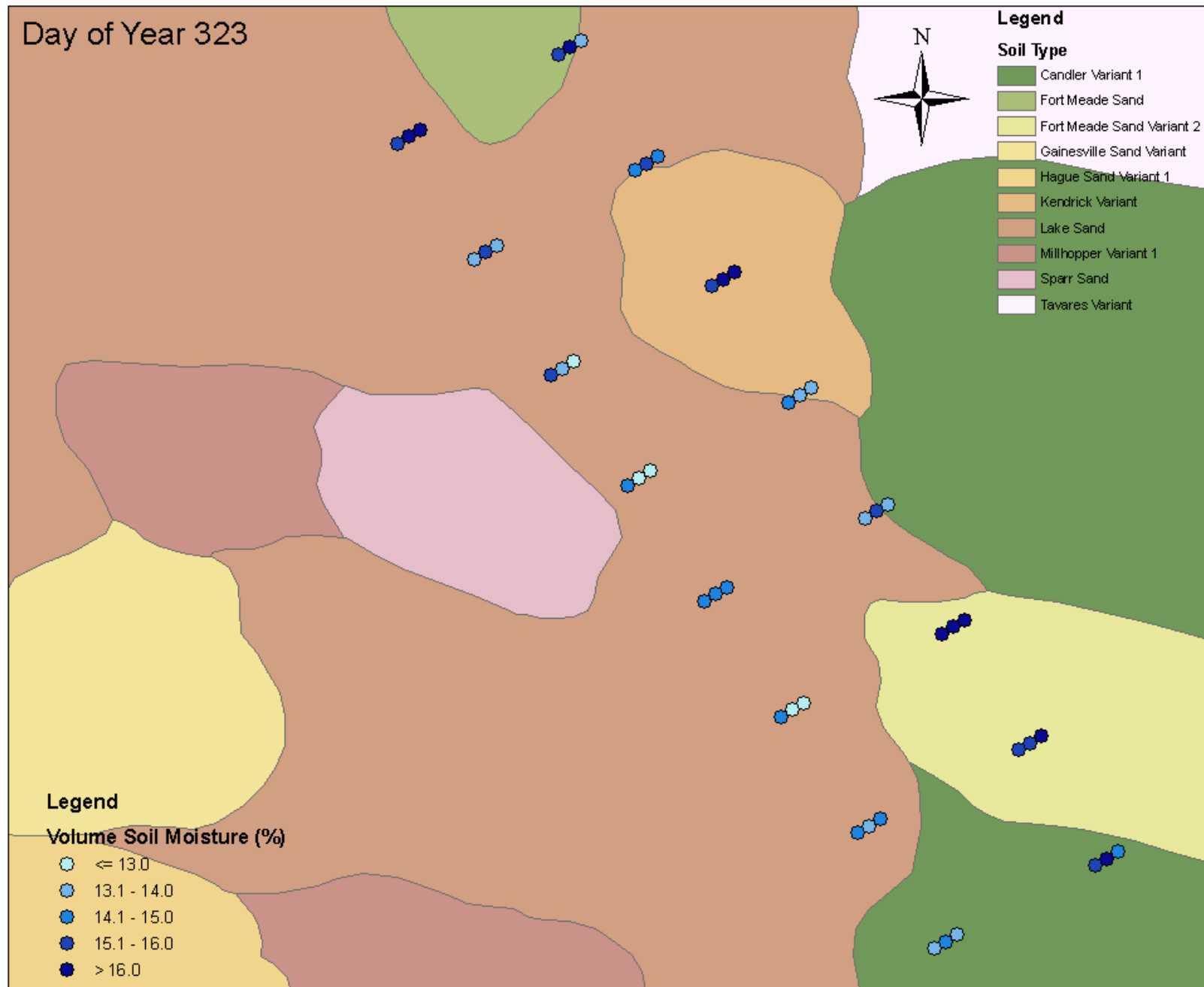


Figure A-68. Soil moisture at in-row; 1/4 row; 1/2 row (left to right) for each designated sampling point, Nov. 18, 2004 (DoY 323)

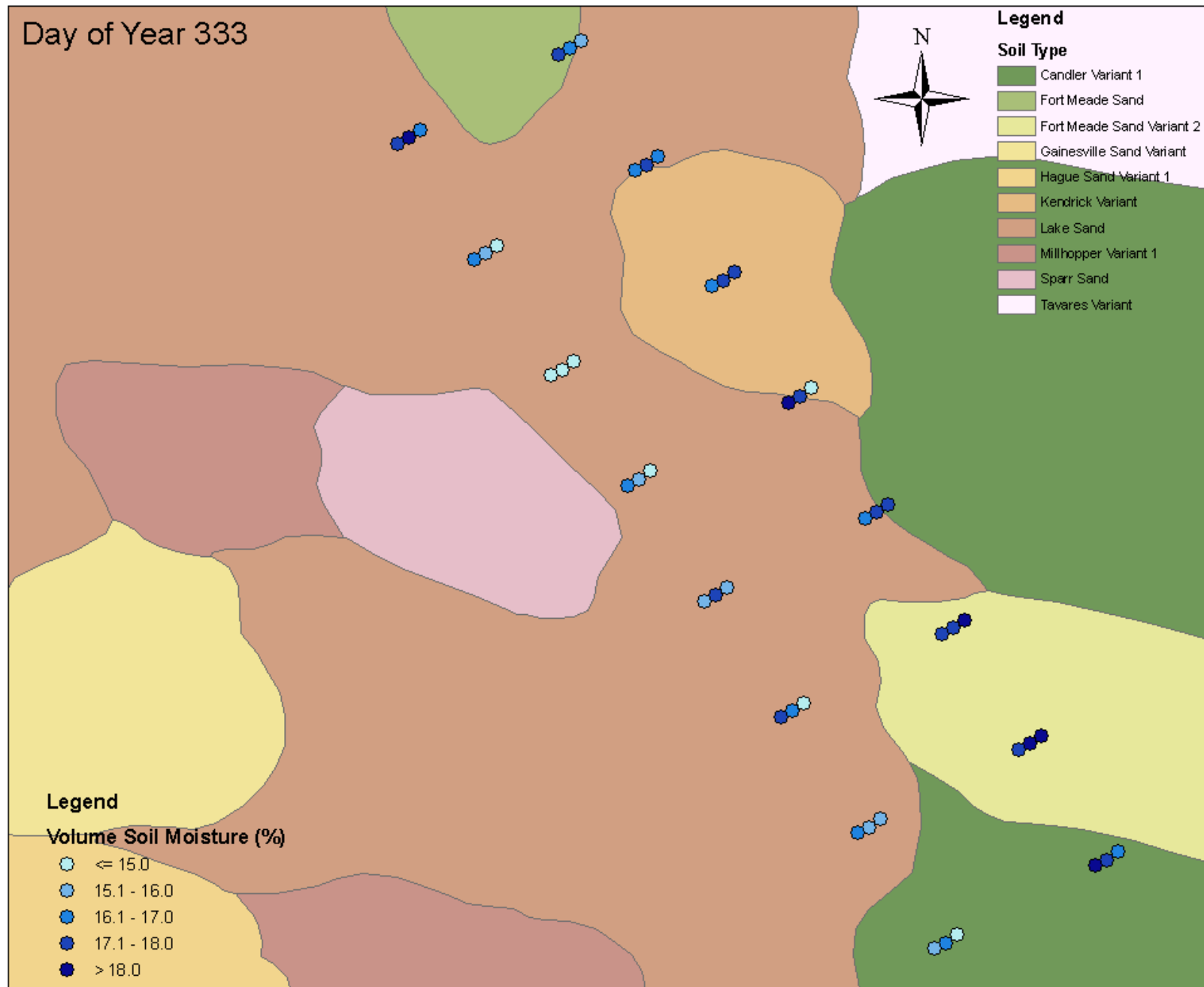


Figure A-69. Soil moisture at in-row; 1/4 row; 1/2 row (left to right) for each designated sampling point, Nov. 28, 2004 (DoY 333)

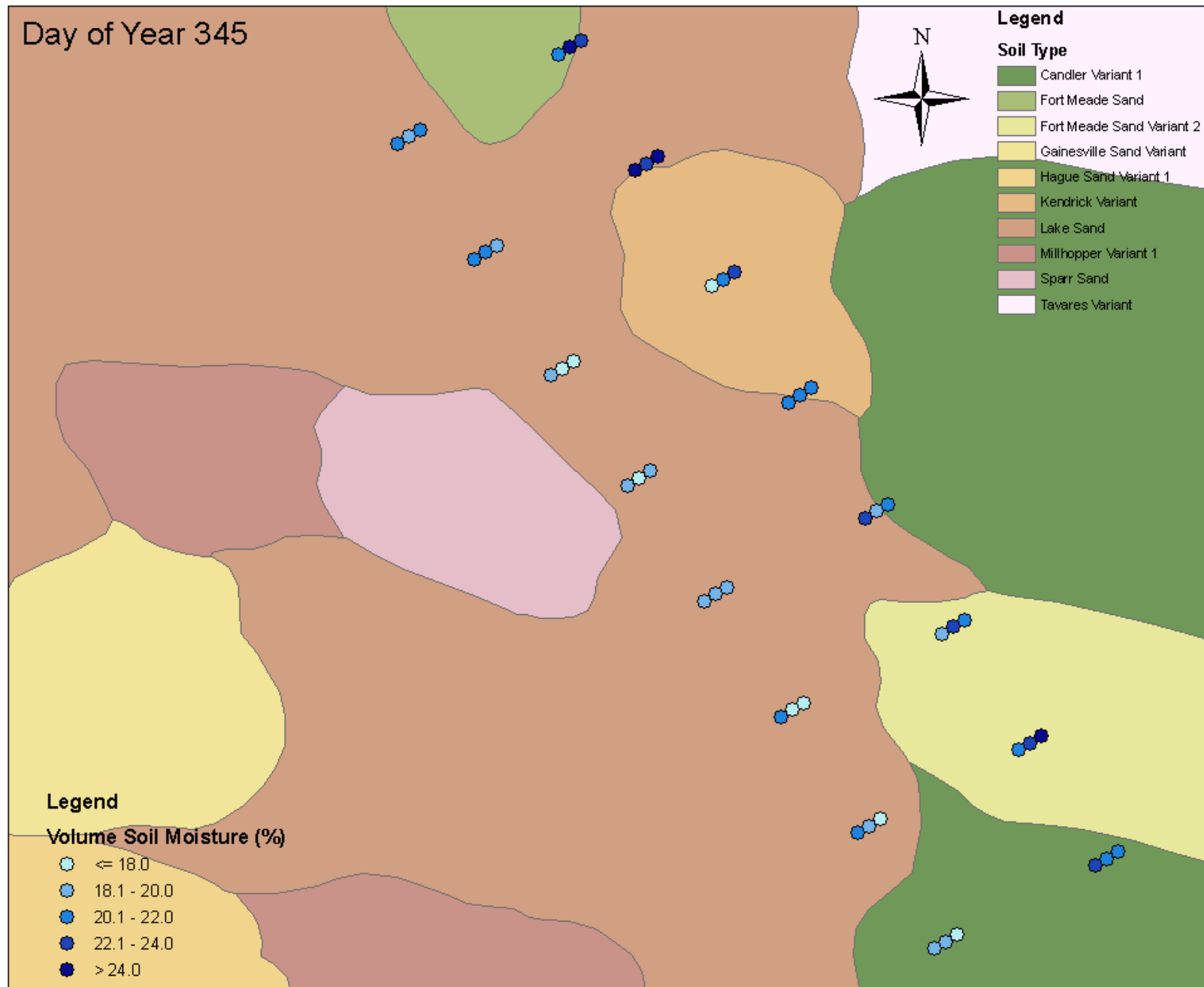


Figure A-70. Soil moisture at in-row; 1/4 row; 1/2 row (left to right) for each designated sampling point, Dec. 10, 2004 (DoY 345)

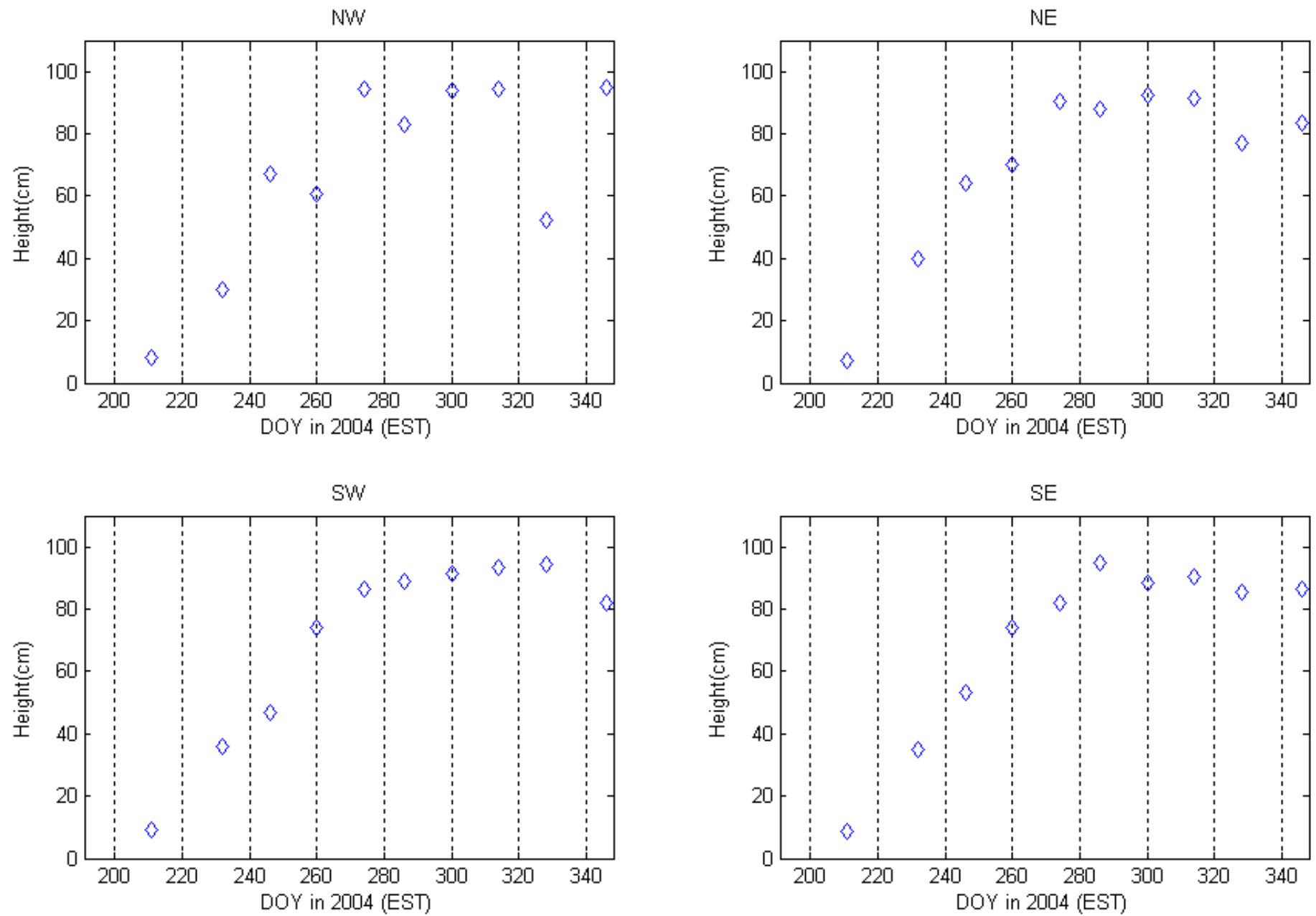


Figure A-71. Average crop heights at vegetation sampling areas

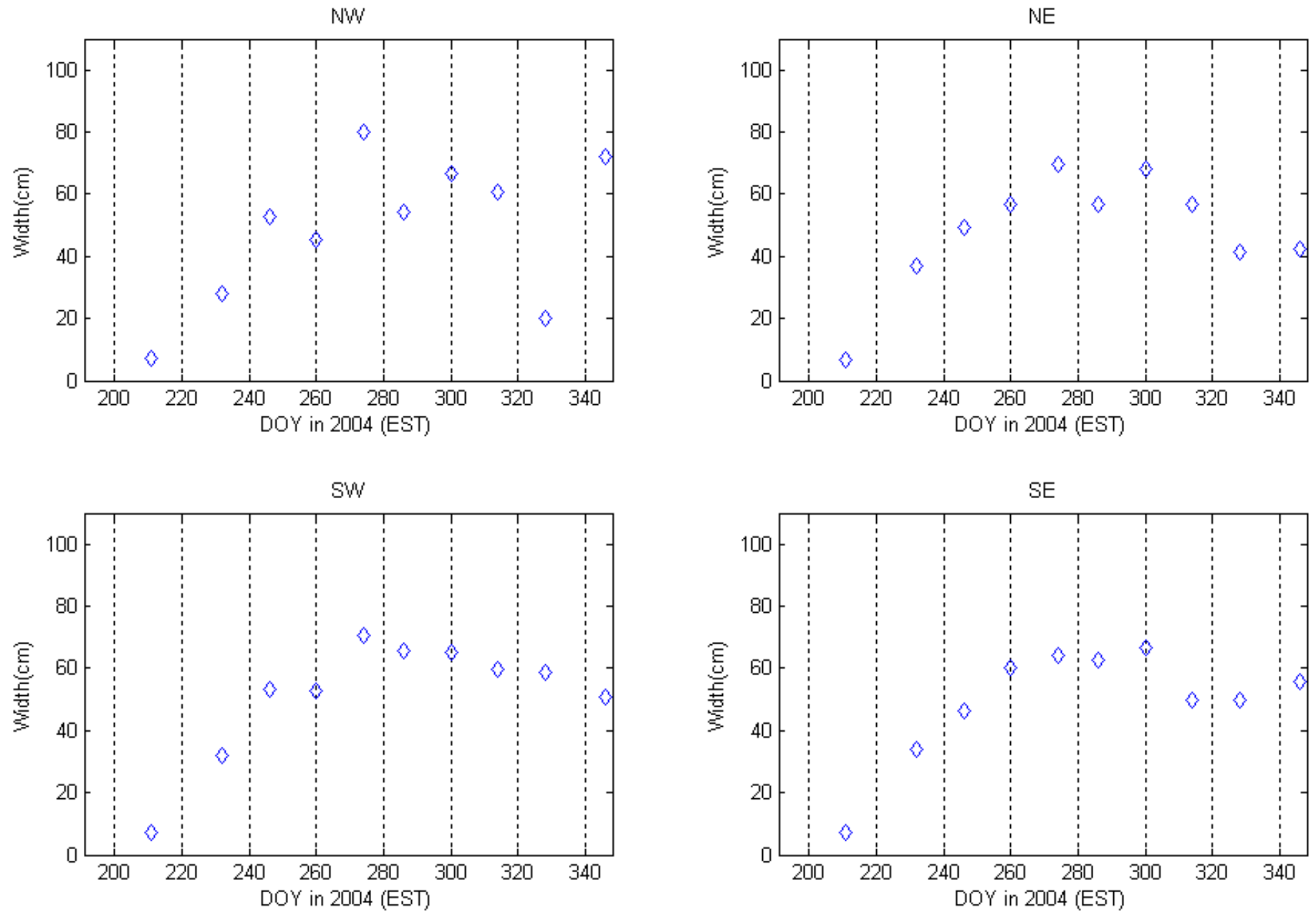


Figure A-72. Average crop widths at vegetation sampling areas

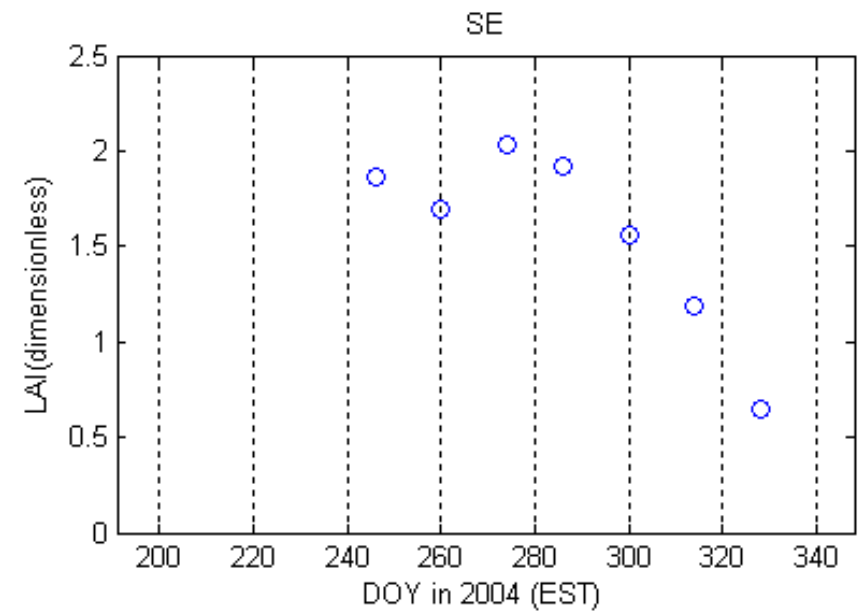
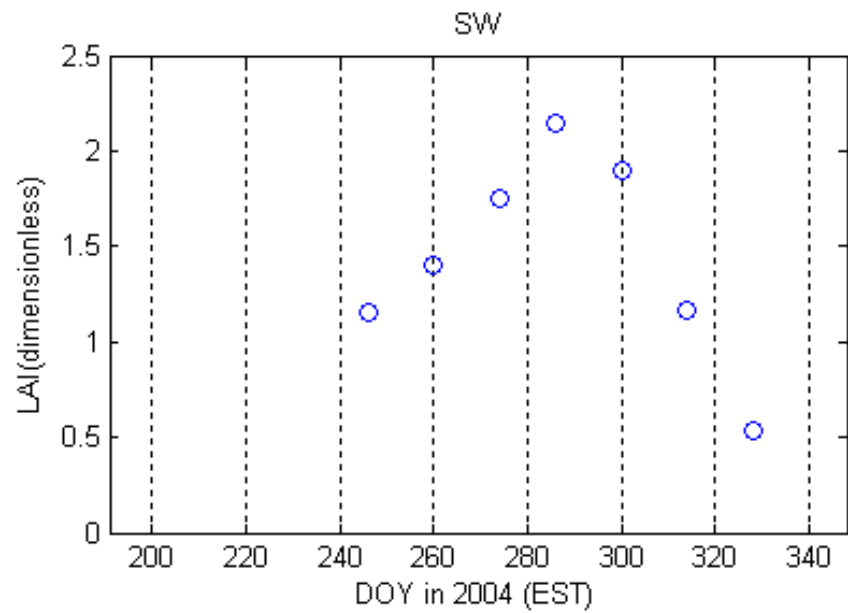
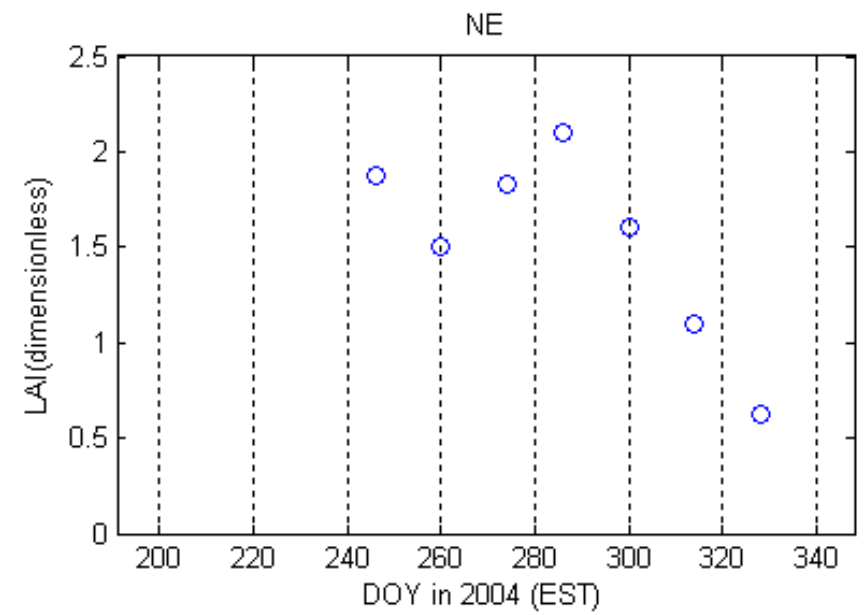
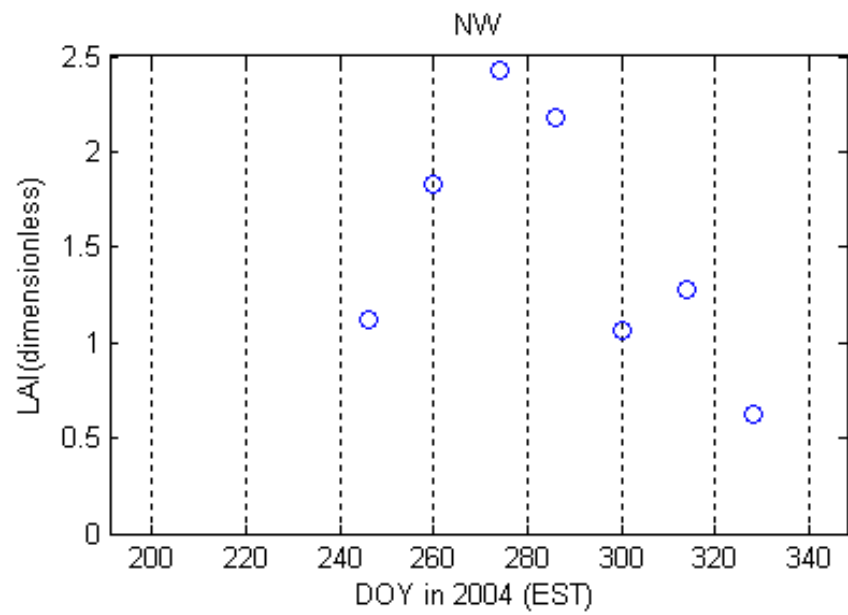


Figure A-73. LAI at vegetation sampling areas

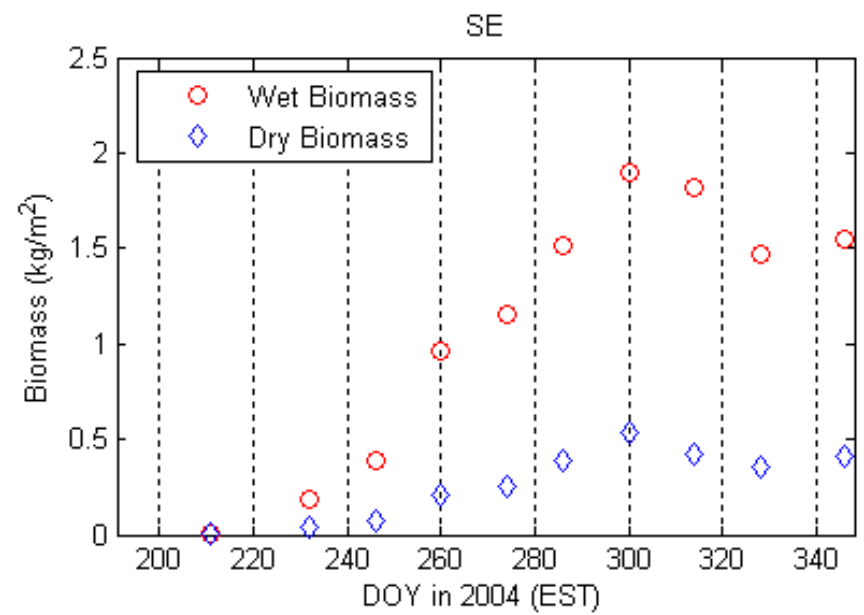
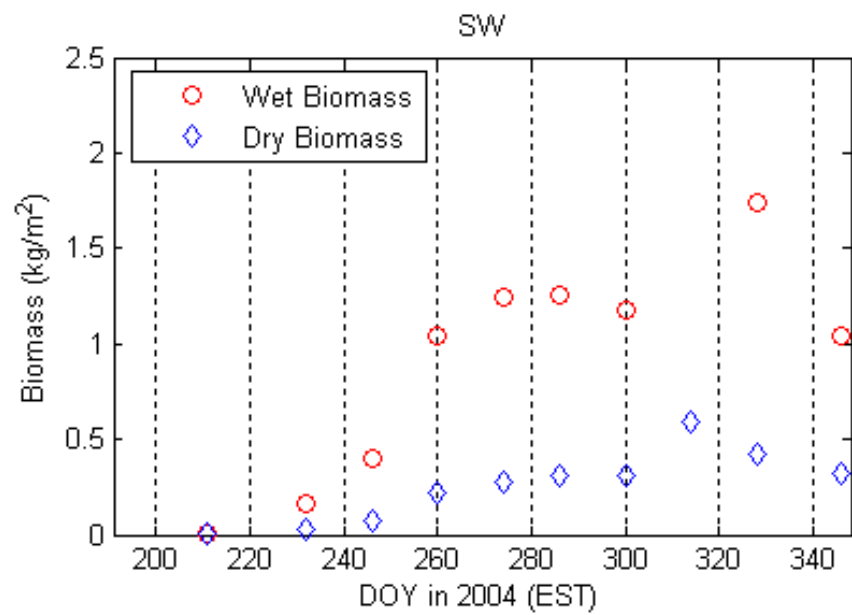
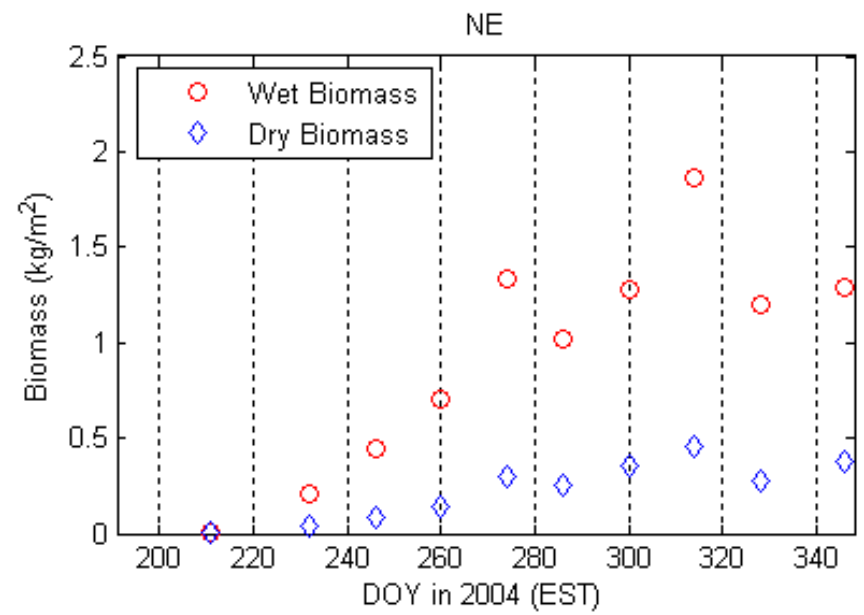
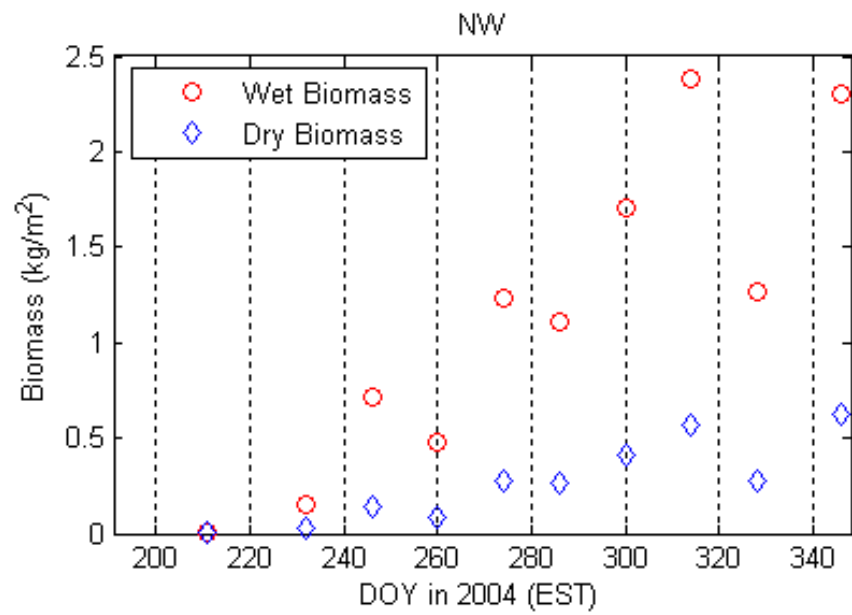


Figure A-74. Wet biomass and dry biomass at vegetation sampling areas

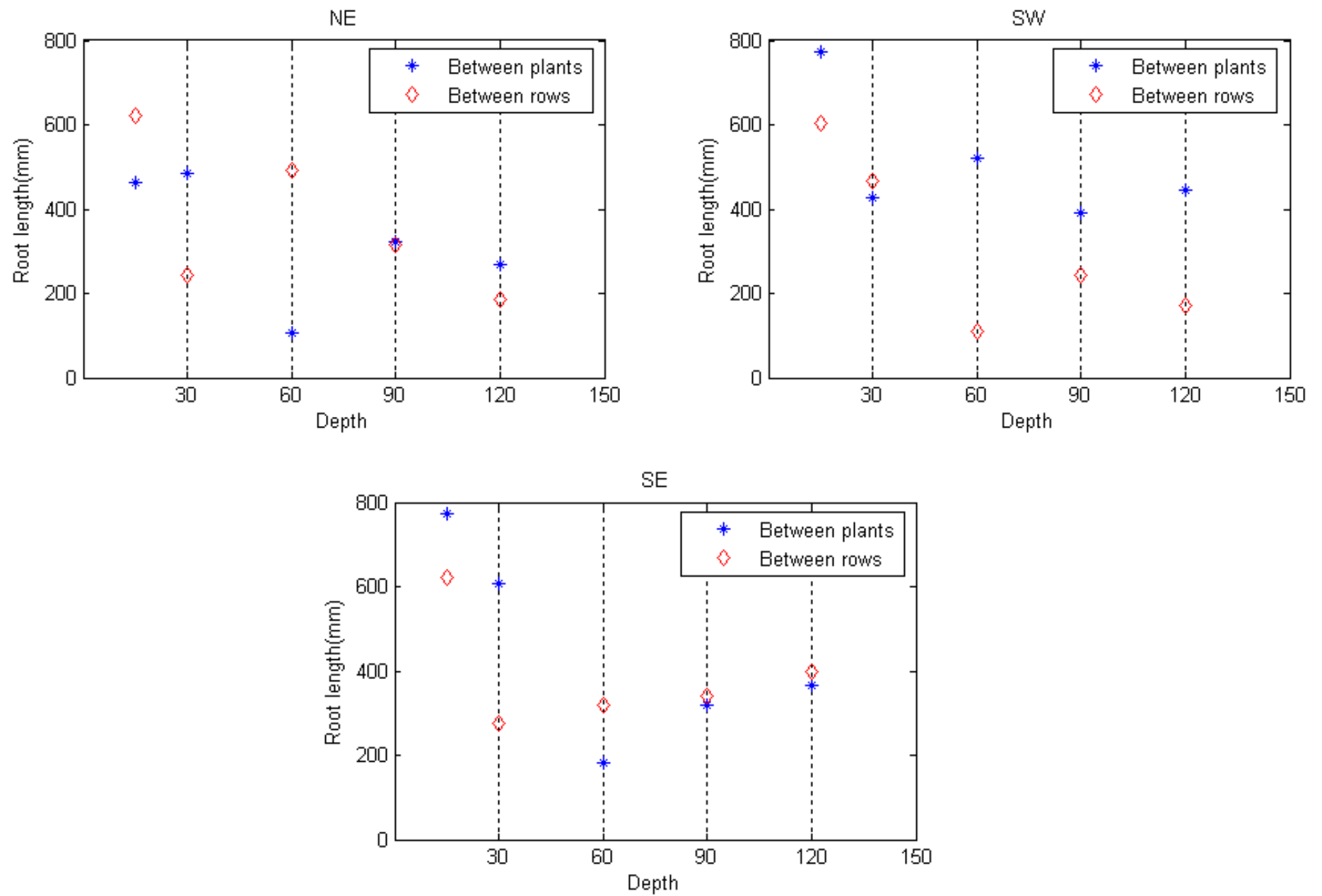


Figure A-75. Total root length at different depths at each vegetation sampling area

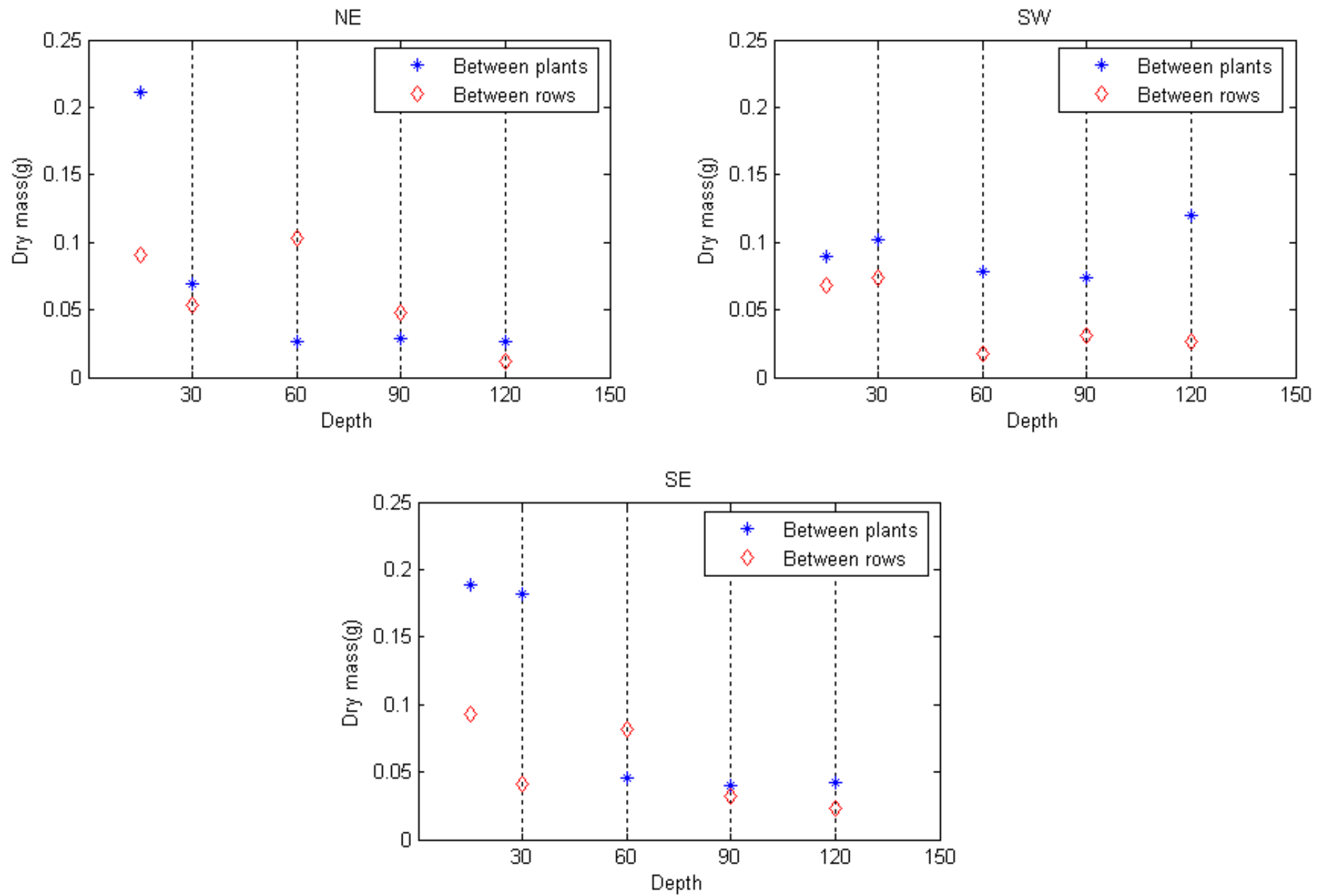


Figure A-76. Dry root mass at different depths at each vegetation sampling area

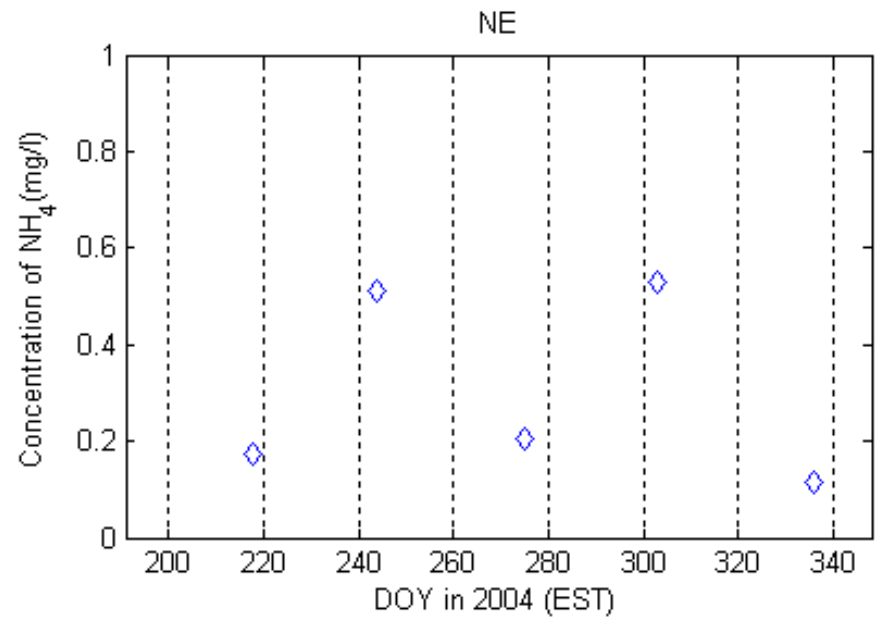
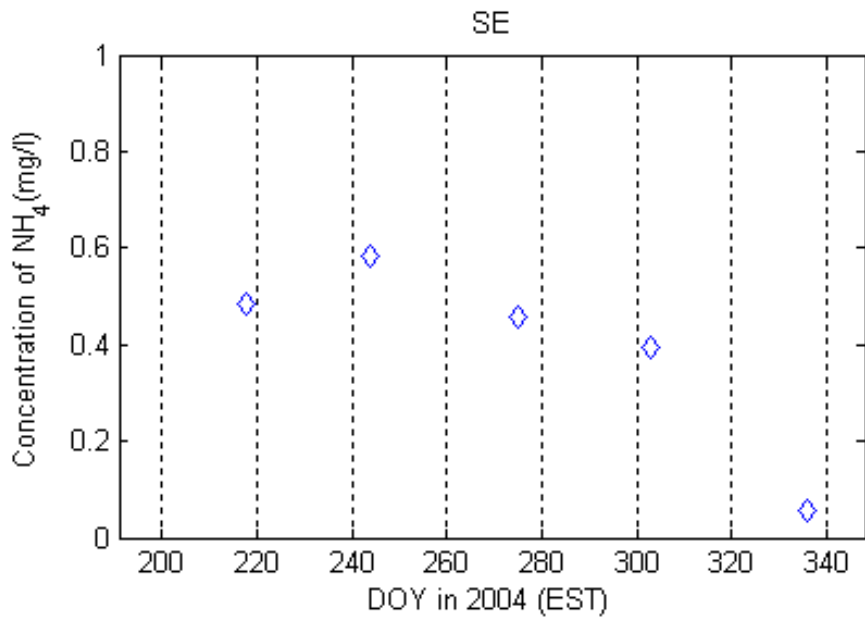
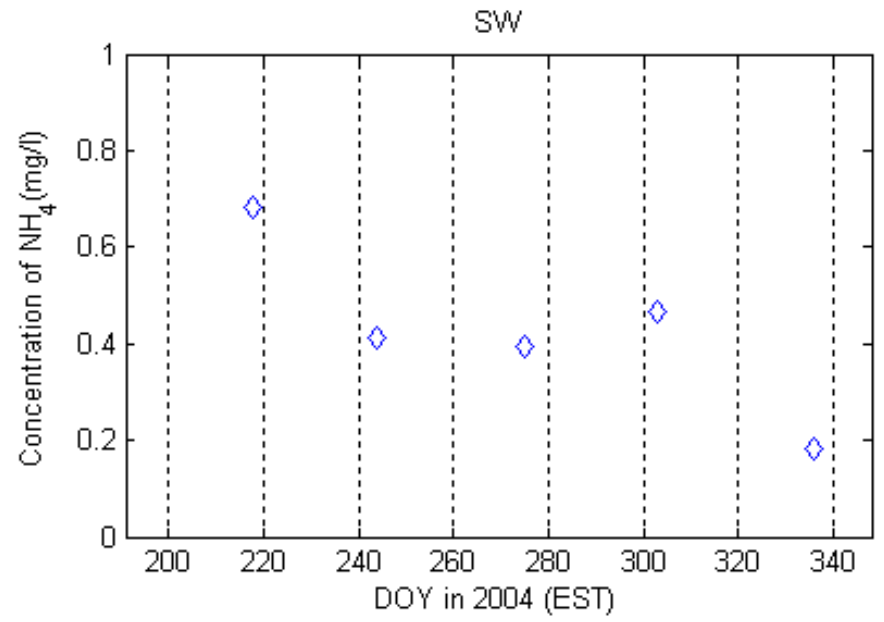
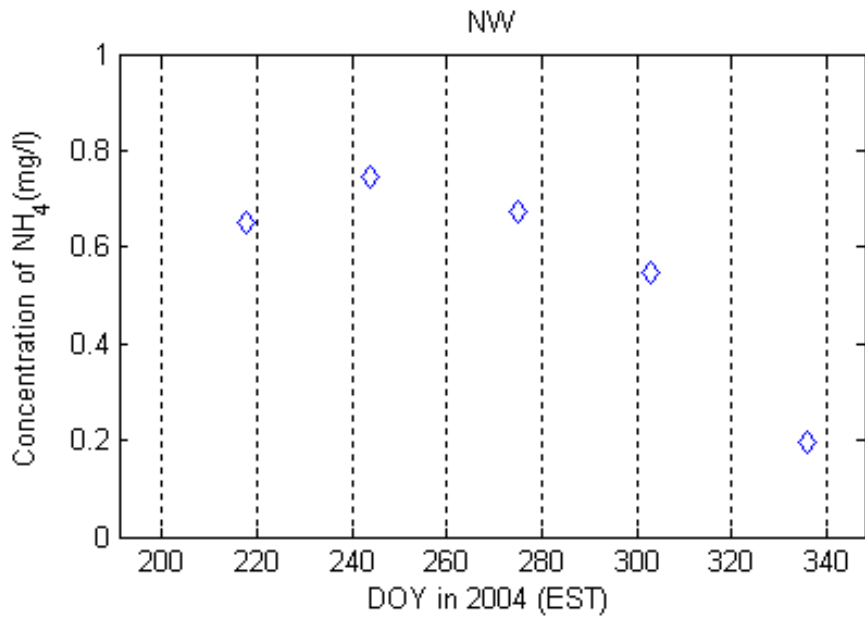


Figure A-77. NO₄ concentration at the monitoring wells

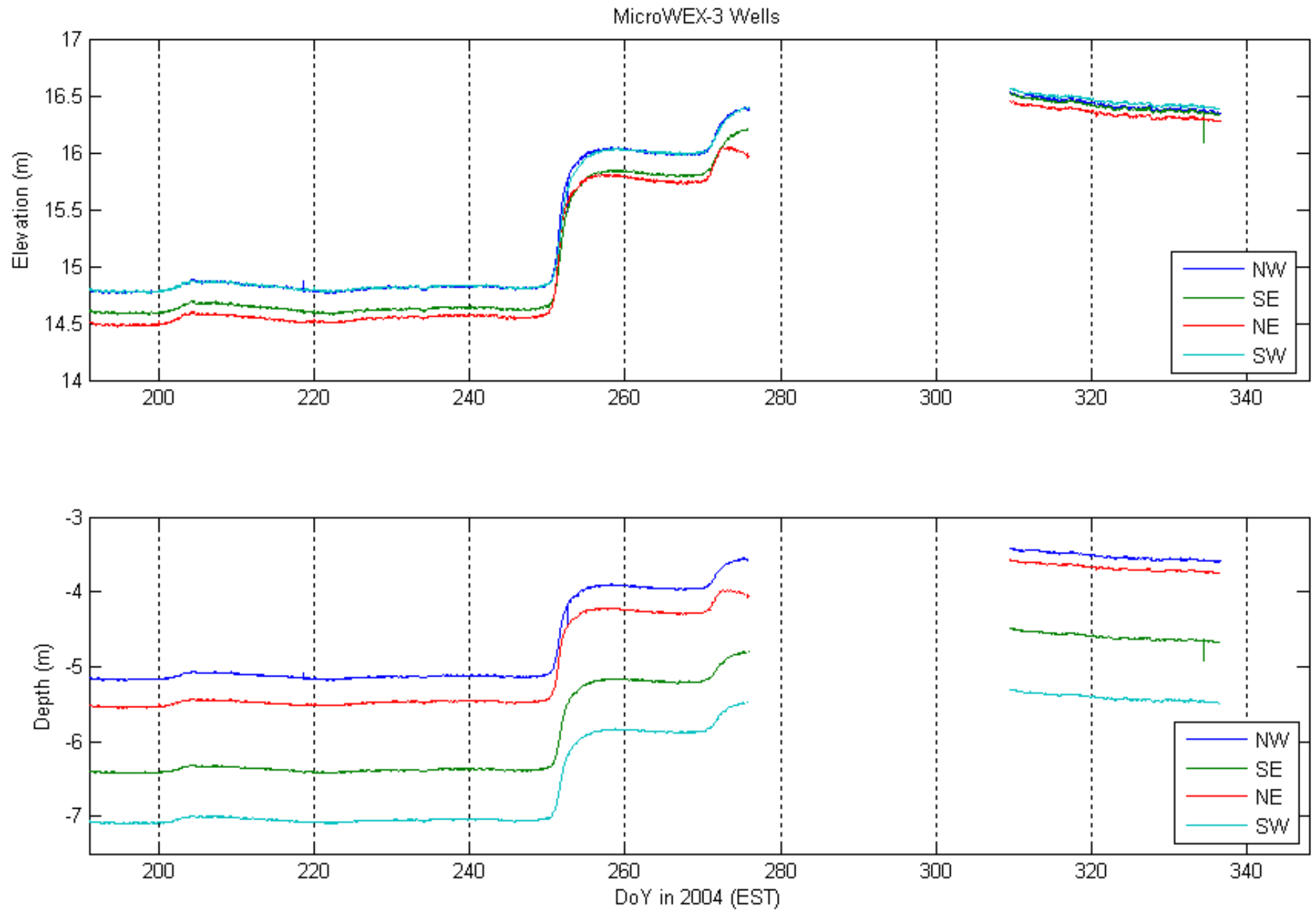


Figure A-78. Ground water level below surface and ground water level above sea level



Figure A-79. Surface roughness measurement at the east side of footprint: along the row

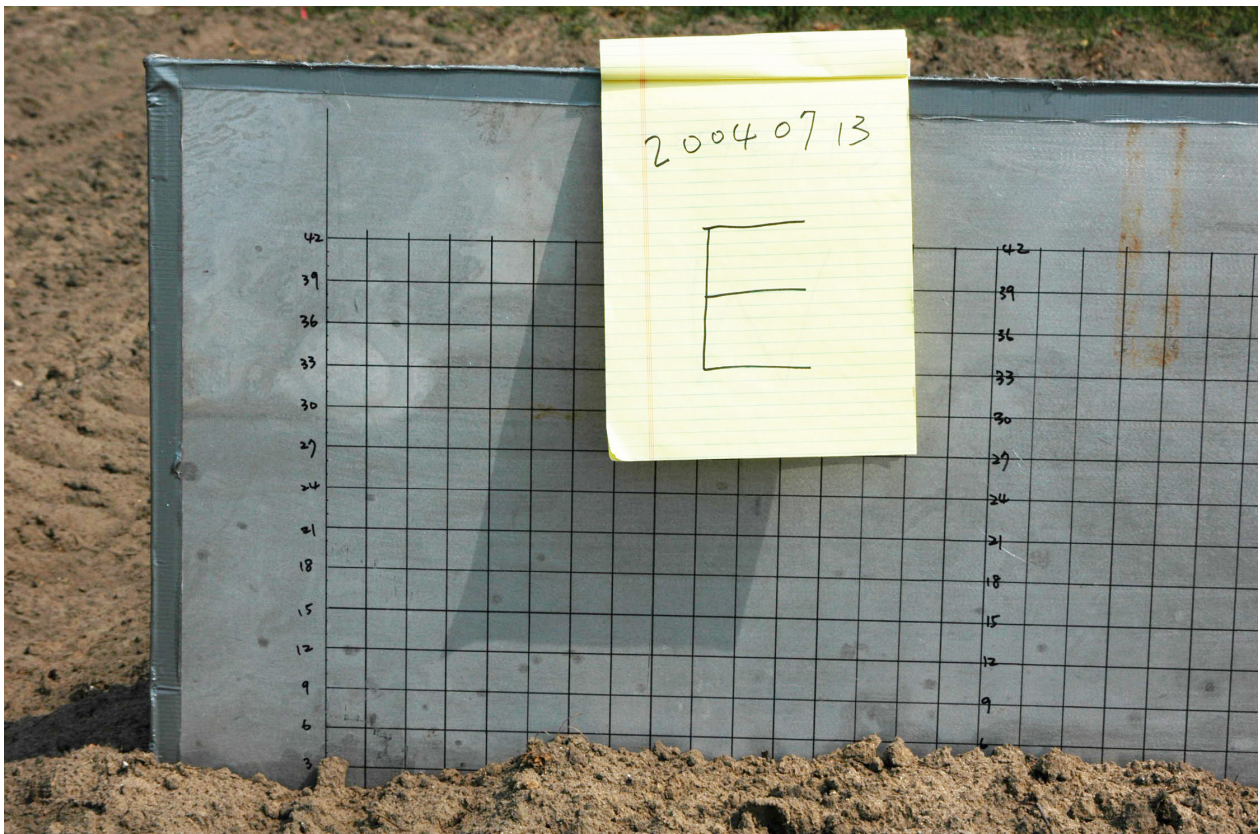


Figure A-80. Surface roughness measurement at the east side of footprint: across the row

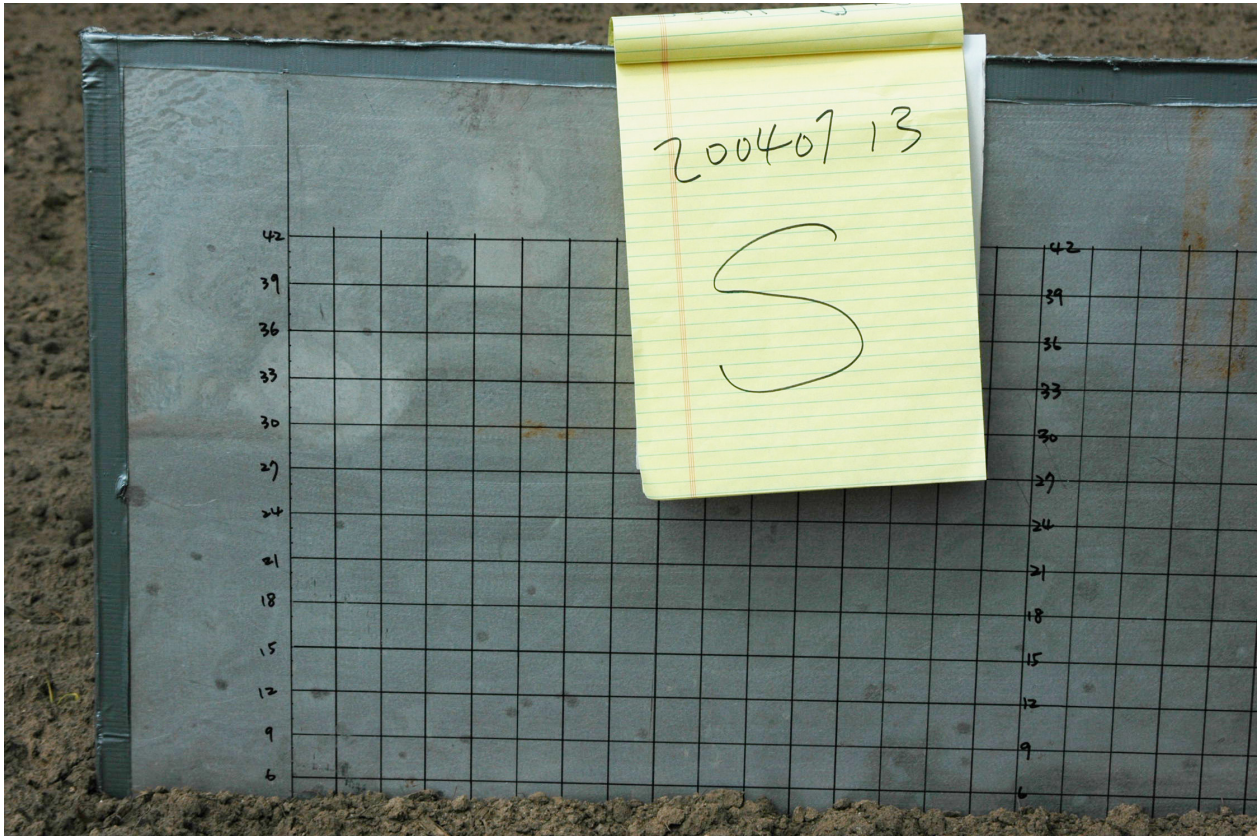


Figure A-81. Surface roughness measurement at the south side of footprint: along the row



Figure A-82. Surface roughness measurement at the south side of footprint: across the row



Figure A-83. Surface roughness measurement at the west side of footprint: along the row



Figure A-84. Surface roughness measurement at the west side of footprint: across the row